January 2015

Stability And Ductility Evaluation Of Thin-Walled Circular Steel Bridge Piers Under Cyclic Loading

Basha Dorose

Follow this and additional works at: https://commons.und.edu/theses

STABILITY AND DUCTILITY EVALUATION OF THIN-WALLED CIRCULAR STEEL BRIDGE PIERS UNDER CYCLIC LOADING

by

Basha Galmessa Dorose
Bachelor of Civil Engineering, University of Minnesota-Twin Cities, 2013

A Thesis
Submitted to the Graduate Faculty

of the

University of North Dakota

in partial fulfillment of the requirements

for the degree of

Masters of Science

Grand Forks, North Dakota

August
2015

Approval Page

This thesis, submitted by Basha Galmessa Dorose in partial fulfillment of the requirements for the Degree of Master of Science in Civil Engineering from the University of North Dakota, has been read by the Faculty Advisory Committee under whom the work has been done and is hereby approved.

Dr. Iraj H.P. Mamaghani (Chair)

Sukhvarsh Jerath
for Iraj H.P. Mamaghani 7/30/2015

Dr. Sukhvarsh Jerath,

Sukhvarsh Jerath 7/30/2015

Dr. Daba Gedafa

7/30/2015

This thesis is being submitted by the appointed advisory committee as having met all of the requirements of the School of Graduate Studies at the University of North Dakota and is hereby approved.

Wayne Swisher
Dean of the School of Graduate Studies

July 30, 2015
Date

PERMISSION

Title   Stability and Ductility Evaluation of Thin-Walled Circular Steel Bridge Piers under Cyclic Loading

Department   Civil Engineering

Degree   Master of Science

In presenting this thesis in partial fulfillment of the requirements for a graduate degree from the University of North Dakota, I agree that the library of this University shall make it freely available for inspection. I further agree that permission for extensive copying for scholarly purposes may be granted by the professor who supervised my thesis work or, in his absence, by the Chairperson of the department or the dean of the School of Graduate Studies. It is understood that any copying or publication or other use of this thesis or part thereof for financial gain shall not be allowed without my written permission. It is also understood that due recognition shall be given to me and to the University of North Dakota in any scholarly use which may be made of any material in my thesis.

Basha Galmessa Dorose
Date: 08/07/2015

TABLE OF CONTENTS

LIST OF FIGURES

LIST OF TABLES

ACKNOWLEDGEMENTS

I wish to express my sincere appreciation and gratitude to the University of North Dakota and especially the Civil Engineering Department for their continued support and guidance throughout my college career. My academic success is a direct impact of the Civil Engineering Department at the University of North Dakota. I would specifically like to thank my graduate advisor, Dr. Iraj Mamaghani, for his supervision and direction throughout the years. The leadership and knowledge provided by Dr. Mamaghani has made a graduate degree a reality for me.

ABSTRACT

Steel bridge piers have found wide application in highway bridge systems around the globe. Steel tubular bridge piers, compared with concrete ones, are light and ductile. They can be built under severe constructional restrictions, such as in limited spaces throughout urban areas like New York and Tokyo, where the effective use of the limited spaces are desired strictly. They are also applied to locations where heavy superstructures are unfavorable, such as on soft ground, reclaimed land and bay areas.

In general, steel bridge piers are designed as single columns of the cantilever type, or one to three-story frames. Steel columns in highway bridge systems are commonly composed of relatively thin-walled members of closed cross-sections, either box or circular in shape, because of their high strength and torsional rigidity. Such structures are considerably different from columns in buildings. The former are characterized by: failure attributed to local buckling in the thin-walled members; irregular distribution of the story mass and stiffness; strong beams and weak columns; low rise (1-3 stories); and a need for the evaluation of the residual displacement. These make them vulnerable to damage caused by local and overall interaction buckling in the event of a severe earthquake. A sound understanding of the inelastic behavior of thin-walled steel tubular columns is important in developing a rational seismic design methodology and ductility evaluation of such structures.

For this purpose, this thesis deals with the stability and ductility evaluation of thin-walled

circular steel bridge piers under cyclic loading. The basic characteristics of the thin-walled circular steel bridge piers and several methods in improving strength and ductility capacity of such structures was investigated. A procedure for ultimate strength and ductility evaluation of thin-walled circular steel bridge piers was developed. The application of the procedure was demonstrated by comparing the computed strength and ductility of some bridge piers with test results. The developed procedure is applicable for both the design of new, and retrofitting of existing, thin-walled circular steel bridge piers. The effects of some important parameters, such as width-to-thickness ratio, column slenderness ratio and residual stress, on the stability and ductility of thin-walled circular steel bridge piers, will be presented and discussed. A reasonably good agreement between the experiment and the analysis confirms the validity of the finite element modeling adopted in this study. From this study it is found that with the increase in eccentric distance, the load-carrying capacity of the eccentrically loaded columns in the eccentric side is greatly decreased, while in the opposite side it is increased. The results of this study also indicate that the buckling modes of the eccentrically in-plane loaded columns are almost the same as those of the centrally loaded columns when the eccentric distance lies within 30 percent of the column height. It was found that the strength and ductility of the eccentrically loaded columns can be conveniently obtained from those of the centrally loaded columns.

CHAPTER I

INTRODUCTION

1.1 Background

Structural engineers are continuously involves in designing structures such as buildings, bridges, tunnels, etc. To design and build structures that will withstand in all loading situations and environmental conditions, such as earthquakes, high wind loads, landslides, and flooding, needs advanced technology. The most extreme conditions any structures will need to resist is the seismic activity which is produced by earthquakes. Structural engineering scholars have made great progresses in predicting the reaction of structures subjected to earthquakes. Recently, the advancement in structural design standards and methods increase the stability and ductility in resisting earthquakes.

Thin-walled steel tubular bridge piers, with and without longitudinal and lateral stiffeners, in the form of cantilever columns and planar rigid frames, have been used in modern highway bridge systems because of their high strength and torsional rigidity. For example, Figure 1 shows bridge piers of thin-walled circular and rectangular box sections supporting an elevated highway bridge in Nagoya, Japan (Mamaghani et al., 2011). These types of structures are susceptible to damage caused by local and overall interaction buckling when subjected to severe earthquakes because their sections are characterized by a large width-to-thickness ratio of the flange plate (for box section), and by a large radius-to-thickness ratio of the circular section.

Figure 1.Thin-Walled Steel tubular Columns Supporting Elevated Highway Bridge in Nagoya, Japan.

Steel tubular bridge piers, compared with concrete ones, are light and ductile. They can be built under severe constructional restrictions, such as in limited spaces in urban areas like New York and Tokyo, where the effective use of the limited spaces are strictly desired. They also may be applied in locations where heavy superstructures are unfavorable, such as on soft ground, on reclaimed land, and in bay areas (Mamaghani et al., 2015a).

In general, because of these restrictions, steel bridge piers are designed as single columns of the cantilever type as shown in Figure 1, or one- to three-story frames, and they are commonly composed of relatively thin-walled members of closed cross-sections, either box or circular in shape because of their high strength and torsional rigidity (Mamaghani, 1996). These make them vulnerable to damage caused by coupled instability, (i.e., the interaction of local and overall buckling) in the event of a major earthquake (Mamaghani et al., 1996a). For example, Figure 2 shows a steel bridge pier of hollow box section,

which was suffered severe local buckling damage near the base of the pier in the 1995 Kobe earthquake. When structural members are composed of thin-walled steel plate elements, the local buckling of the component plates may influence the strength and ductility of those members (Mamaghani, 1997, 2006).

Figure 2. Damaged Bridge Pier Due to January 1995 Kobe Earthquake, Japan.

To improve seismic capacity of steel bridge piers of tubular sections, a number of researchers, among others, Banno et al. (1998), Fukumoto (2004), Gao et al. (2006, 2000a, 2000b, 1998), Hajjar (2000), JRA(1996), Kitada et al. (2000), Mamaghani (2015, 2008,2006a, 2006b, 2006c, 2005, 1996), Mamaghani et al. (2015a - 2015d, 2014a - 2014 d, 2011, 2008, 1997, 1996a, 1996b, 1995), Mamaghani and Packer (2002), Nakanishi et al. (1999), Nishikawa et al. (1998, 1996), Obata and Goto (2004), Shen et al. (1995), Uenoya et al. (2003), and Usami et al. (1995, 1996) have experimentally and theoretically investigated the stability and plastic ductility of steel tubular columns. Based

on the damage sustained by steel bridge piers in the Kobe earthquake and extensive test results, one of the important challenges of seismic design and retrofit of steel tubular columns is to increase the ductility of the columns while keeping their ultimate strength almost unchanged. Therefore a sound understanding of the cyclic inelastic behavior of thin-walled steel tubular columns is important in developing a rational performance-based seismic design methodology and ductility evaluation of such structures. Also seismic retrofits of existing steel tubular columns that do not satisfy the new seismic design method regulations are needed in order to enhance their strength and ductility.

Since 1995 Kobe earthquake, the Japanese seismic design code adopted a new design for highway bridges where the damages of columns are controlled, so the deformations under input earthquake waves are within acceptable values (Goto et al, 2006). For this, it is necessary to correctly forecast the ultimate behavior of thin-walled steel columns so that it can sustain during severe earthquakes. It is essential to examine the ultimate behavior of thin-walled steel columns under cyclic bidirectional lateral loading in the presence of a constant compressive centric or eccentric axial load (Gao et al., 2000a; Gao et al., 2000b).

This study examines the behavior of thin-walled steel columns subjected to a constant compressive centric/eccentric axial load and cyclic in-plane/out-of-plane lateral loading using a nonlinear finite element analysis software program (ABAQUS, 2013). A number of different specimens are modeled in ABAQUS (2013) and subjected to different loading programs at different eccentric distance from the center of top columns. The experimental and analytical results are compared by plotting the hysteretic behaviors of the columns. The deformation patterns of each model is also examined.

In what follows, the finite element modelling of thin-walled steel columns under eccentric in-plane and out-of-plane loading will be presented in chapter 2. The stability evaluation of thin-walled steel tubular bridge piers subjected to cyclic eccentric in plane lateral loading will be discussed in chapter 3. The stability evaluation of thin-walled steel tubular bridge piers subjected to cyclic eccentric out-of-plane lateral loading will be discussed in chapter 4. The application of the method will be demonstrated by comparing the computed strength and ductility of some bridge piers with test results. The method will be applicable for both the design of new, and retrofitting of existing, thin-walled steel tubular bridge piers. The effects of some important parameters, such as width-to-thickness ratio, column slenderness ratio and residual stress, on the ultimate strength and ductility of thin-walled steel tubular bridge piers, will be presented and discussed. The overall conclusions and future research needs will be presented in chapter 5.

CHAPTER II

FINITE ELEMENT MODELLING OF THIN-WALLED STEEL TUBULAR COLUMNS UNDER ECCENTRIC IN-PLANE AND OUT-OF-PLANE LOADING

2.1 Introduction

A large number of eccentrically loaded steel column have been constructed in many countries, especially in Japan, due to several factors, such as ground conditions, shape of the bridge piers and eccentric load from the superstructure. An additional bending moment, which is a function of eccentricity, is generated due to the eccentric load which comes from the superstructure as a term of dead load or live load. The load carrying capacity of the column decreases in the eccentric side due to this additional bending moment. Introducing torsional moment makes the structure more complicated. A study conducted by Nagoya Public Highway Corporation shows the importance of considering eccentricity in predicting seismic behavior of steel bridge piers. In practice, the eccentricity could be as large as 0.1 to 0.5 of height of column (Gao et al., 2000a). Recently an extensive study was carried out to investigate the behavior of concentrically-loaded hollow steel column but the behavior of eccentrically loaded column has hardly investigated. In the past three decades several tests were conducted by Nagoya University to investigate the behavior of cyclic eccentrically-loaded steel tubular bridge piers (Gao et al., 2000b). Usami (1999) compared the test result with concentrically loaded steel column to show the differences in behavior. Ge et al. (2000) compared the test result with analytical modeling and after extensive studies established a correlation between

concentric and eccentrically loaded column. In this chapter, first the characteristics of thin-walled steel tubular bridge piers will be reviewed and discussed. Then finite element modelling of the eccentrically loaded bridge piers will be presented.

2.2 Characteristics of Thin-Walled Steel Tubular Bridge Piers

Steel tubular columns in highway bridge systems are commonly composed of relatively thin-walled members of closed cross-sections, either box or circular shape, because of their high strength and torsional rigidity. Such structures are considerably different from columns in buildings. The failure characterization of the former one is attributed to local buckling in the thin-walled members, irregular distribution of the story mass and stiffness, strong beams and weak columns, low rise (1-3 stories). Hence there is a need for the evaluation of the residual displacement. These can make the columns vulnerable to damage caused by local and overall buckling in the event of a severe earthquake (Mamaghani, 2006a; Mamaghani, 2006b).

Different parameters for steel columns are considered in analysis and compared to the experimental results. The most important parameters consider in the practical design and ductility evaluation of thin-walled steel hollow columns are the radius-to-thickness ratio for circular sections, R_t, and the slenderness ratio parameter, λ of the columns (Mamaghani, 2006a). R_t influence the local buckling of the section while λ controls the global stability (Mamaghani, Khavanin, Erdogan, & Falken, 2008a). They are given by

$$R_t = \frac{r}{t}\sqrt{3(1-v^2)}\frac{\sigma_y}{E} \quad \text{(for circular section)} \tag{1}$$

$$\lambda = \frac{2h}{r_g}\frac{1}{\pi}\sqrt{\frac{\sigma_y}{E}} \tag{2}$$

in which, b = flange width; t = plate thickness; σ_y = yield stress; E = Young's modulus; v = Poison's ratio; n = number of subpanels divided by longitudinal stiffeners in each plate panel (n = 1 for unstiffened sections); r = radius of the circular section; h = column height; r_g = radius of gyration of the cross section.

The elastic strength and deformation capacity of the column are expressed by the yield strength H_{y0}, and the yield deformation (neglecting shear deformations) δ_{y0}, respectively, corresponding to zero axial load. They are given by:

$$H_y = \frac{M_y}{h} \tag{3}$$

$$\delta_y = \frac{H_y h^3}{3EI} \tag{4}$$

Where: M_y = yield moment, I = moment of inertia of the cross section. Under the combined action of buckling under constant axial and monotonically increasing lateral loads, the yield strength is reduced from H_y to a value denoted by H_y. The corresponding yield deformation is denoted by δ_y. The value H_y is the minimum of yield, local buckling, and instability loads evaluated by the following equations:

$$\frac{P}{P_u} + \frac{0.85 H_y h}{M_y\left(1 - \frac{P}{P_E}\right)} = 1 \tag{5}$$

$$\frac{P}{P_u} + \frac{H_y h}{M_y} = 1 \tag{6}$$

Where: P = the axial load; P_y = the yield load; P_u = the ultimate load and; P_E = the Euler load.

2.1 Loading

In case of out-of-plane moment, despite complex loading, out-of-plane bending moment M_1 is more dominant than torsional moment, T and in-plane moment, M_0 because of its high magnitude. M_1, T, and M_0 are expressed by the following equations:

$$M_o = P.e$$

(7)

$$M_1 = H.h$$

(8)

$$T = H.e \tag{9}$$

Here, P = Vertical load; e = eccentricity; H = transverse load acting in the out-of-plane direction; and h = height of the column.

Usually eccentricity e, which is obtained from practical investigation, is taken 30%-40% of column height h. The intention of this study is to make a relation between concentrically loaded hysteresis diagrams with eccentrically loaded hysteresis diagram as a lot of study is carried out on concentrically loaded column. Another purpose is to study the effect of several factor such as, eccentricity e, radius-thickness ratio, R and column slenderness ratio, λ. These parameters are expressed by following equations (Nishino, 1987):

$$R_t = \frac{\sigma_y}{\sigma_{cr.pipe}} = \sqrt{3(1 - \vartheta^2)}\, \frac{\sigma_y}{E} \frac{D}{2t}$$

(10)

$$\overline{\lambda} = \frac{2h}{r}\frac{1}{\pi}\sqrt{\frac{\sigma_y}{E}}$$

(11)

2.3 Finite Element Modeling of the Eccentrically Loaded Steel Tubular Bridge Piers

2.3 .1 Material Modeling

The cyclic behavior of structure depends on the mechanical property of the material represented by the stress-strain hysteresis loops such as bilinear kinematic hardening and multi-linear kinematic hardening rule. The effects of mechanical properties of material on cyclic behavior of steel structures were studied by many researchers. Schneider (1998) considered structural steel as elastic-perfectly plastic material while Guo (2007) considered linear kinematic hardening and Han (2007) considered multinear kinematic hardening. The behavior of structure greatly depend on the material model (constitutive law) used in the analysis, namely isotropic hardening model and kinematic hardening model. The effect of constitutive law on cyclic behavior of steel structures were studied by Mamaghani (1996) and Gao et. al. (1998). The cyclic behavior of structure such as, hysteresis loops, which represent the energy absorption by the structure, and buckling shape is considerably different under isotropic hardening and kinematic hardening material models. The reason is due to the fact that in the isotropic hardening material model strain hardening takes place in both tension and compression directions due to cyclic loading. In contrast, the kinematic hardening rule consider the Bauschinger effect, while the yield surface with a constant radius translates. The yield surface translation results in strain-hardening of the material in loading direction and softening of the

material in opposite (unloading) direction. In this study, the multilinear kinematic hardening material model is used in the analysis as it predicts material behavior better than the isotropic hardening material model (Gao et al., 1998; Mamaghani et al. 1997).

2.3 .2 Modeling of Bridge Piers under Eccentric In-Plane Loading

The bridge piers under eccentric in-plane loading is modelled as shown in figure 3. In this study full scale model was analyzed to obtain reasonably accuracy result. The vertical load *P* is applied at the eccentric distance *e*. The load *P* is transmitted to the bridge pier through rigid bars connecting the loading point to several points at the top of pier, Figure 3.
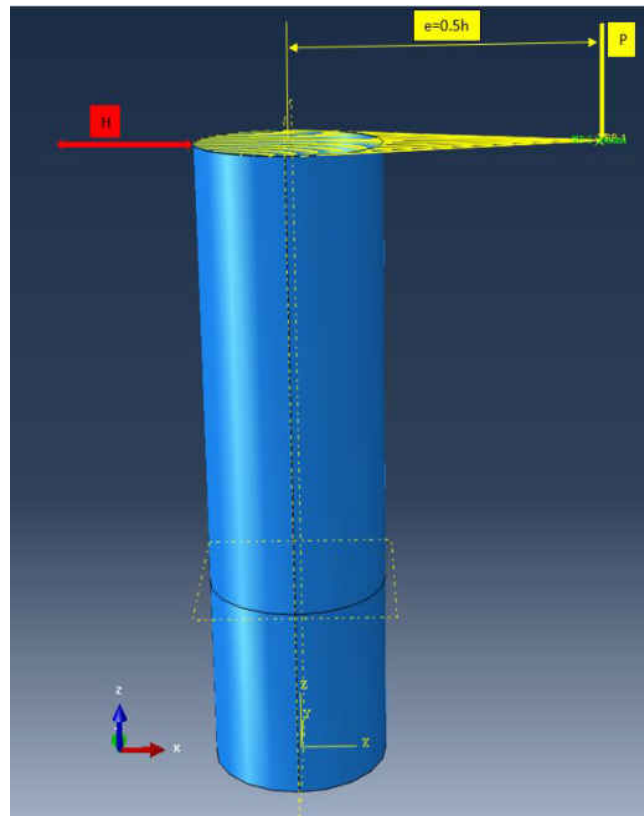
Figure 3.In-Plane Loading of the Analyzed Column.

2.3.3 Finite Element Discretization of Bridge Piers

The finite element modeling of tubular column is shown in Figure 4. For thin-walled steel columns, local buckling always occurs near the base of the columns. Therefore, a coarse mesh discritization is employed for the upper part of the column; while finer mesh discritization is adopted for the lower part of the column to consider the effect of local buckling, see Figure 4. The length from the base, which equals the radius of the column, is divided into 15 segments, while the following length of the column is divided into 30 segments along the column length. In the circumferential direction, both meshing patterns consist of 20 segments. Adopting these two different meshing patterns reduces the computation time and required memory space in the analysis.

The above stated mesh divisions are determined by trial and error method. It is found that such mesh divisions can give an accurate result. The initial deflections of the column are not considered in the analysis as their effect is insignificant on the cyclic behavior (Banno et al., 1998).

(a)   (b)
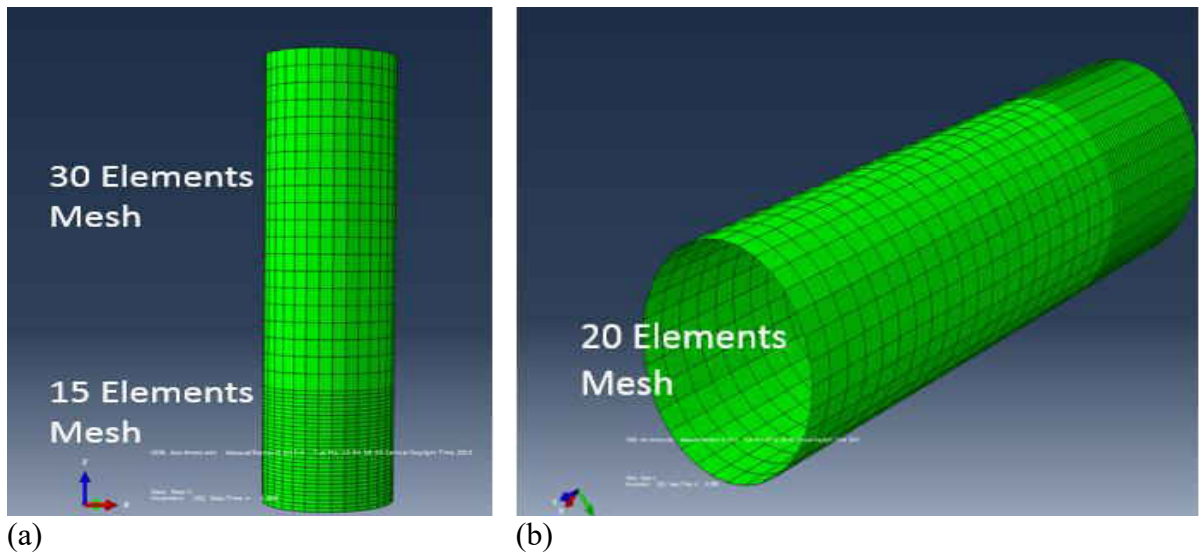
Figure 4.Meshing Details of Bridge Piers, (a) Elevation, (b) Circumferential Direction

Column was modeled using shell element S4R, a 4 node reduced integration shell element. Plasticity was assumed distributed along cross section of shell element and along the length of column. Five Gaussian integration point is used across the cross section to distribute the plasticity along cross section. Figure 5 shows a schematic diagram of S4R element.
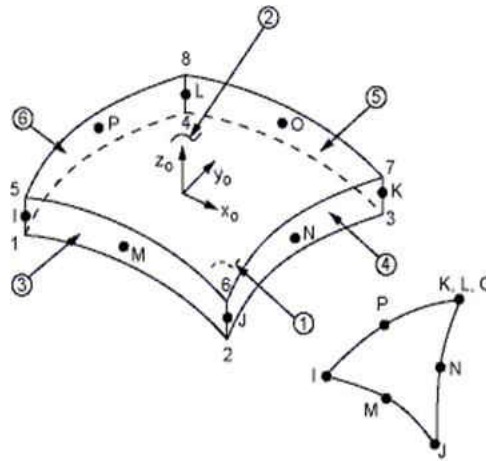
Figure 5.Shell Element (S4R)

2.3.4 Loading History

The objective of the present study is to evaluate possible maximum deterioration in strength and ductility of thin-walled tubular steel bridge piers caused by eccentrically applied in-plane and out-of-plane constant axial load and cyclic lateral loads in-comparison with the conventional centrically applied constant axial load and cyclic lateral loads. While keeping the vertical compressive load constant ($P/P_y = 0.15$), the lateral displacement amplitude is monotonically increased by the integer multiples of the initial yield displacement given by δ_{y0} (cyclic lateral displacements of increasing amplitude $\pm\delta_{y0}$, $\pm2\delta_{y0}$, …, $\pm8\delta_{y0}$ at the top of the column). Under the same amplitude, one

loading cycle is given to the columns. Most of the cyclic unidirectional loading tests conducted for thin-walled columns adopt one loading cycle (Mamaghani et al., 2008) The applied axial force $P/Py = 0.15$, where P is a dead load acting at the top of the column and $P_y = \sigma_y A$ is a yield compressive strength of the column.
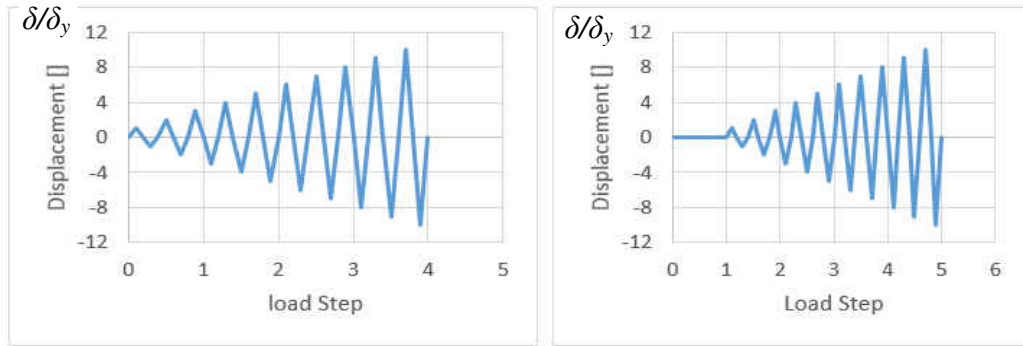
(a) Centrally Loaded, e=0.0h   (b) Eccentrically Loaded, e=0.5h

Figure 6. Eccentric In-Plane Cyclic Loading
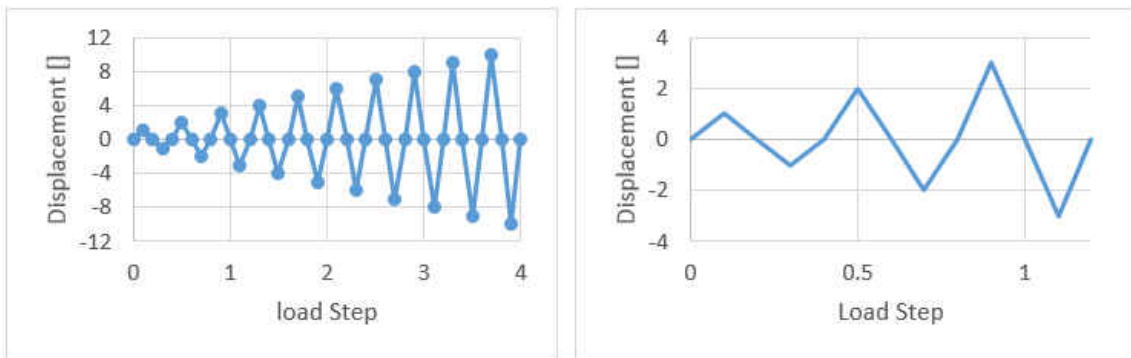
(a) Centrally Loaded, e=0.0h   (b) Eccentrically Loaded, e=0.4h

Figure 7. Eccentric Out-of-Plane Cyclic Loading

14

CHAPTER III

ANALYSIS AND STABILITY EVALUATION OF THIN-WALLED STEEL TUBULAR BRIDGE PIERS SUBJECTED TO CYCLIC-IN- PLANE ECCENTRIC LOADING

3.1 Introduction

In recent years thin-walled steel tubular columns have found a wide range of usage as bridge piers for highway bridge systems in Japan and other countries. These steel bridge piers are beneficial compared to concrete piers. They are light, ductile, and they can be built under severe constructional restriction, such as highly populated urban areas like New York and Tokyo due to their small cross sectional areas. They are also advantageous in environments that cannot support heavy superstructures, such as areas with soft ground, reclaimed land and, bay areas (Mamaghani et al., 2010).

Thin-walled steel columns are preferred in Japan as bridge piers for elevated bridges in urban areas because of the stated advantages and high earthquake resistance. After lessons learned from the 1995 Kobe earthquake (JSCE Earthquake Engineering Committee, 2000), the Japanese seismic design code (Japan Road Association, 2002) for highway bridges adopted a new design concept where the damages of columns are controlled, so the residual deformations after being subjected to earthquake waves are within an allowable value. Therefore, when these thin-walled steel columns are subjected to severe earthquakes it is necessary to accurately predict the ultimate behavior (Goto et al., 2006).

Steel bridge piers because of the stated restrictions generally designed as single columns of the cantilever type, or one to three-story frames, most commonly composed of relatively thin-walled circular or box shape members of closed cross-sections because of their high strength and torsional rigidity (Mamaghani et al., 1996). This can make them susceptible to damage caused by the coupled instability, i.e., the interaction of local and overall buckling, in the event of a major earthquake (Mamaghani et al, 2008b). For example, Figure 2 shows a hollow steel bridge pier which suffered severe local buckling near the base of the pier in the Kobe earthquake. While structural members are composed of thin-walled steel plate elements, the inelastic seismic behaviors of thin-walled steel columns are affected by the cyclic metal plasticity as well as the local buckling behavior of individual plate elements (Gao, et al., 1998).

In this chapter, the behavior of thin-walled steel tubular columns under the cyclic eccentric in-plane loads was examined. This study examined the ultimate strength and ductility capacity and correlation between centrally and eccentrically loaded steel columns subjected to cyclic transverse (horizontal) load at the top of columns. All columns were considered as circular sections. An extensive elastoplastic finite-element analysis was conducted on the eccentrically loaded columns subjected to cyclic transverse loading to find a correlation between the eccentrically and centrally loaded columns.

3.2 Loading Program

Each test model was subjected to a specific central/eccentrical loading pattern at the top of the column controlled by displacement. Figure 6 illustrates the specific cyclic loading

program for P13. In the model, a horizontal displacement, δ_y, was applied at the top of the model with a constant compressive force, P, which is illustrated in Figure 3. Where δ_y is the horizontal displacement at the loading point when the model begins to yield. δ_y is calculated here by Equation (7)

$$\delta_y = \frac{H_y h^3}{3EI} \qquad (7)$$

Where H_y represents the horizontal force corresponding to h = the column height, EI = the bending rigidity. Table 1 lists the loading parameters for each respective models.
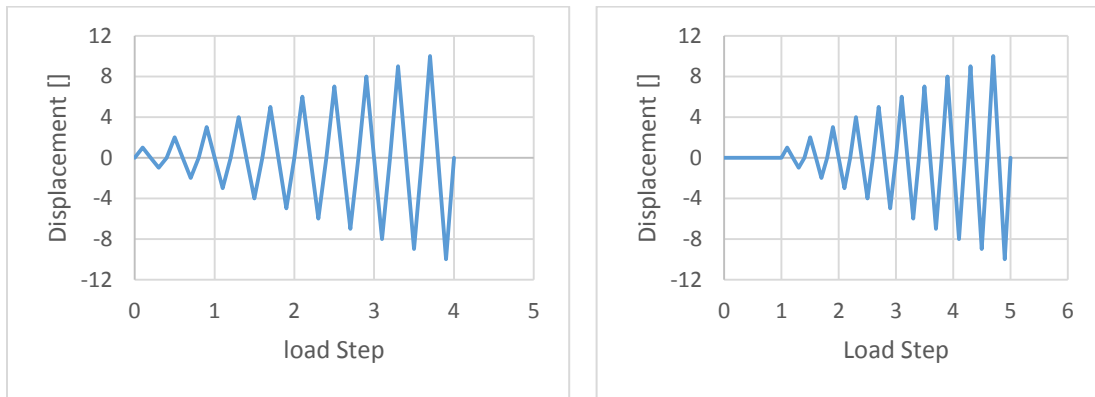
(a) Centrally Loaded, e=0.0h   (b) Eccentrically Loaded, e=0.5h

Figure 8. Model P13 Loading Programs

Table 1: Models Loading Parameters.

Model	$\alpha=P/P_y$	P_y [KN]	P [KN]	H_y [KN]	δ_y[m]	δ_0[m]
P1-e0	0.12	7222	867	408	0.0107	0.0000
P1-e1	0.12	7222	867	408	0.0107	0.0034
P1-e2	0.15	7222	867	408	0.0107	0.0068
P3-e0	0.15	4784	718	122	0.0389	0.0000
P3-e1	0.15	4784	718	122	0.0389	0.0344
P8-e0	0.15	7287	1093	306	0.0140	0.0000
P8-e1	0.15	7287	1093	306	0.0140	0.0075
P8-e2	0.15	7287	1093	306	0.0140	0.0150
P9-e0	0.15	7287	1093	184	0.0389	0.0000
P9-e1	0.15	7287	1093	184	0.0389	0.0347
P12-e0	0.15	10861	1629	451	0.0140	0.0000
P12-e2	0.15	10861	1629	451	0.0140	0.0076
P13-e0	0.15	7287	1093	460	0.0062	0.0000
P13-e1	0.15	7287	1093	460	0.0062	0.0022
P13-e2	0.15	7287	1093	460	0.0062	0.0044
P13-e3	0.15	7287	1093	460	0.0062	0.0067
P13-e4	0.15	7287	1093	460	0.0062	0.0089
P13-e5	0.15	7287	1093	460	0.0062	0.0110

3.3 Numerical Method

Numerical studies on the cyclic behavior of thin-walled steel tubular columns were carried out using the computer program ABAQUS (2013). Figure 6 shows the analytical model of an eccentrically loaded column that is simplified to centrally loaded column conducted that an eccentric load P is now treated as a concentric load, and an additional bending moment, M_0, is introduced. The results from the finite element analysis are compared with the experimental results (Gao et al., 2000b). The experimental data was used to validate the accuracy of the cyclic elastoplastic large displacement finite element analysis procedure used in ABAQUS (2013). Table 2 lists the geometrical parameters for

the thirteen specimens used in this study. Here, R_t = radius-thickness ratio of cross section; λ= column slenderness ratio; h = column height; D = diameter of pipe section; t = plate thickness; and e=eccentric distance. In this study, the eccentric distance, e, was assumed to be range from 0 to 0.5h. In the case of e = 0 refers to the centrally loaded column. The axial force, P, was taken as 0.15P_y (P_y = squash load) for all the columns except for the P1 series, where 0.12Py was applied (Gao et al., 2000b).

Table 2: Geometrical Properties of Analyzed Columns

Model	h [m]	D [m]	t [m]	A [m²]	R_t	λ	e/h
P1	3.403	0.891	0.009	0.024938	0.0115	0.26	0.0
P1-e1	3.403	0.891	0.009	0.024938	0.0115	0.26	0.1
P1-e2	3.403	0.891	0.009	0.024938	0.0115	0.26	0.2
P3	7.319	0.891	0.00732	0.020322	0.0115	0.50	0.0
P3-e1	7.319	0.891	0.00732	0.020322	0.0115	0.50	0.1
P8	4.391	0.891	0.0112	0.030957	0.075	0.30	0.0
P8-e1	4.391	0.891	0.0112	0.030957	0.075	0.30	0.1
P8-e2	4.391	0.891	0.0112	0.030957	0.075	0.30	0.2
P9-e0	7.319	0.891	0.0112	0.030957	0.075	0.50	0.0
P9-e1	7.319	0.891	0.0112	0.030957	0.075	0.50	0.1
P12	4.391	0.891	0.0168	0.046139	0.050	0.30	0.0
P12-e2	4.391	0.891	0.0168	0.046139	0.050	0.30	0.2
P13	2.927	0.891	0.0112	0.030957	0.075	0.20	0.0
P13-e1	2.927	0.891	0.0112	0.030957	0.075	0.20	0.1
P13-e2	2.927	0.891	0.0112	0.030957	0.075	0.20	0.2
P13-e3	2.927	0.891	0.0112	0.030957	0.075	0.20	0.3
P13-e4	2.927	0.891	0.0112	0.030957	0.075	0.20	0.4
P13-e5	2.927	0.891	0.0112	0.030957	0.075	0.20	0.5

(a) Centerally Loaded Column
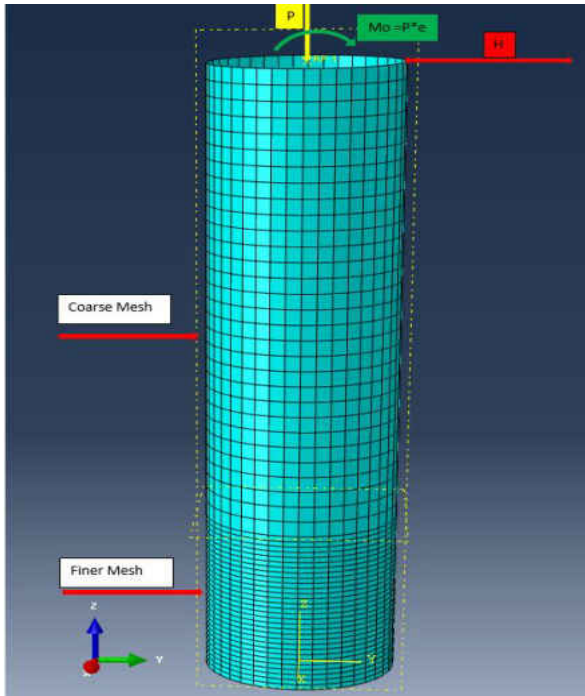
(b) Eccentrically Loaded in-Plane Column

Figure 9. Numerical Analytical Model

Figure 10. View of Eccentrically Loaded Steel Circular Section Bridge pier Constructed in Urban Area of Japan.

3.4 Finite Element Analysis

The computer program ABAQUS 6.13(2013) which is a finite element analysis program, which was used to study the behavior of the thin-walled steel tubular columns. Each column was created using SHELL 281 elements. Local buckling generally occurs near the base of the columns. Therefore, a finer mesh was adopted for the lower part of the column to consider the effect of local buckling, while a coarser mesh is adopted for the upper part of the column. The fine mesh was used to a height equal to the diameter, D from the base of the column. The finite element model of the tubular column and mesh is shown in Figure 4. For Meshing, lower part of the column, which is equal to the diameter of the column, was divided into 15 segments, while the rest of the column was divided into 30 segments along the length. In the circumferential direction, column is divided into 20 segments. The above stated mesh divisions are determined by trial and error method and it is found that such mesh divisions give an accurate result.

All input data for geometric and material parameters in ABAQUS (2013) is listed in Tables 2 and 3. Initial imperfections of thin-walled circular columns such as initial deflections and residual stresses were not considered in the analysis. The initial deflections of the plates were not considered in the analysis as their effect is insignificant on the cyclic behavior (Banno et al., 1998).

Table 3: Model Material Properties

Model	E [Gpa]	σ_y [Mpa]	σ_u [Mpa]	υ [m/m]	ε_y	ε_{st}
P1	206	289.6	576	0.3	0.001406	0.019682
P1-e1	206	289.6	576	0.3	0.001406	0.019682
P1-e2	206	289.6	576	0.3	0.001406	0.014058
P3	206	235.4	426.1	0.3	0.001143	0.011427
P3-e1	206	235.4	426.1	0.3	0.001143	0.011427
P8	206	235.4	426.1	0.3	0.001143	0.011427
P8-e1	206	235.4	426.1	0.3	0.001143	0.011427
P8-e2	206	235.4	426.1	0.3	0.001143	0.011427
P9	206	235.4	426.1	0.3	0.001143	0.011427
P9-e1	206	235.4	426.1	0.3	0.001143	0.011427
P12	206	235.4	426.1	0.3	0.001143	0.011427
P12-e2	206	235.4	426.1	0.3	0.001143	0.011427
P13	206	235.4	426.1	0.3	0.001143	0.011427
P13-e1	206	235.4	426.1	0.3	0.001143	0.011427
P13-e2	206	235.4	426.1	0.3	0.001143	0.011427
P13-e3	206	235.4	426.1	0.3	0.001143	0.011427
P13-e4	206	235.4	426.1	0.3	0.001143	0.011427
P13-e5	206	235.4	426.1	0.3	0.001143	0.011427

3.5 Comparison between Computed Hysteresis Curves of Centrally and Eccentrically Loaded Columns

The objective of the study was to evaluate possible maximum deterioration in strength and ductility of thin-walled tubular steel columns caused by in-plane cyclic unidirectional lateral load and constant axial centric compressive load in comparison with the constant axial eccentric compressive load. Therefore, to determine the transverse load versus transverse displacement relationship between the centrally and eccentrically loaded columns, 12 columns, including six centrally loaded columns, were analyzed. The Figures 12 to 38 compare the analytical hysteresis curves of the centrally and eccentrically loaded columns. Here, H_y is the lateral yield load of the centrally loaded column and was taken as the smaller of equations (5 and 6) (Gao et al., 2000b):

Where M_y = yield moment of cross section; P_E = Euler's buckling load of cantilever column; P_u = ultimate strength of centrally loaded column; and δ_y = yield displacement (Gao et al., 2000b).

3.6 Correlation between Centrally and Eccentrically Loaded Columns

Sketches of centrally and eccentrically loaded columns are shown in Figure 11. In this figure, H_c indicates the transverse load of centrally loaded column and H_e indicates the transverse load of eccentrically loaded columns, respectively while δ_c and δ_e denote the corresponding transverse displacements of two types of columns. According to the elastic theory, neglecting shear deformation, δ_c and δ_e can be written as follows:

$$\delta_c = \frac{H_c h^3}{3EI} \tag{8}$$

$$\delta_e = \delta_o + \frac{H_e h^3}{3EI} \tag{8}$$

Where E = Young's modulus; I = inertial moment of cross section; and h = column height. Moreover, δ_0 is the initial transverse displacement resulting from the eccentric vertical load, and given by equation (10 and 11) :

$$\delta_o = \frac{M_o h^2}{2EI} \tag{10}$$

Form equation 11 to 13

$$\delta_e - \delta_c - \delta_o = \frac{h^3}{3EI}(H_e - H_c) \tag{11}$$

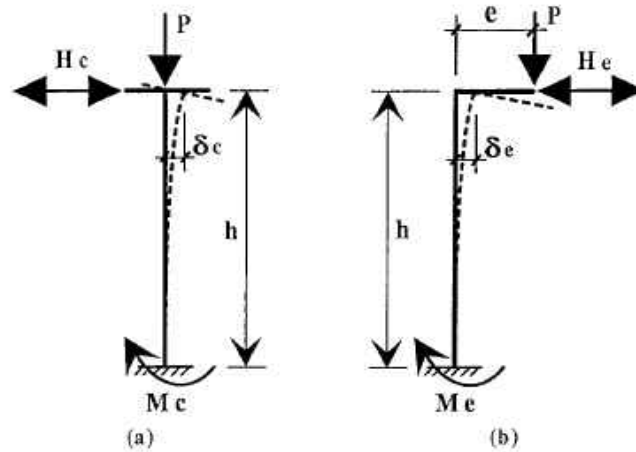Where$M_o = P * e$; and e is the eccentric distance (Gao et al., 2000b).

Figure 11. Sketches of (a) Centrally Loaded Column; (b) Eccentrically Loaded Column

3.7 Numerical Results

Using ABAQUS (2013), finite element analysis results for each models were produced. Some of the model results obtained by (Gao et al., 2000b) were used to validate the analysis results. Figures 12, 13, and 15 to 23 show comparison of the analytical hysteresis curves of the centrally and eccentrically loaded columns. In each plot of Figure 12, 13, and 15- 23, the dashed lines are the results of the centrally loaded column, whereas the solid lines are for the results of the eccentrically loaded column. It is noticed from the figures that the load-carrying capacity in the eccentric side is significantly reduced due to the presence of the eccentric load. On the other hand, the maximum strength in the other side is much larger than that of the centrally loaded column.

To determine the most accurate results considering (Gao et al., 2000b) data and the results were plotted in Figures 31-38. Results obtained were used to validate the finite element model and were plotted for comparison with experimental values. The finite element analysis results were used to plot hysteretic curves. Finite element analysis and

experimental results for normalized lateral load (H/H_y) versus normalized lateral displacement (δ/δ_y) were plotted and compared. Comparisons of buckling, model stress distribution and deformation level near the base of the columns at the $\delta/\delta_{y\,=}$ +8 stage for p1 and P8 series was plotted. Also, Stress distribution and deformation level near the base of the columns at the $\delta/\delta_{y\,=}$ +10 load stage for p12 and P13 series was plotted. And also for p3 series at $\delta/\delta_{y\,=}$ 6 displacement. Envelopment curves of the horizontal load-displacement relations are plotted for each analysis shown in Figures 25-30. Comparison of Hysteresis Curves plotted for P13 series in Figures 19-24. Also, comparison of Envelope Curves between analysis and experimental results were plotted for P1and P13 series in Figures 35-38.

Figure 12. Model P1and P1-e1 Comparison of Normalized Lateral Load vs. Lateral Displacement of Centrally Concentric Load and Eccentrically Concentric Load.

Figure 13: Model P1 and P1-e2 Comparison of Normalized Lateral Load vs. Lateral Displacement of Centrally Concentric Load and Eccentrically Concentric Load.

(a) P1-e0

(b) P1-e1

(c) P1-e2

Figure 14. Comparison of Buckling Modes of Columns P1 Series :(a) P1-e0; (b) P1-e1; (c) P1-e2
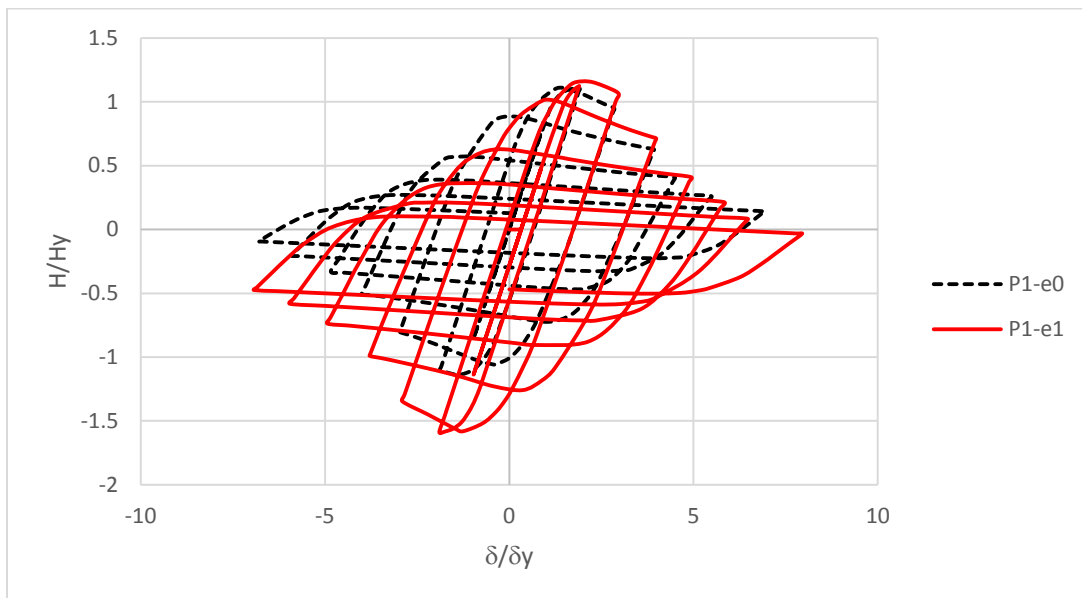
Figure 15. Model P3 and P3-e1 Comparison of Normalized Lateral Load Vs. Lateral Displacement of Centrally Concentric Load and Eccentrically Concentric Load.

Figure 16. Model P8, P8-e1 Comparison of Normalized Lateral Load Vs. Lateral Displacement of Centrally Concentric Load and Eccentrically Concentric Load.
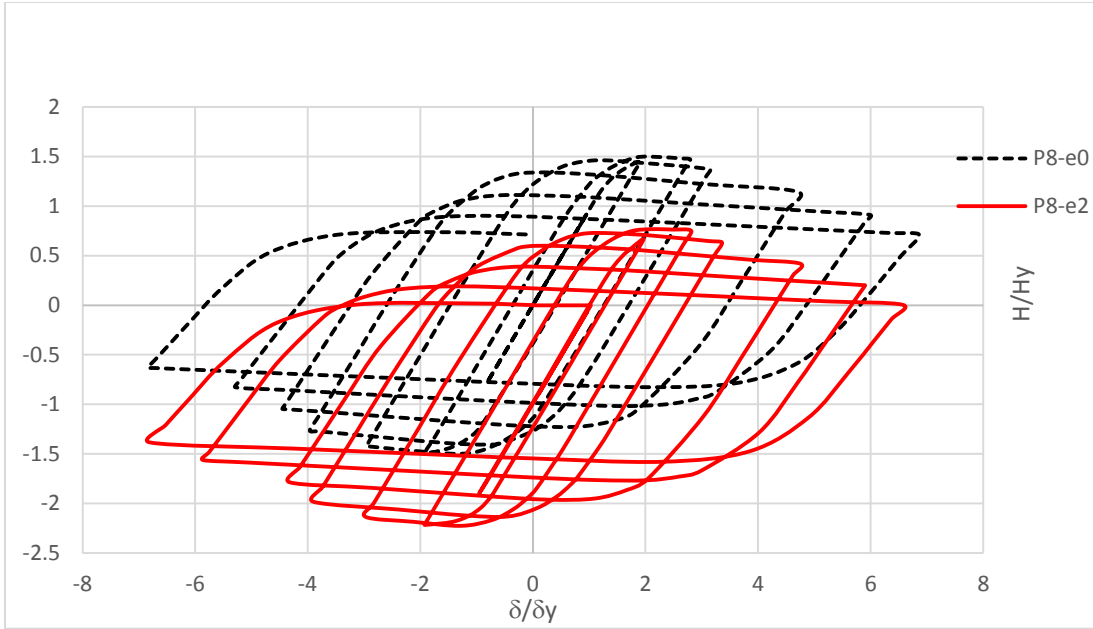
Figure 17. Model P8 and P8-e2 Comparison of Normalized Lateral Load Vs. Lateral Displacement of Centrally Concentric Load and Eccentrically Concentric Load.
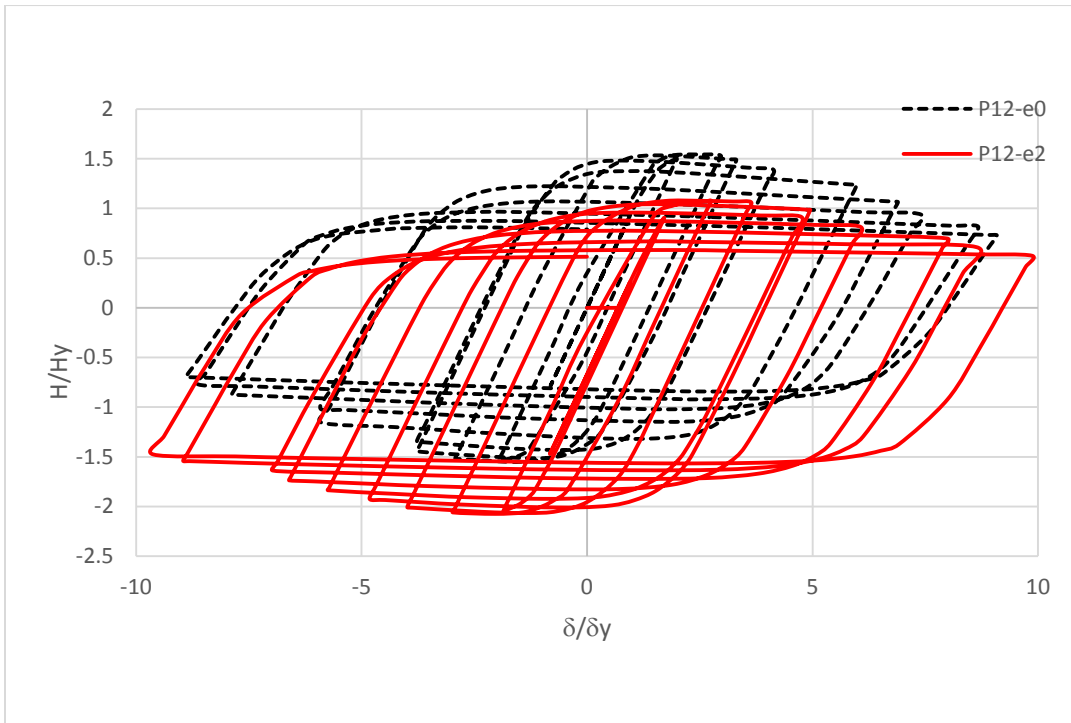
Figure 18. Model P12 and P12-e2 Comparison of Normalized Lateral Load Vs. Lateral Displacement of Centrally Concentric Load and Eccentrically Concentric Load.
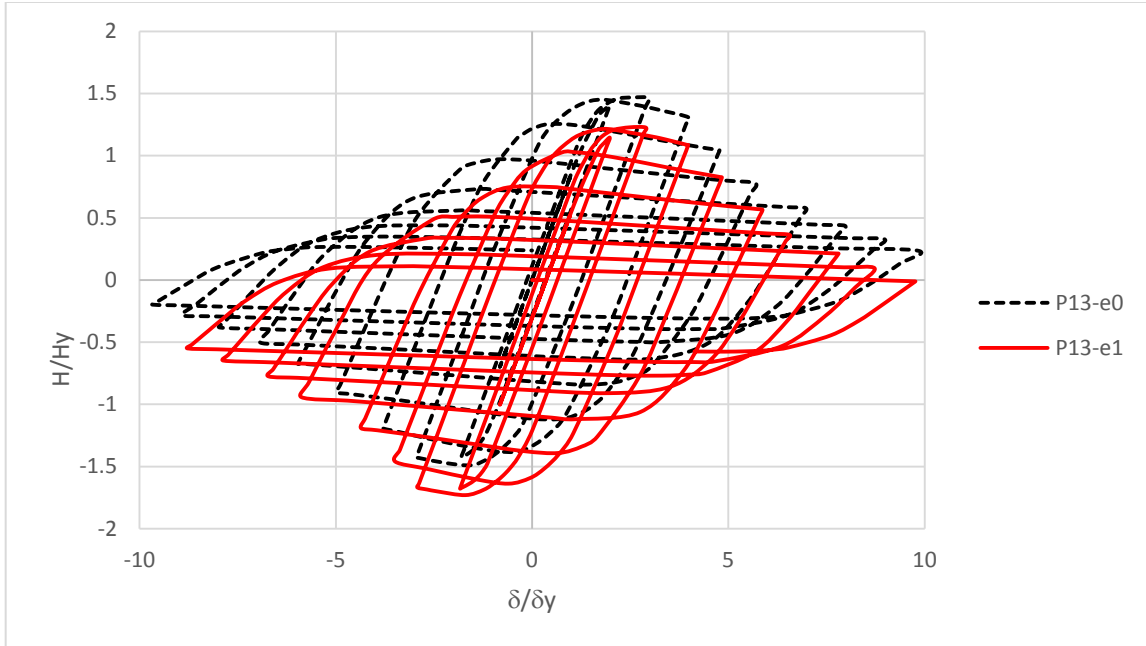
Figure 19. Model P13 and P13-e1 Comparison of Normalized Lateral Load Vs. Lateral Displacement of Centrally Concentric Load and Eccentrically Concentric Load.
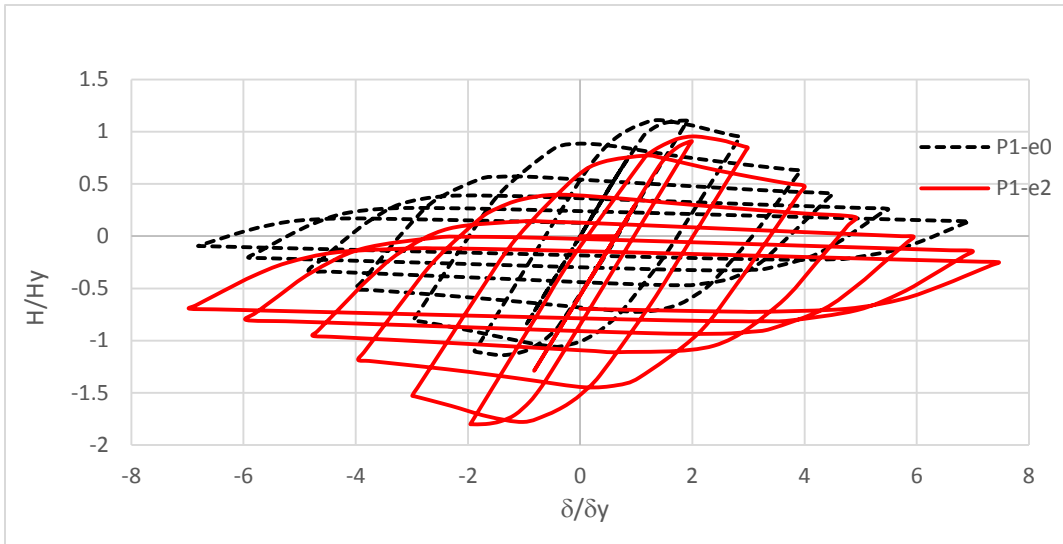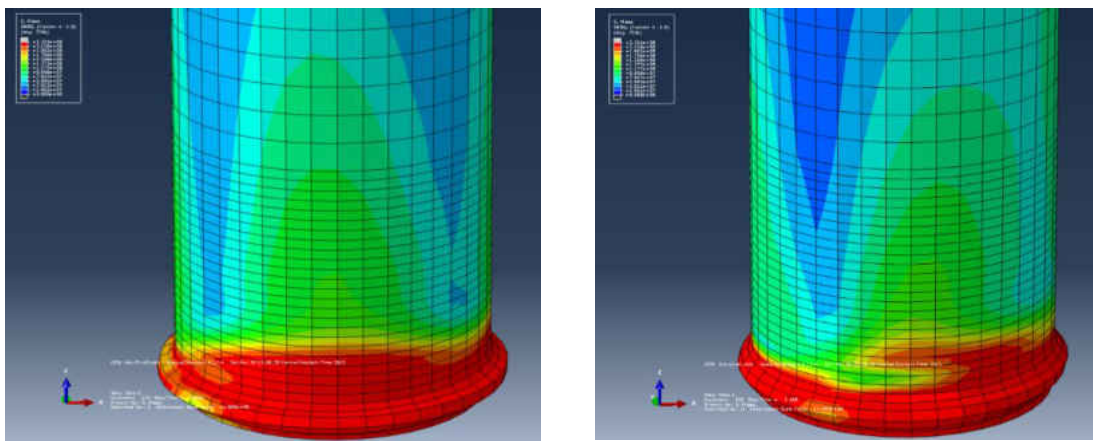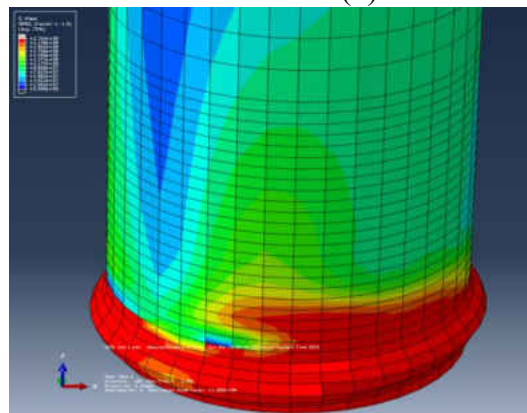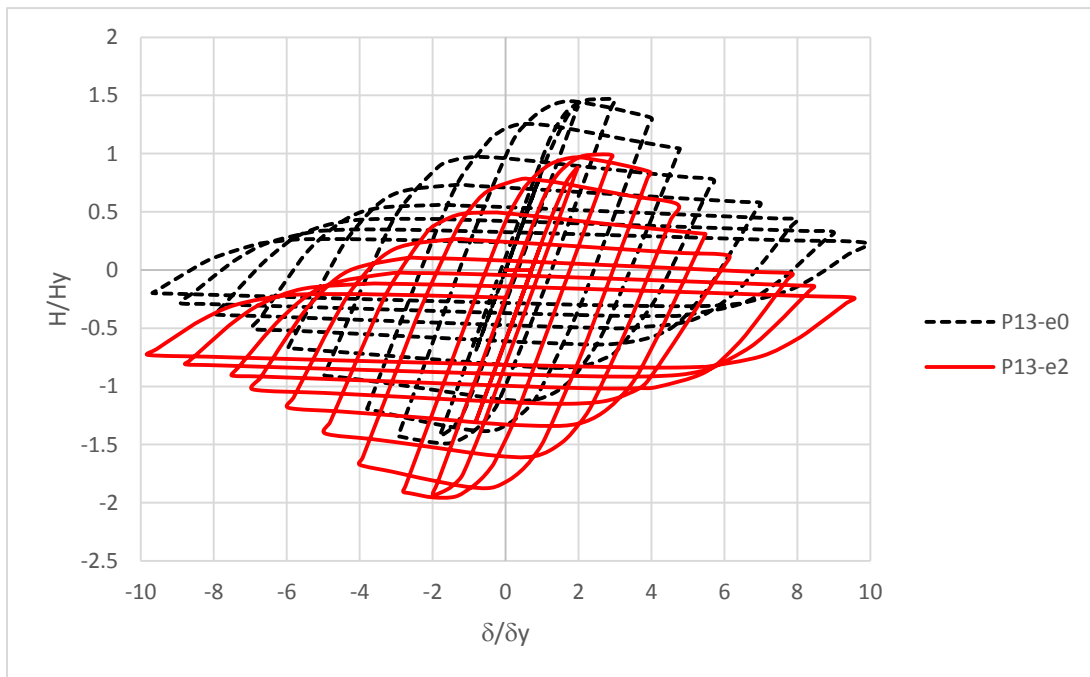

Figure 20. Model P13 and P13-e2 Comparison of Normalized Lateral Load Vs. Lateral Displacement of Centrally Concentric Load and Eccentrically Concentric Load.
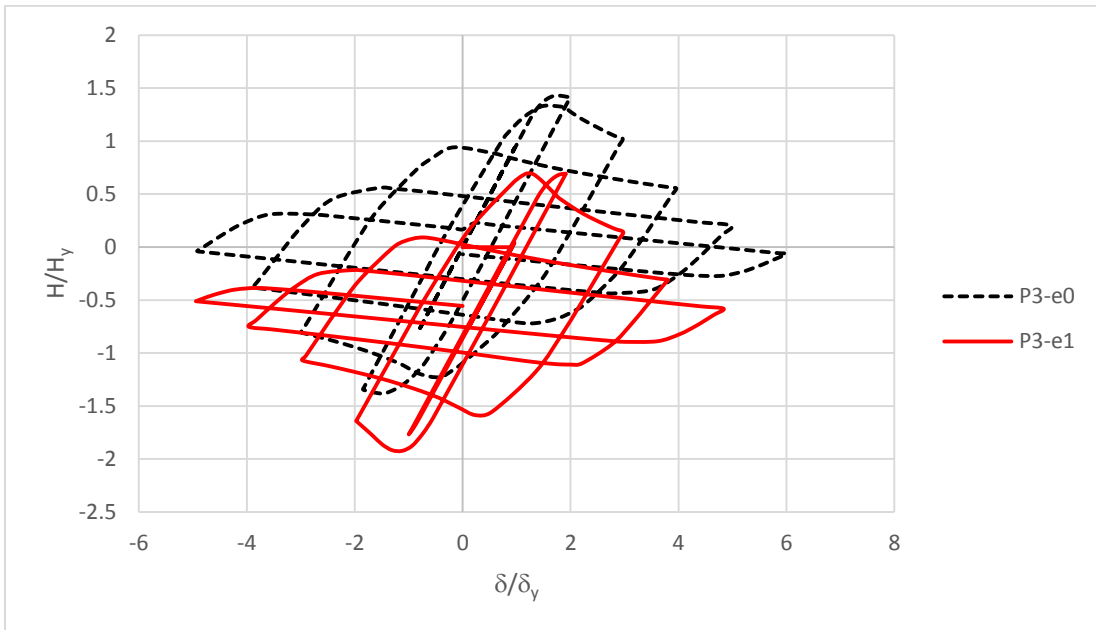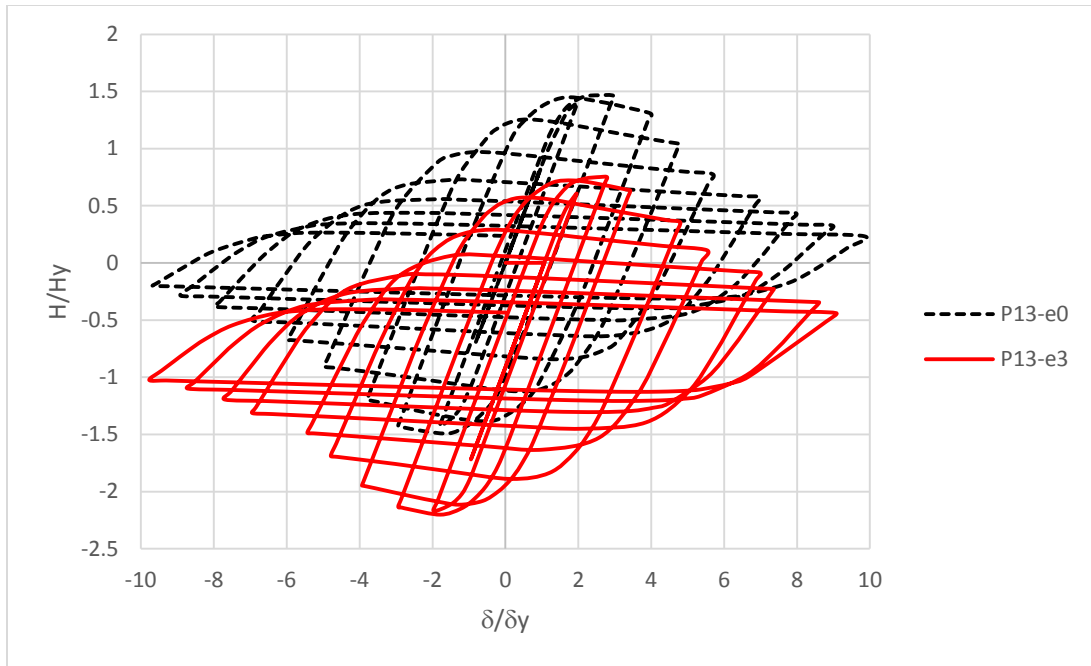
Figure 21. Model P13 and P13-e3 Comparison of Normalized Lateral Load Vs. Lateral Displacement of Centrally Concentric Load and Eccentrically Concentric Load.
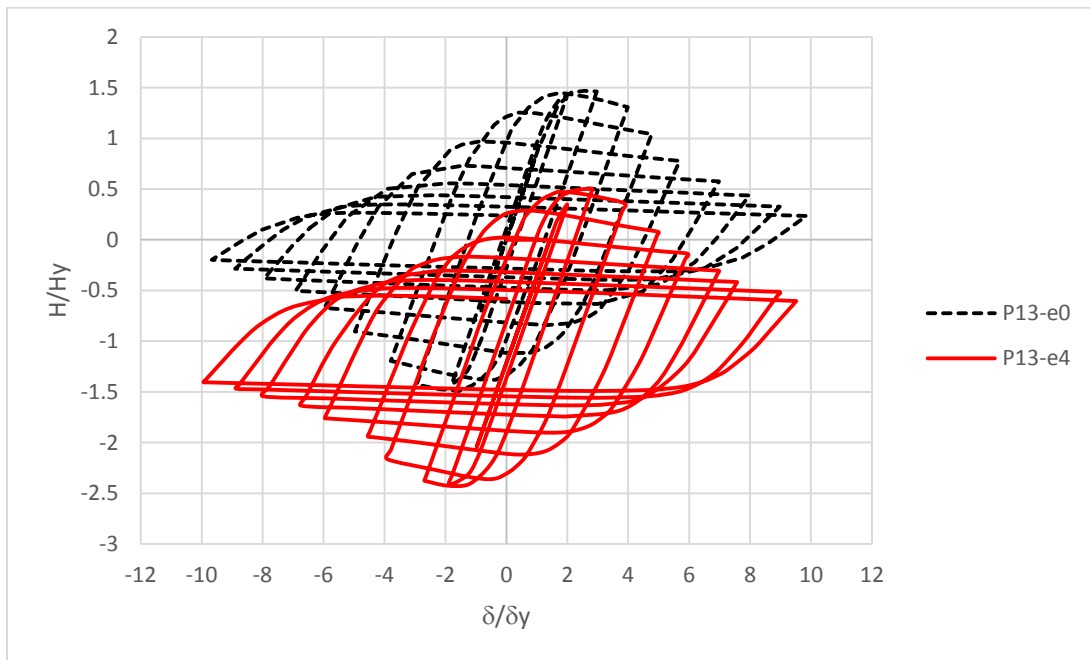
Figure 22. Model P13 and P13-e4 Comparison of Normalized Lateral Load Vs. Lateral Displacement of Centrally Concentric Load and Eccentrically Concentric Load.
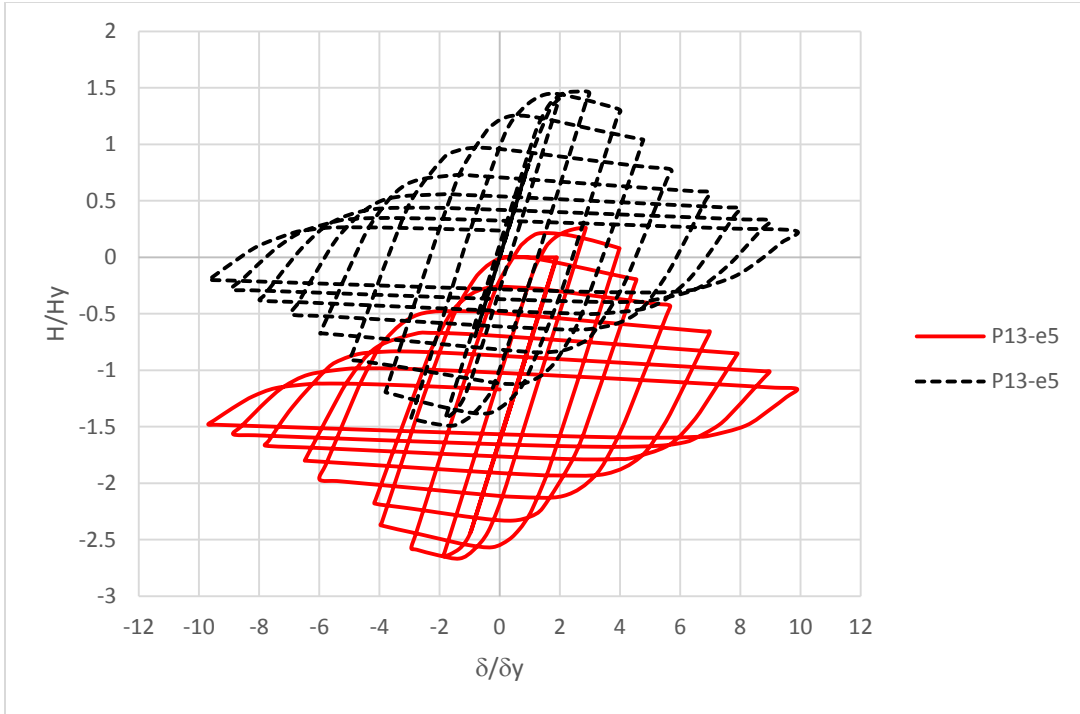
Figure 23. Model P13and P13-e5 Comparison of Normalized Lateral Load Vs. Lateral Displacement of Centrally Concentric Load and Eccentrically Concentric Load.
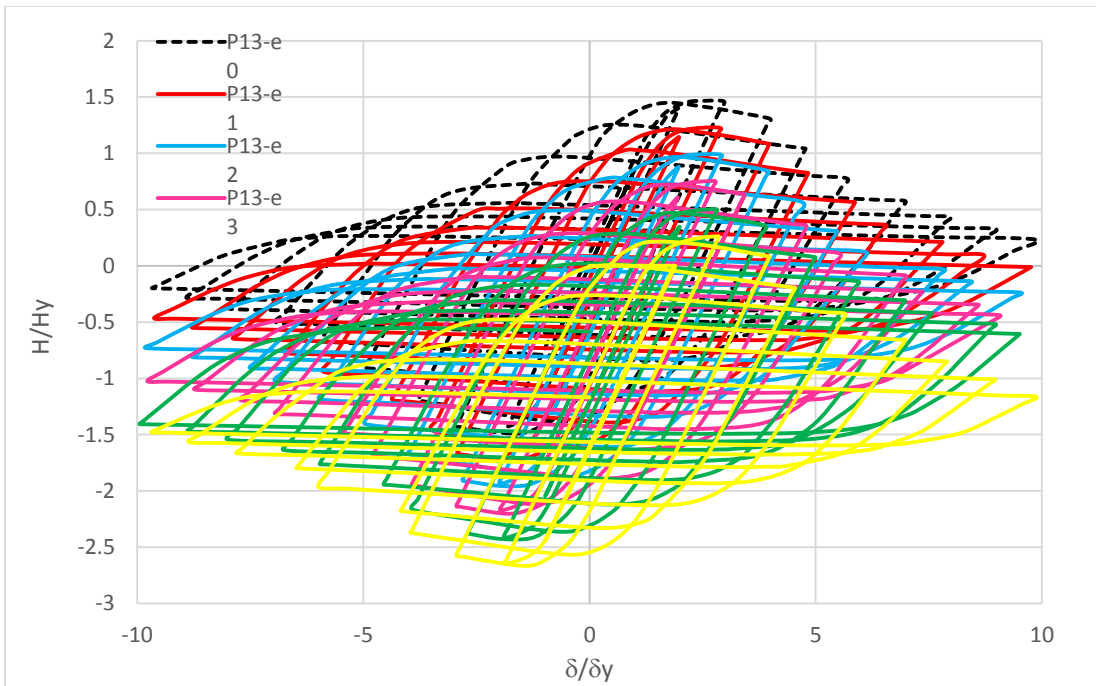
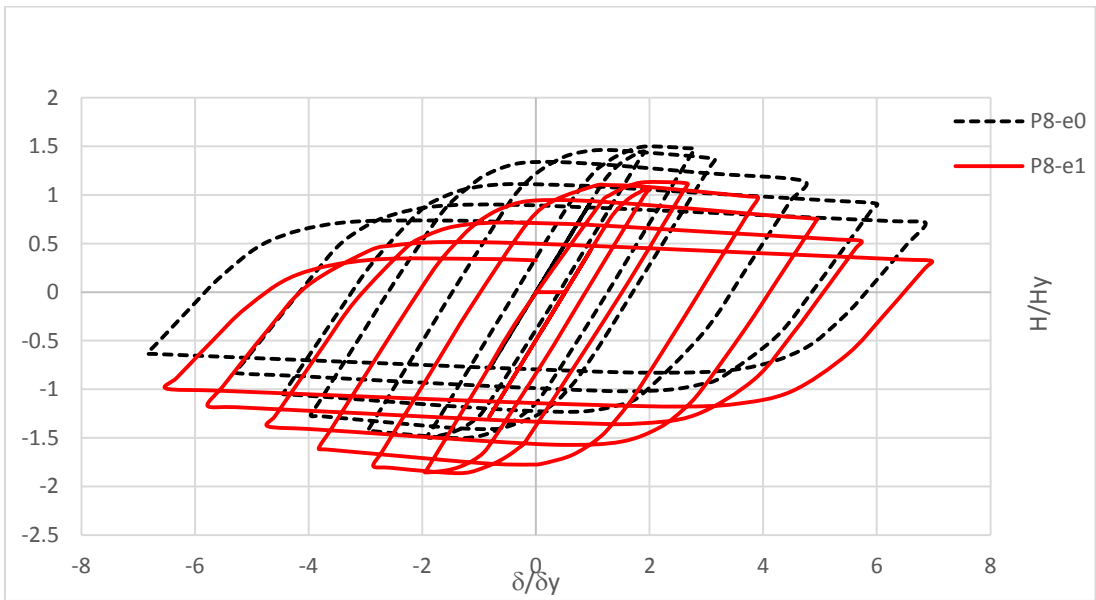
Figure 24. Model P13 toP13-e5 Comparison of Normalized Lateral Load Vs. Lateral Displacement of Centrally Concentric Load and Eccentrically Concentric Load.
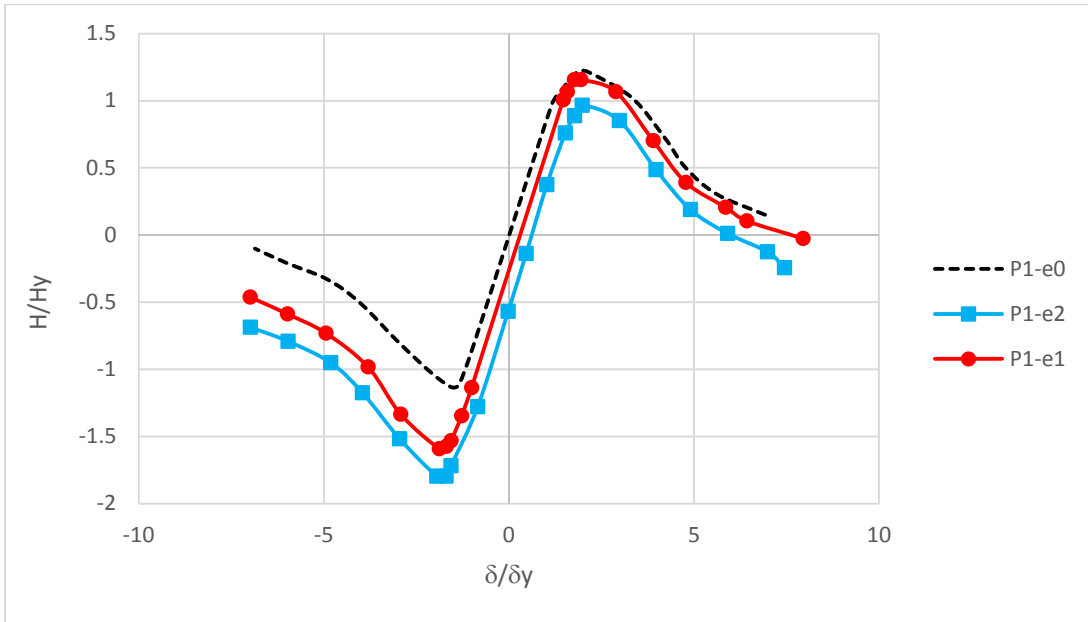
Figure 25. Model P1 Series Envelopment Curves of Horizontal Load Vs. Displacement Relation.
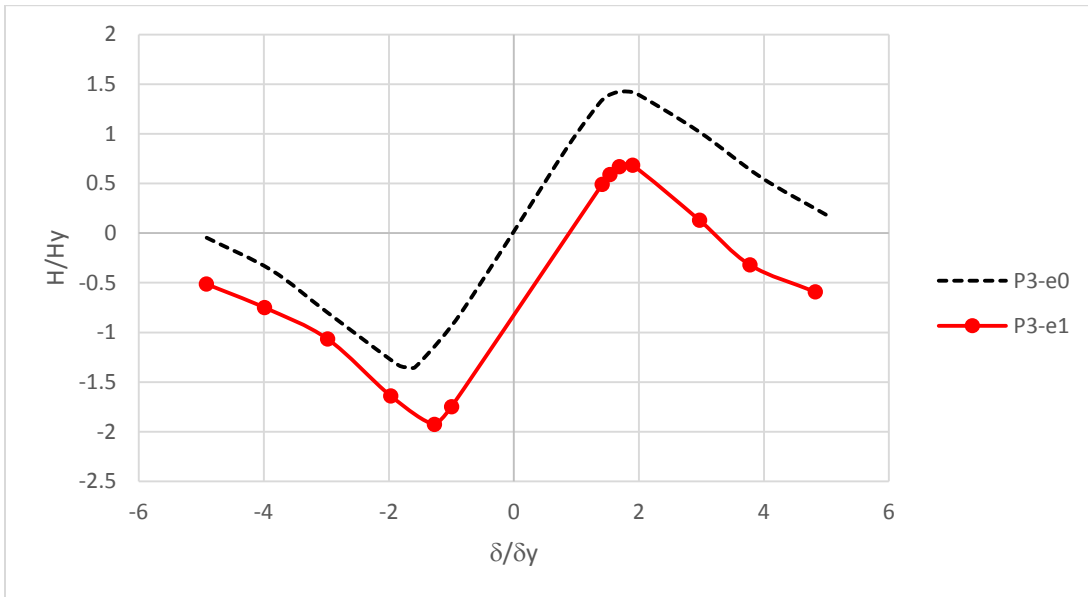
Figure 26. Model P3 Series Envelopment Curves of Horizontal Load Vs. Displacement Relation.

32
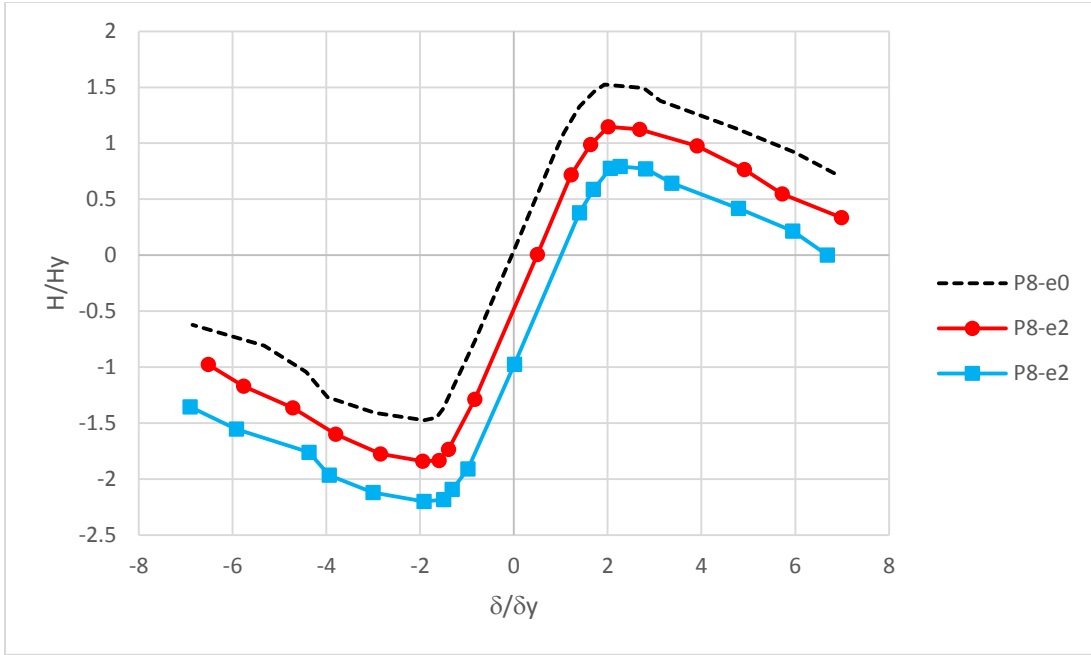
Figure 27. Model P8 Series Envelopment Curves of Horizontal Load Vs. Displacement Relation.
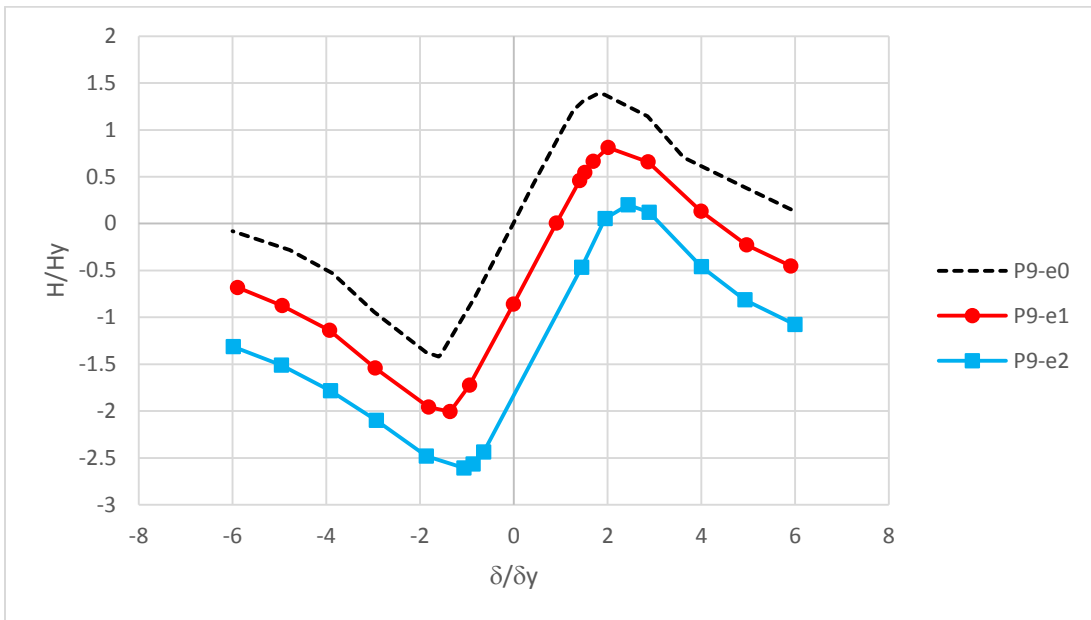
Figure 28. Model P9 Series Envelopment Curves of Horizontal Load Vs. Displacement Relation.
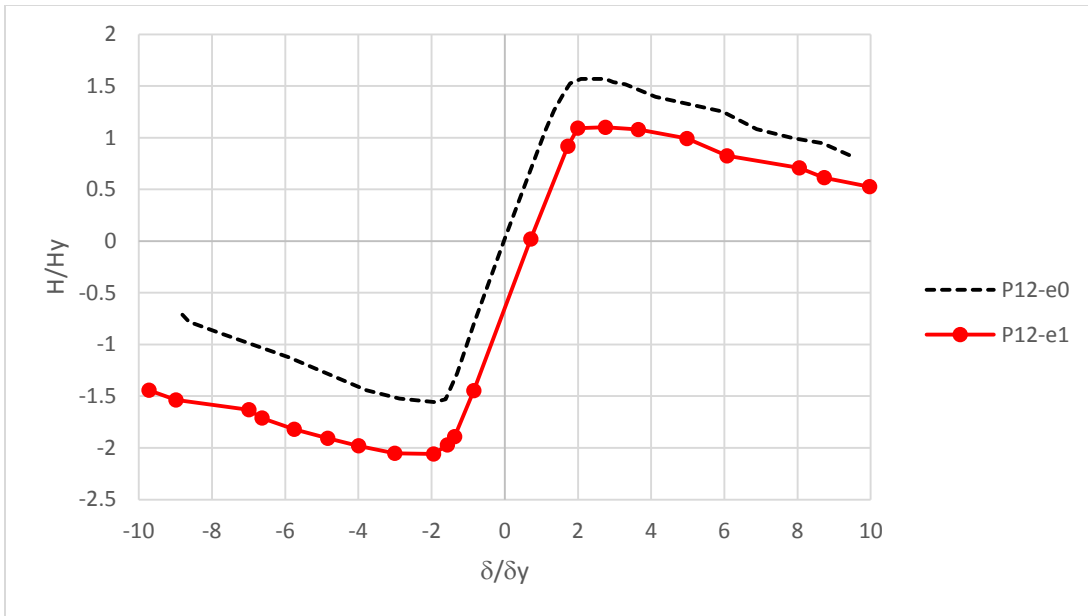
Figure 29. Model P12 Series Envelopment Curves of Horizontal Load Vs. Displacement Relation.
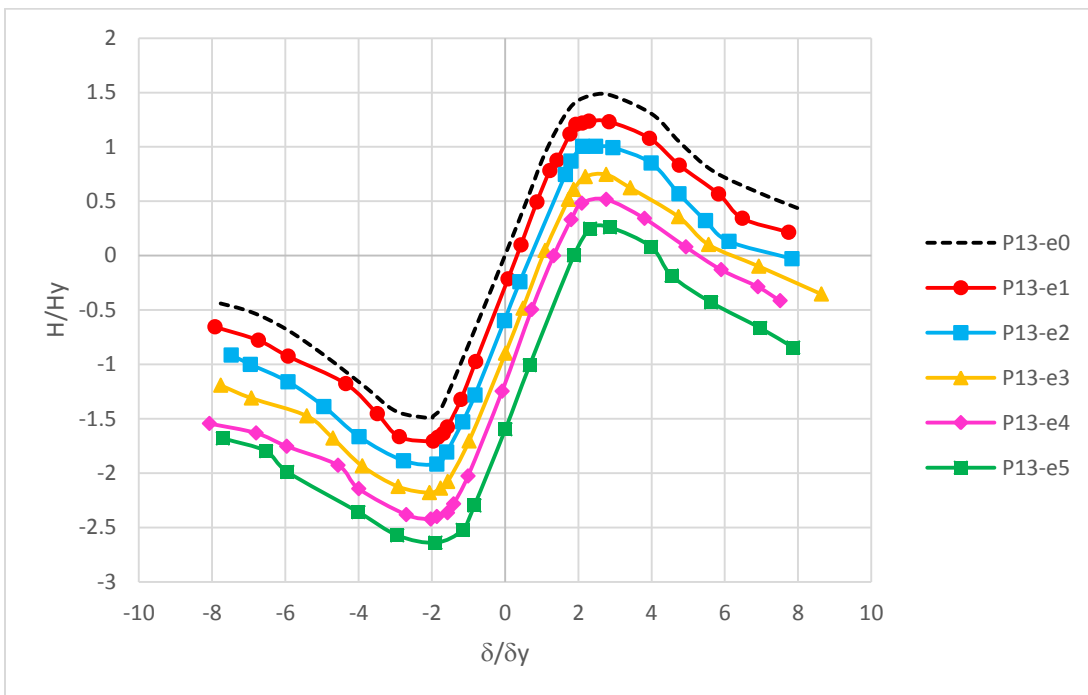
Figure 30. Model P13 Series Envelopment Curves of Horizontal Load Vs. Displacement Relation.
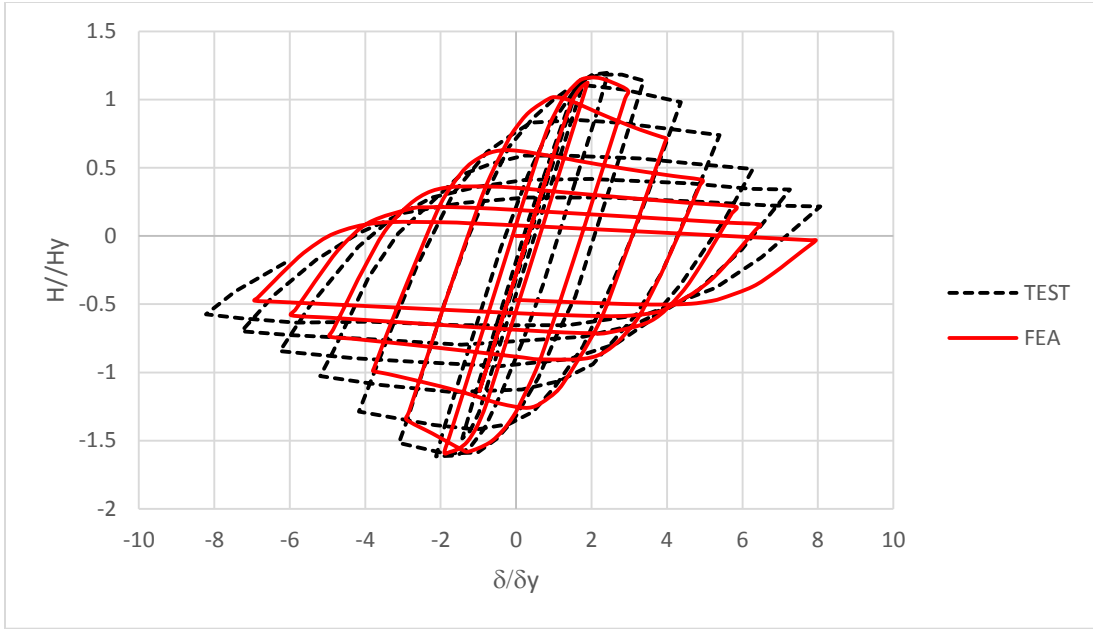
Figure 31. Comparison of Hysteresis Curves of Steel Circular Columns between FEA Analysis and Experimental P1-e1
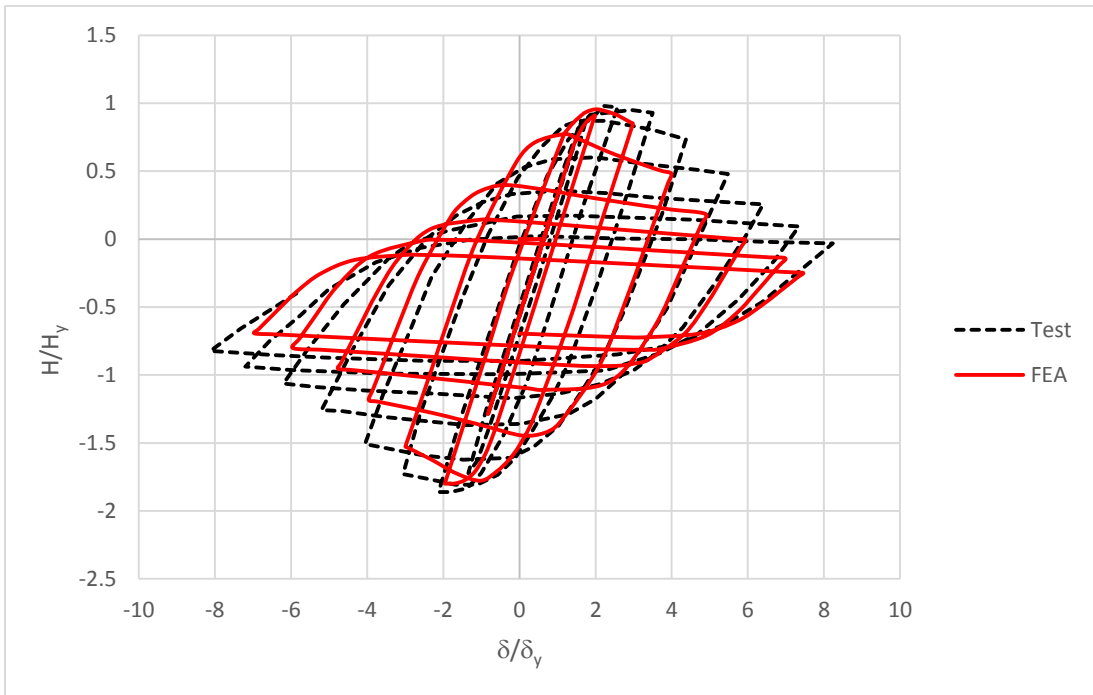
Figure 32. Comparison of Hysteresis Curves of Steel Circular Columns between FEA Analysis and Experimental P1-e2
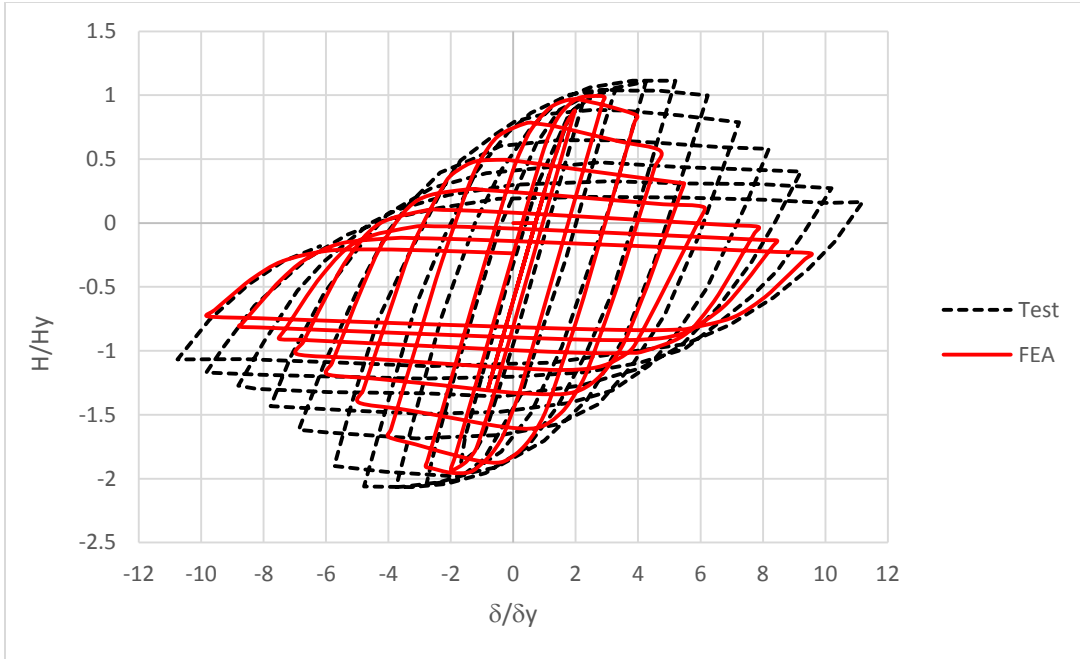
Figure 33. Comparison of Hysteresis Curves of Steel Circular Columns between FEA Analysis and Experimental P13-e2
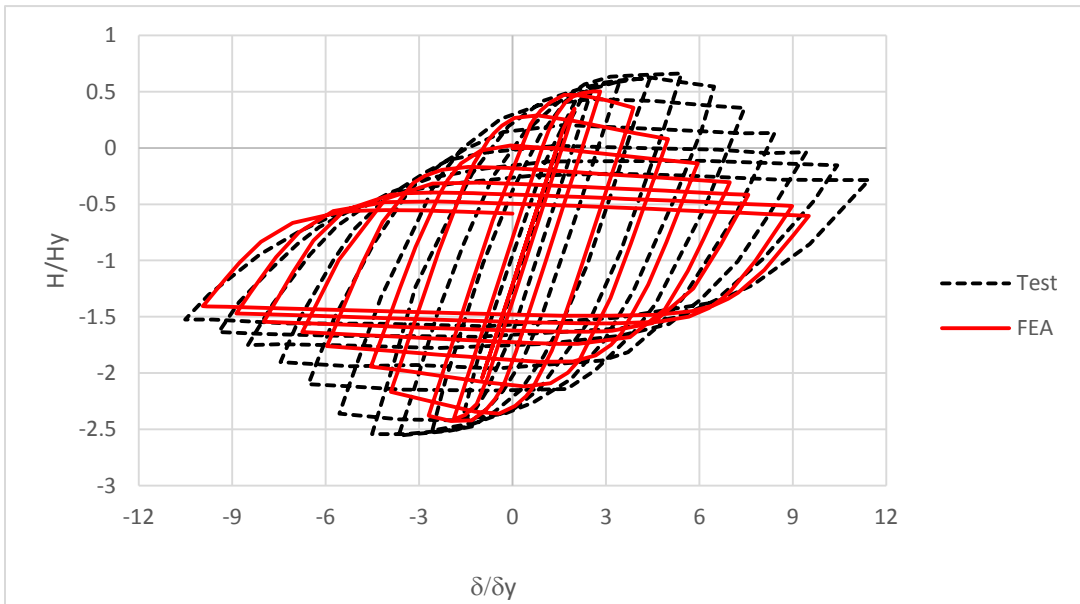
Figure 34. Comparison of Hysteresis Curves of Steel Circular Columns between FEA and Experimental P13-e4
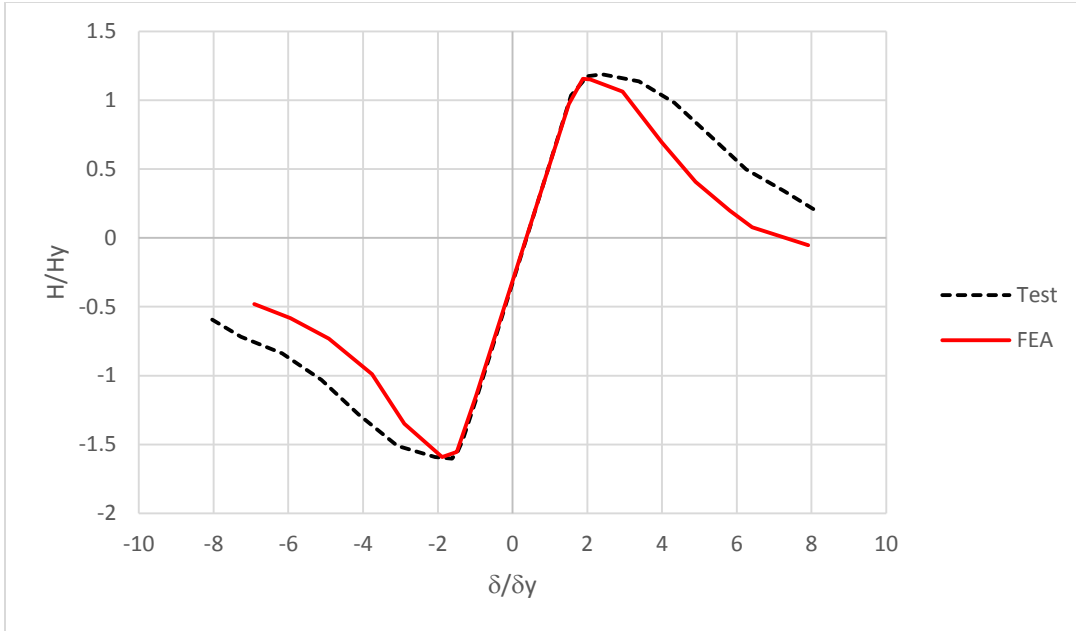
Figure 35. Comparison of Envelope Curves between Analysis and Experimental P1-e1
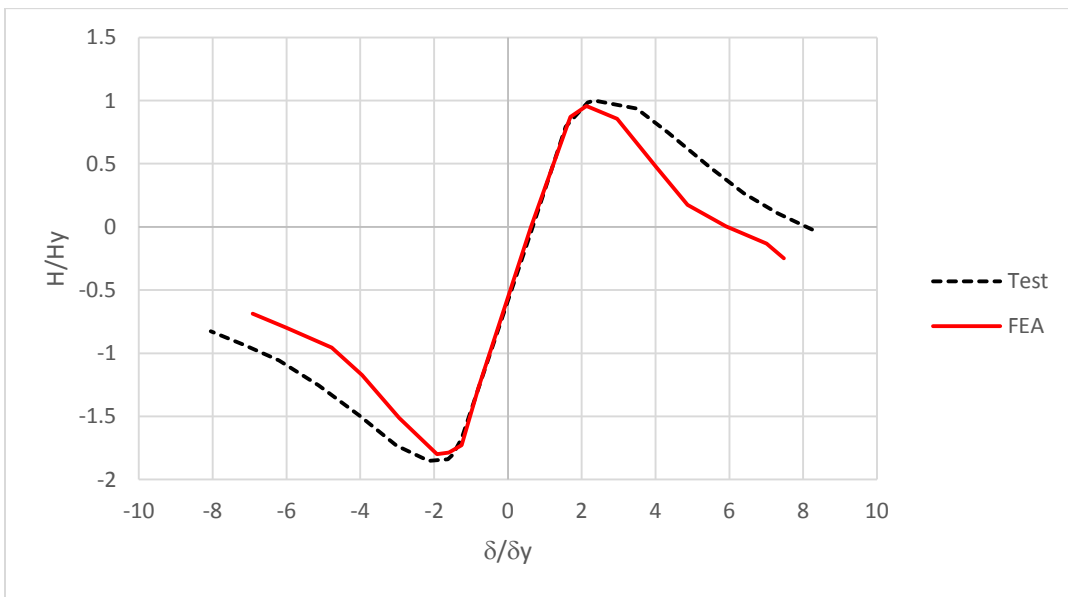
Figure 36. Comparison of Envelope Curves between FEA Analysis and Experimental, P1-e2
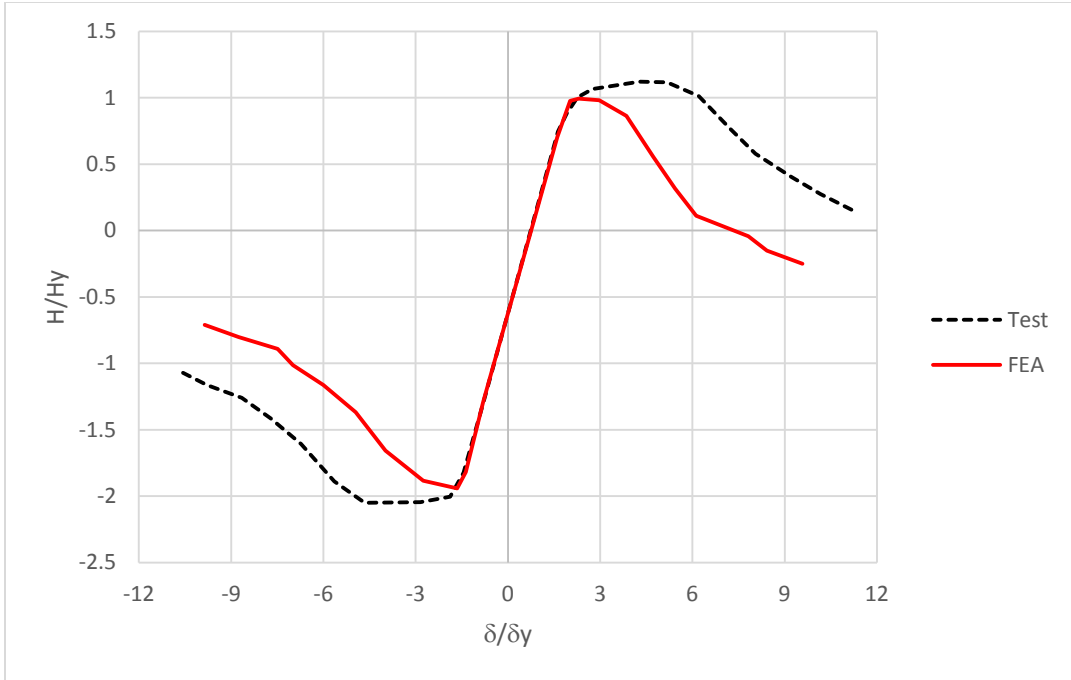
Figure 37. Comparison of Envelope Curves between FEA Analysis and Experimental
P13-e2
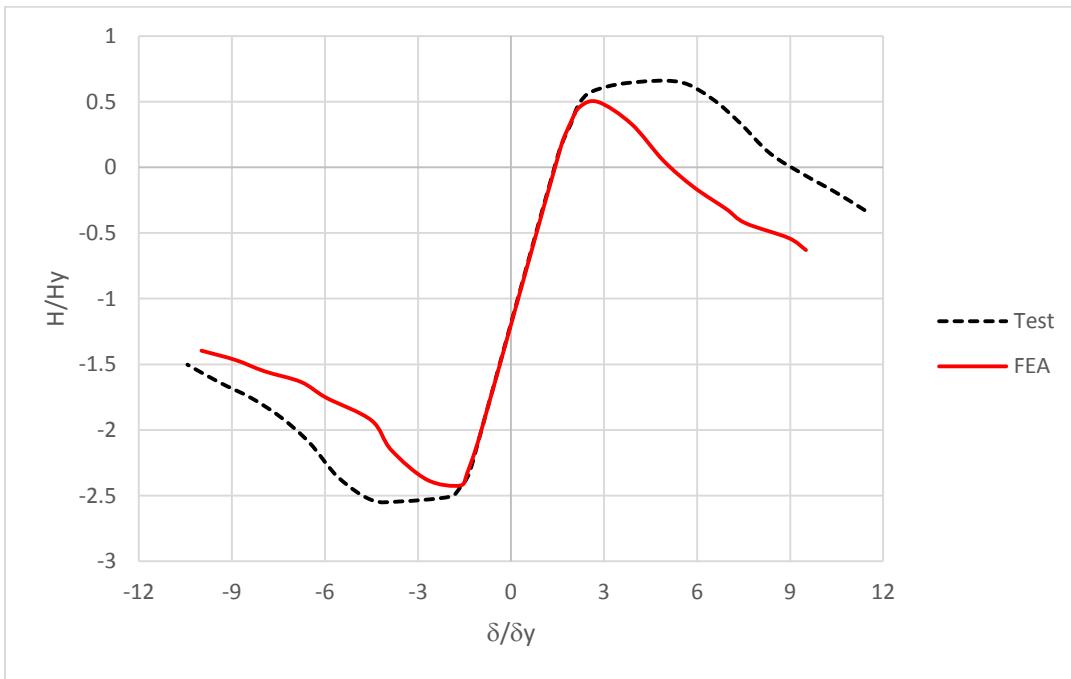
Figure 38. Comparison of Envelope Curves between FEA Analysis and Experimental
P13-e4

3.8 Conclusion

The study deals with the stability evaluation of thin-walled steel tubular columns exposed to cyclic elastoplastic in plane eccentric lateral loading. Thin-walled steel tubular columns used as bridge piers have found a variety of usage in highway bridge systems in constructional restricted urban areas, such as Japan and New York. Compared with concrete, steel tubular bridge piers are light and ductile, it can be applied in locations that heavy superstructures are unfavorable, such as bay areas, soft ground, and reclaimed land. Finite element analysis computer program, ABAQUS (2013) was used to run analysis the models that are exposed to centrally and eccentrically loads. The experimental results are obtained from (Gao et al., 2000b) and were used to validate the finite element analysis results.

Based on finite element analysis the followings are concluded:

- The load-carrying capacity of the eccentrically loaded columns in the eccentric side is significantly decreased with the increase in eccentric distance, whereas in the opposite side it is increased.

- When the eccentric distance e lies 0- $0.4h$ for pipe columns, the buckling modes of the eccentrically loaded columns are almost the same as those of the centrally loaded columns.

CHAPTER IV

ANALYSIS AND STABILITY EVALUATION OF THIN-WALLED STEEL TUBULAR BRIDGE PIERS SUBJECTED TO CYCLIC-OUT- PLANE ECCENTRIC   LOADING

4.1 Introduction

For generations, the main concern for the society of structural engineers is the effects of an earthquake on structure. Constantly structural engineers are designing structures with consideration of severe earthquakes. In Japan where earthquakes are very common, elevated highway bridge often use thin-wall steel columns composed of stiffened plate elements as piers. Thin-walled steel columns are advantageous because of their small cross-sectional areas and high earthquake resistance. It is crucial to predict their ultimate hysteretic behaviors accurately to make sure that the safety of the structures under major earthquakes (Japanese Road Association, 1996).

In chapter 3, the strength and ductility correlation between the centrally and eccentrically loaded columns, subjected to cyclic in-plane transverse (horizontal) loading, has been discussed. It was discovered that the ultimate strength on the eccentric side has been significantly reduced with the increase of eccentric distance, and the strength and ductility of the eccentrically loaded columns can be conveniently obtained from those of the centrally loaded columns (Gao et al., 2000b). In this chapter, an eccentrically loaded steel circular section column was exposed to cyclic out-of-plane transverse loading, in addition to a constant eccentric load, at the tip was considered. Bending moments in two

directions and increasing twisting moment with respect to axial direction were applied to the column. It becomes complex to find the column's relationship with the centrally loaded columns. The structural stiffness with respect to the out-of-plane direction has been greatly enriched by the bridge decks. The eccentrically loaded bridge piers are probably damaged by the combination of the bending and twisting moments during a severe earthquake event (Gao et al., 2000b). The out-of-plane bending moment, M_1, mainly controls the hysteretic behavior of the column since the in-plane bending moment, M_o, and the twisting moment, T, are relatively small compared to the value of M_1. The expressions of M_1, M_o, and T are as follows:

$$M_o = P*e;$$

$$M_1 = H*h;$$

$$T = H*e$$

(9)

Where P = vertical load; e = eccentric distance; H = transverse load in the out-of-plane direction; and h = column height. The eccentric distance, e, is taken to range from *0.1h to 0.4h* based on the result of a practical investigation on the eccentric distance.

The inelastic seismic behaviors of thin-walled steel columns are affected by the cyclic metal plasticity as well as the local buckling behavior of individual plate elements and eccentric load. Various numerical techniques have been developed to improve the accuracy of the geometrical nonlinear analysis, which takes into account the local buckling of plated structures. Over the years, many reliable numerical methods have been available in commercial general purpose finite element analysis programs (Goto et al., 1998). This study focused on using the finite element analysis program, ABAQUS

(2013), to accurately model and predict the behavior of steel bridge piers subjected to cyclic loading. To demonstrate the validity of the analysis, I analyzed the numerical method presented by Ge et al. (2000). Total of 21 columns were analyzed to obtain the hysteretic behavior of the centrally and eccentrically loaded columns for comparison. It was found that the ultimate strength and ductility formulas of the centrally loaded columns can be used for the eccentrically loaded columns subjected to cyclic out-of-plane loading by introducing a modification coefficient for the initial structural stiffness.

4.2 Numerical Analytical Method

4.2.1 Analytical Model

All columns were modelled considering twisting moment. Buckling deformation of the out-of-plane will controlled by bending moment because of its larger influence compare to in-plane and twisting moments. Numerical studies on the cyclic behavior of thin-walled steel tubular columns were conducted using the computer program ABAQUS (2013). A total of twenty one hollow circular columns were analyzed. Table 4 lists the specific geometrical parameters of each models.

Numerical studies on the cyclic behavior of thin-walled steel tubular columns are carried out using the computer program ABAQUS (2013). Figure 39 shows the analytical model of an eccentrically and centrally loaded columns conducted. An eccentric load P is now treated as a combination of a concentric load, P and a bending moment, M_0. In addition to bending moment, M_1 a twisting moment, T was also introduced due to transverse out-of-plane load, H. The results from the finite element analysis were compared with the proposed results obtained by (Gao et al., 2000b). The experimented data was used to

validate the accuracy of the cyclic elastoplastic large displacement finite element analysis procedure used in ABAQUS (2013). Table 4 lists the geometrical parameters for the twenty one specimens used in this study. Here, R_t = radius-thickness ratio of cross section; λ= column slenderness ratio; h = column height; D = diameter of pipe section; t = plate thickness; and e=eccentric distance. In this study, the eccentric distance, e, is assumed to be range from *0 to 0.4h*. In the case of e = 0 refers to the centrally loaded column. The axial force, P, is taken as $0.15P_y$ (P_y = squash load) for all the columns (Gao et al., 2000b).

Table 4: Geometrical Properties of Analyzed Columns

Model	h [m]	D [m]	t [m]	A [m^2]	R_t	λ	e/h
P5-e0	4.391	0.891	0.008412	0.02332	0.1000	0.30	0.0
P5-e1	4.391	0.891	0.008412	0.02332	0.1000	0.30	0.1
P5-e2	4.391	0.891	0.008412	0.02332	0.1000	0.30	0.2
P8-e0	4.391	0.891	0.011217	0.03100	0.0750	0.30	0.0
P8-e1	4.391	0.891	0.011217	0.03100	0.0750	0.30	0.1
P8-e2	4.391	0.891	0.011217	0.03100	0.0750	0.30	0.2
P9-e0	7.319	0.891	0.011217	0.03100	0.0750	0.50	0.0
P9-e1	7.319	0.891	0.011217	0.03100	0.0750	0.50	0.1
P12-e0	4.391	0.891	0.016825	0.04621	0.0050	0.30	0.0
P12-e1	4.391	0.891	0.016825	0.04621	0.0050	0.30	0.1
P12-e2	4.391	0.891	0.016825	0.04621	0.0050	0.30	0.2
P13-e0	2.927	0.891	0.011217	0.03100	0.0750	0.20	0.0
P13-e2	2.927	0.891	0.011217	0.03100	0.0750	0.20	0.1
P13-e2	2.927	0.891	0.011217	0.03100	0.0750	0.20	0.2
P13-e3	2.927	0.891	0.011217	0.03100	0.0750	0.20	0.3
P13-e4	2.927	0.891	0.011217	0.03100	0.0750	0.20	0.4
P14-e0	2.927	0.891	0.008412	0.02332	0.1000	0.20	0.0
P14-e1	2.927	0.891	0.008412	0.02332	0.1000	0.20	0.1
P14-e2	2.927	0.891	0.008412	0.02332	0.1000	0.20	0.2
P15-e0	2.927	0.891	0.016825	0.04621	0.0500	0.20	0.0
P15-e1	2.927	0.891	0.016825	0.04621	0.0500	0.20	0.1
P15-e2	2.927	0.891	0.016825	0.04621	0.0500	0.20	0.2
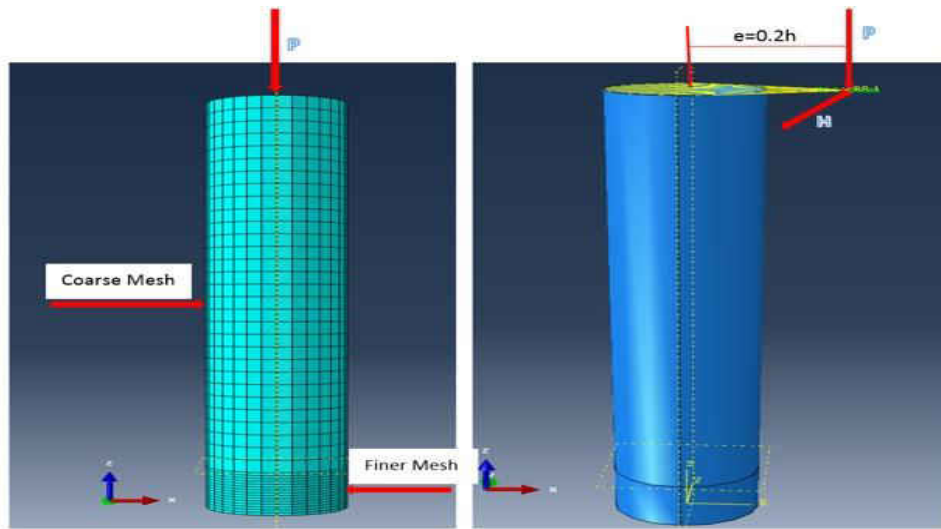
(a) Centerally Loaded Column   (b)   Eccentrically Out-of-Plane Loaded Column

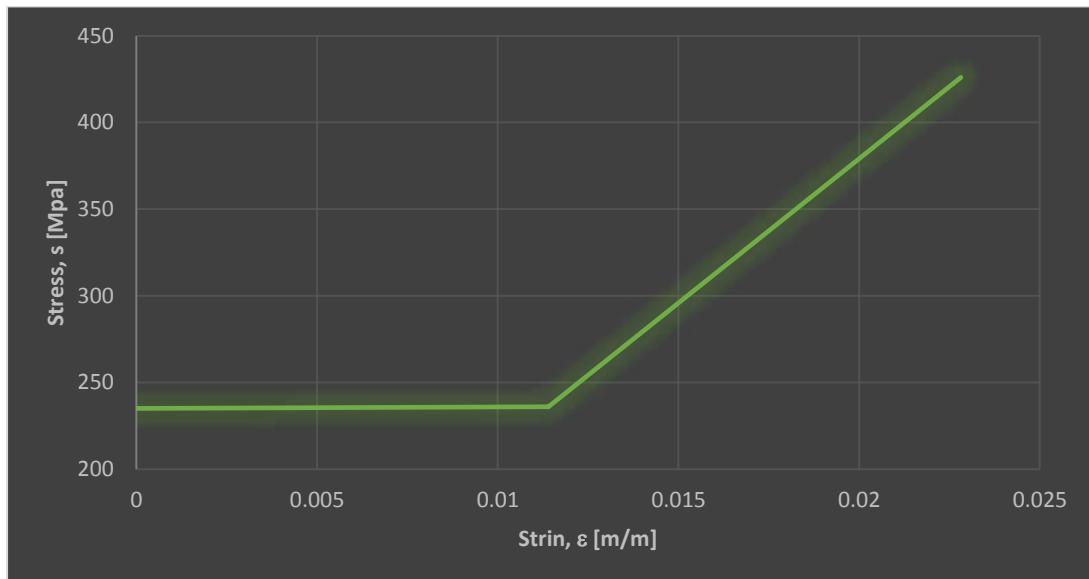Figure 39. Numerical Analytical Model.

Figure 40: Model Stress-Strain Curve.

4.2.2 Finite Element Analysis

Several numerical methods have been developed to improve the accuracy of geometrical

nonlinear analysis that takes into account the local buckling. The finite element analysis

program which was used to assess the hysteretic ultimate behavior of the thin-walled

steel piers was ABAQUS (2013). The analysis results are compared with the proposed results to validate the finite element analysis. The input geometrical and material properties are listed in Tables 4 and 5. Each model was created using SHELL 281 elements having the specified properties that is used in the experimental model. For thin-walled steel columns, local buckling usually occurs near the base of the columns. Therefore, a coarse mesh discretization was implemented for the upper part of the column; while a finer mesh discretization was implemented for the lower part of the column to consider the effect of local buckling. The fine mesh discretization was used to a height equal to the radius, r, of the model from the base of the column. The finite element modeling of the tubular columns and mesh discretization is shown in Figure 34 (a). The plasticity spread is considered both through the thickness and in the plane of the elements. The shell element employed is a four-node doubly curved shell element (S4R) in which there is only one sample point, but five layers were assumed across the thickness. These element types can account for the effect of transverse shear deformation. Initial geometrical imperfections and residual stresses were neglected in this analysis (Shen et al., 1995).

It also should be noted that the steel pier models are moderately thin. The bending moment force is more dominant to the cyclic behavior of the piers than the vertical compressive force. Therefore, the effects of the initial imperfections on the present pier models are less significant than those on the extremely thin columns under purely compressive loads. Finally, the large amplitudes of alternating loads will also reduce the effect of initial imperfections (Goto et al., 1998).

Table 5: Material properties of Analyzed Columns

Model	E [Gpa]	σ_y [Mpa]	σ_u [Mpa]	υ [m/m]	ε_y	ε_{st}	$\varepsilon_{st}/\varepsilon_y$	ε_u
P5-e0	206	235	426	0.3	0.001141	0.011408	10	0.020534
P5-e1	206	235	426	0.3	0.001141	0.011408	10	0.020534
P5-e2	206	235	426	0.3	0.001141	0.011408	10	0.020534
P8-e0	206	235	426	0.3	0.001141	0.011408	10	0.020534
P8-e1	206	235	426	0.3	0.001141	0.011408	10	0.020534
P8-e2	206	235	426	0.3	0.001141	0.011408	10	0.020534
P9-e0	206	235	426	0.3	0.001141	0.011408	10	0.020534
P9-e1	206	235	426	0.3	0.001141	0.011408	10	0.020534
P12-e0	206	235	426	0.3	0.001141	0.011408	10	0.020534
P12-e1	206	235	426	0.3	0.001141	0.011408	10	0.020534
P12-e2	206	235	426	0.3	0.001141	0.011408	10	0.020534
P13-e1	206	235	426	0.3	0.001141	0.011408	10	0.020534
P13-e2	206	235	426	0.3	0.001141	0.011408	10	0.020534
P13-e3	206	235	426	0.3	0.001141	0.011408	10	0.020534
P13-e4	206	235	426	0.3	0.001141	0.011408	10	0.020534
P14-e0	206	235	426	0.3	0.001141	0.011408	10	0.020534
P14-e1	206	235	426	0.3	0.001141	0.011408	10	0.020534
P14-e2	206	235	426	0.3	0.001141	0.011408	10	0.020534
P15-e0	206	235	426	0.3	0.001141	0.011408	10	0.020534
P15-e1	206	235	426	0.3	0.001141	0.011408	10	0.020534
P15-e2	206	235	426	0.3	0.001141	0.011408	10	0.020534

4.3 Loading Program

All models were subjected to a specific central/eccentrical out-of-pane loading pattern at the top of the column controlled by displacement. Figure 41 shows the specific cyclic loading program for P13. In the model, the specified alternating horizontal load under displacement control was squash, load applied to the top of the model with a constant compressive force, *P,* illustrated in Figure 1, where δ_y is the horizontal displacement of the loading point when the model begins to yield. δ_y is calculated here by the Equation:

$$\delta_y = \frac{H_y h^3}{3EI} \qquad\qquad (13)$$

Where H_y represents the horizontal force corresponding to, h = the column height, EI = the bending rigidity. Table 4 lists the loading parameters for each respective models.
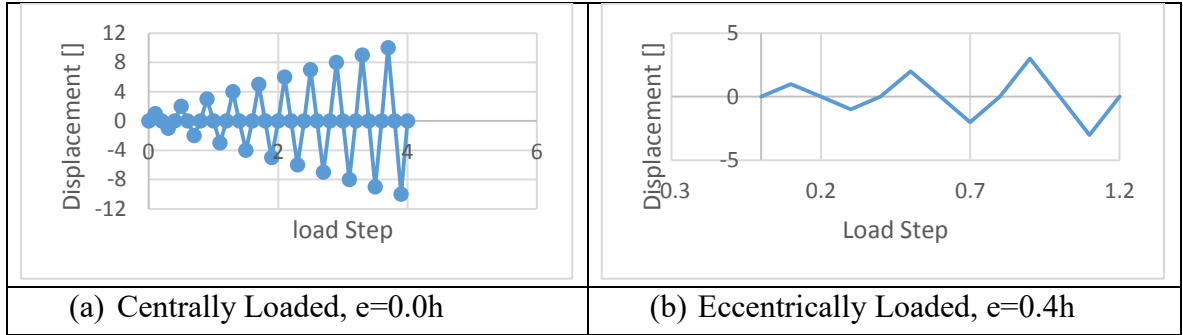
(a) Centrally Loaded, e=0.0h	(b) Eccentrically Loaded, e=0.4h

Figure 41: Model P13 Loading Programs.

Table 6: Models Loading Parameters.

Model	$\alpha = P/P_y$	P_y [KN]	P [KN]	H_y [KN]	δ_y[m]	β
P5-e0	0.15	5481	822	232	0.0140	1.000
P5-e1	0.15	5481	822	232	0.0140	1.039
P5-e2	0.15	5481	822	232	0.0140	1.156
P8-e0	0.15	7286	1093	306	0.0140	0.000
P8-e1	0.15	7286	1093	306	0.0140	1.039
P8-e2	0.15	7286	1093	306	0.0140	1.156
P9-e0	0.15	7286	1093	184	0.0389	0.000
P9-e1	0.15	7286	1093	184	0.0389	1.039
P12-e0	0.15	10859	1629	451	0.0140	0.000
P12-e1	0.15	10859	1629	451	0.0140	1.039
P12-e2	0.15	10859	1629	451	0.0140	1.156
P13-e0	0.15	7286	1093	460	0.0062	0.000
P13-e2	0.15	7286	1093	460	0.0062	1.039
P13-e2	0.15	7286	1093	460	0.0062	1.156
P13-e3	0.15	7286	1093	460	0.0062	1.351
P13-e4	0.15	7286	1093	460	0.0062	1.624
P14-e0	0.15	5481	822	348	0.0062	0.000
P14-e1	0.15	5481	822	348	0.0062	1.039
P14-e2	0.15	5481	822	348	0.0062	1.156
P15-e0	0.15	10859	1629	676	0.0062	0.000
P15-e1	0.15	10859	1629	676	0.0062	1.039
P15-e2	0.15	10859	1629	676	0.0062	1.156

4.4 Results

A series of numerical analyses were conducted to investigate the effect of the main parameters on the hysteretic behavior of the eccentrically loaded columns. The geometrical parameters of the analyzed columns are given in Table 4. The axial load, P, was kept constant as $0.15Py$ and applied at a point with a distance e from the centroid of the column section. The same size section was also centrically loaded by $0.15P_y$. Here, P_y stands for squash load. In this presentation, JIS SS400 mild steel (equivalent to ASTM A36) was employed. Here, eccentric distance, e was taken from $0.1h$ to $0.4h$ with the material properties as listed yield stress $\sigma y = 235$ MPa; ultimate tensile stress $\sigma u = 426$ MPa; initial strain hardening modulus $E_{st} = E/40$; Young's modulus $E = 206$ GPa; strain at the onset of strain hardening, $\varepsilon_{st} = 10\varepsilon_y$; yield strain, $\varepsilon_y = 0.114\%$; and Poisson's ratio n $= 0.3$. To compare the analytical results with those of the centrically loaded columns, the stepwise increased displacement, $\pm 1\delta y$, $\pm 2\delta y$, . . . ,was applied till it failed to the free end of the cantilever model. Here, δy is the yield displacement of the corresponding centrically loaded column without including the effect of the transverse shear deformation (Gao et al., 2000b).

The finite element analysis results were produced for each model using ABAQUS (2013). The results were then compared to proposed data presented by (Gao et al., 2000) to validate the analysis. For comparison finite element analysis and proposed results of normalized lateral load (H/H_y) versus normalized lateral displacement (δ/δ_y) hysteretic curves in the out-of-plane direction were plotted for P5-e1, P5-e2, P13-e2, and P13-e4 models. For comparison, the result of a corresponding centrically loaded column is also

plotted for all models. Also, the deformation pattern and stress distribution was compared for P13 series models.

From the hysteresis diagrams, it is noted that the initial structural stiffness of the eccentrically loaded column decreases with the increase in eccentric distance mainly because of the twisting moment. A modification coefficient was derived to match the initial structural stiffness of the eccentrically loaded column with that of the centrally loaded column. According to the elastic theory, the transverse displacement, δ_e, and the transverse load, H_e, of the eccentrically loaded columns in the out-of-plane direction can be expressed as:

$$\delta_e = \frac{H_e h^3}{3EI} + \frac{T.h*e}{GI_p} \tag{14}$$

Where $G = \dfrac{E}{[2(1+v)]}$ =shear modulus, Ip = polar moment of inertia

$\dfrac{H_e h^3}{3EI}$ = bending deformation; $\dfrac{T.h*e}{GI_p}$ = twisting deformation

In the case of thin-walled pipe section column it can be written as follows

$$\delta_e = \frac{H_e h^3}{3EI}\left[1 + 3(1+v)\left(\frac{e}{h}\right)^2\right] = \frac{\beta H_e h^3}{3EI} \tag{15}$$

Where $\quad \beta = \left[1 + 3(1+v)\left(\frac{e}{h}\right)^2\right]$ $\tag{10}$

Centrally loaded column, the transverse displacement, δ_c is as follows:

$$\delta_c = \frac{H_c h^3}{3EI} \tag{17}$$

Transverse load correlation between centrally and eccentrically loaded columns can be obtained when δc and δe.

$$H_e = \frac{H_c}{\beta} \tag{18}$$

If given displacement δ, point P_1 will be transferred to point P_2 after H_e multiplied by β. Then, the initial structural stiffness of the eccentrically loaded columns was modified to match that of the centrally loaded columns. Figures 75-81 illustrates comparisons of computed envelope curves by using $\beta H/H_y$ for all models.

Comparison between experimental and analyzed models envelope curves were also plotted in Figures 82-90. From the analysis, the following observations can be made: When the eccentric distance increase the maximum strength and ductility capacity of the eccentrically loaded columns decrease. But, deteriorations in both strength and ductility are relatively small in the case of $e =0.1h$. A large difference in strength and ductility was observed in the cases of $e = 0.2h$ and $e = 0.3h$. It should also be noted that the initial structural stiffness of the eccentrically loaded column decreases with the increase in eccentric distance, mostly largely due to the influence of the twisting moment.

Figure 42 compares the buckling modes of the column P13 series. Figure 42 (a) shows the buckling of centrally loaded model. Figure 42 (b-e) shows buckling for eccentrically loaded models having eccentricity $e=0.1h$ to $0.4h$. The figure shows that the buckling deformation from the in-plane direction. It indicates that the out-of-plane bending moment dominates the hysteretic behavior of the columns. While eccentricity increase by 10% loading amplitude $(\delta/\delta y)$ decrease by 1. Shell elements near the base of the column on the eccentric side deform inward due to the presence of the cyclic twisting moment. For the thin walled pipe member subjected to a pure torque, a diamond buckling mode can be observed. Hence, for such cantilever columns, the inward deformation on the eccentric side can be attributed to the effect of the cyclic twisting moment (Timoshenko, 1961).

(a) e =0.0h (δ/δ_y =10) (b) e=0.1h (δ/δ_y =6)

(c) e=0.2h (δ/δ_y =5) (d) e=0.3h (δ/δ_y =4)
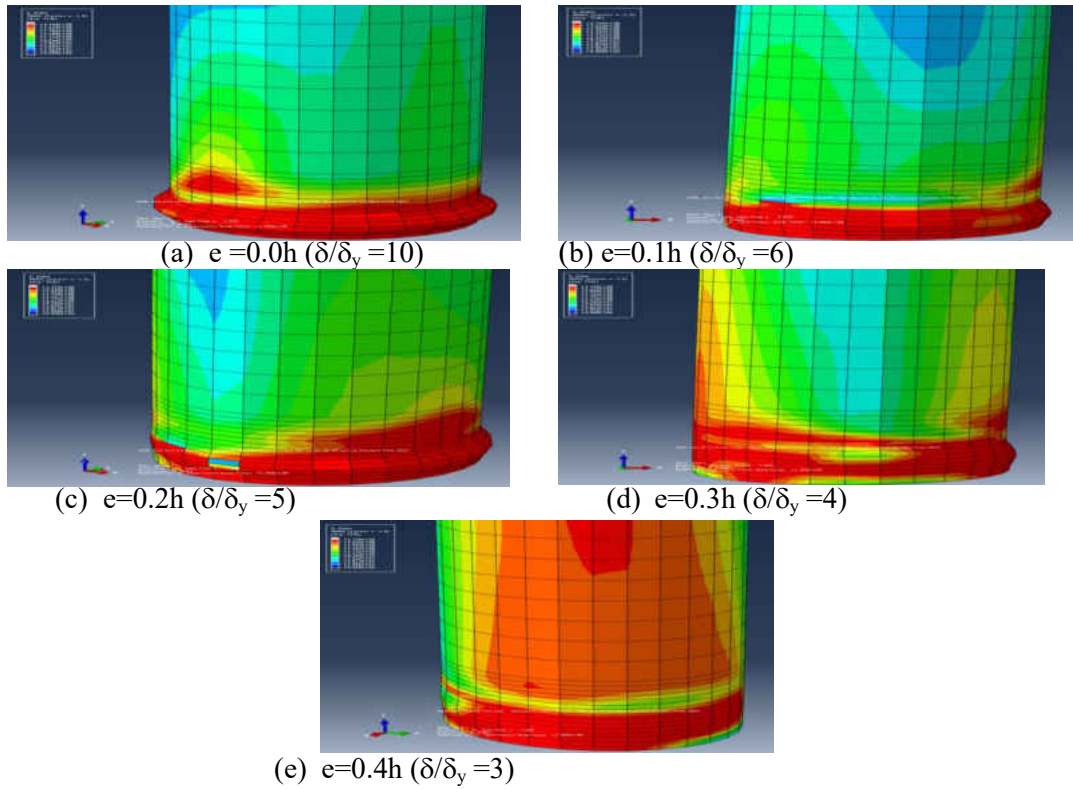
(e) e=0.4h (δ/δ_y =3)

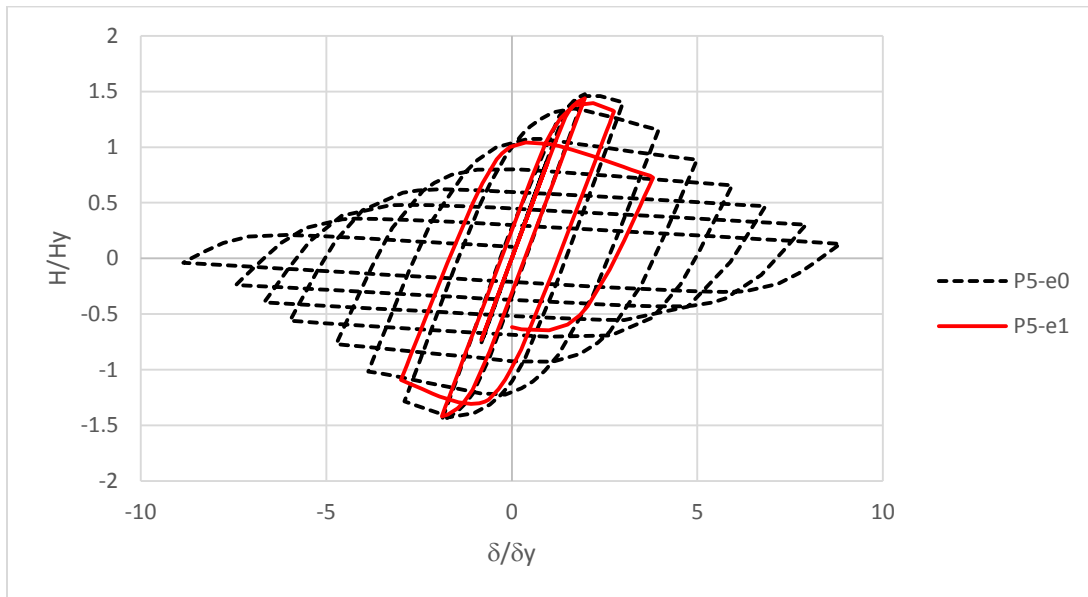Figure 42. Comparison of Buckling Modes of Column P13 Series

Figure 43. Model P5-e0 and P5-e1 Comparison of Normalized Lateral Load Vs. Lateral Displacement of Centrally Concentric Load and Eccentrically Concentric Load.
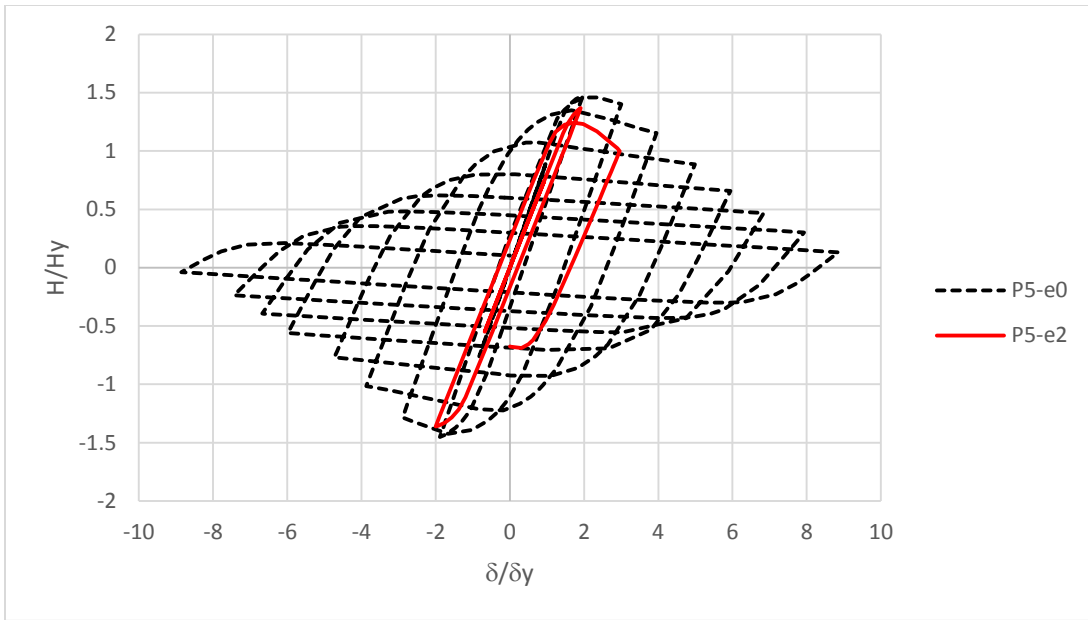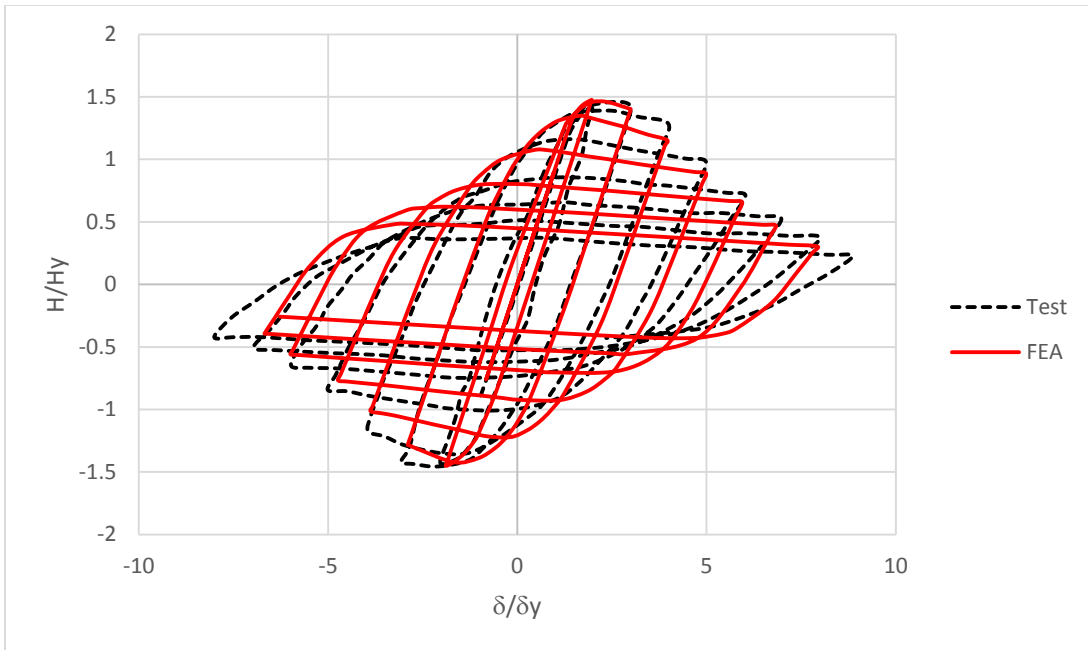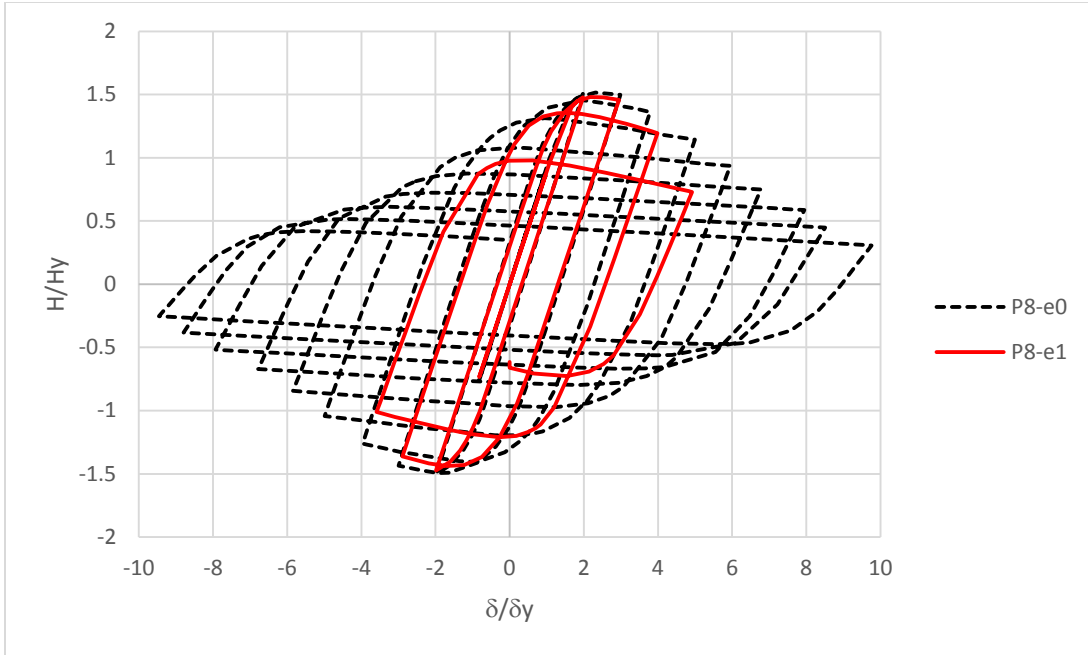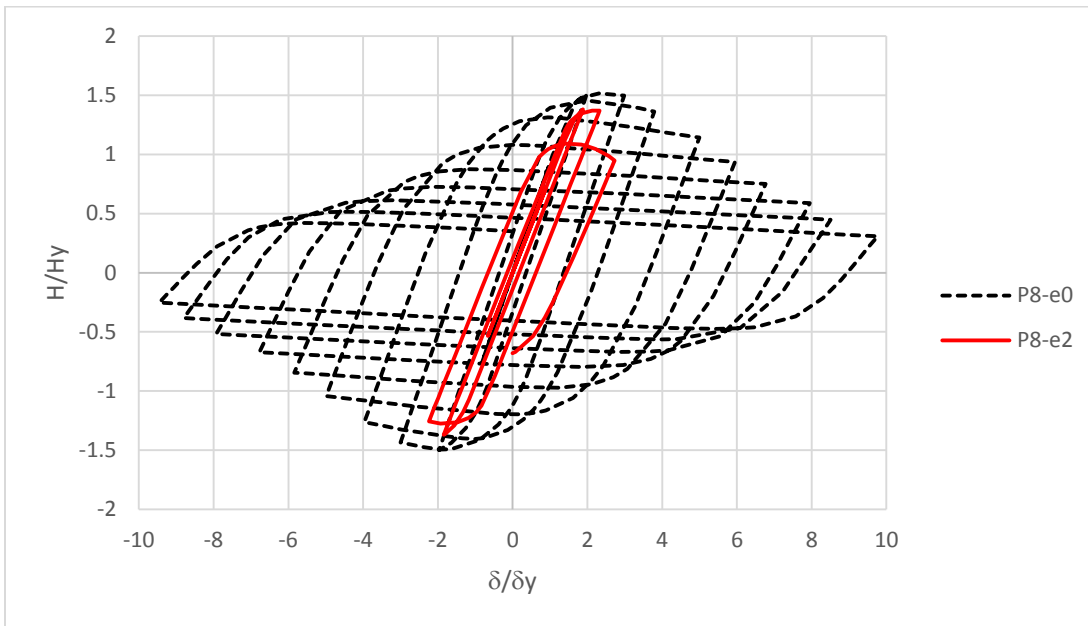
Figure 44. Model P5-e0 and P5-e2 Comparison of Normalized Lateral Load Vs. Lateral Displacement of Centrally Concentric Load and Eccentrically Concentric Load.
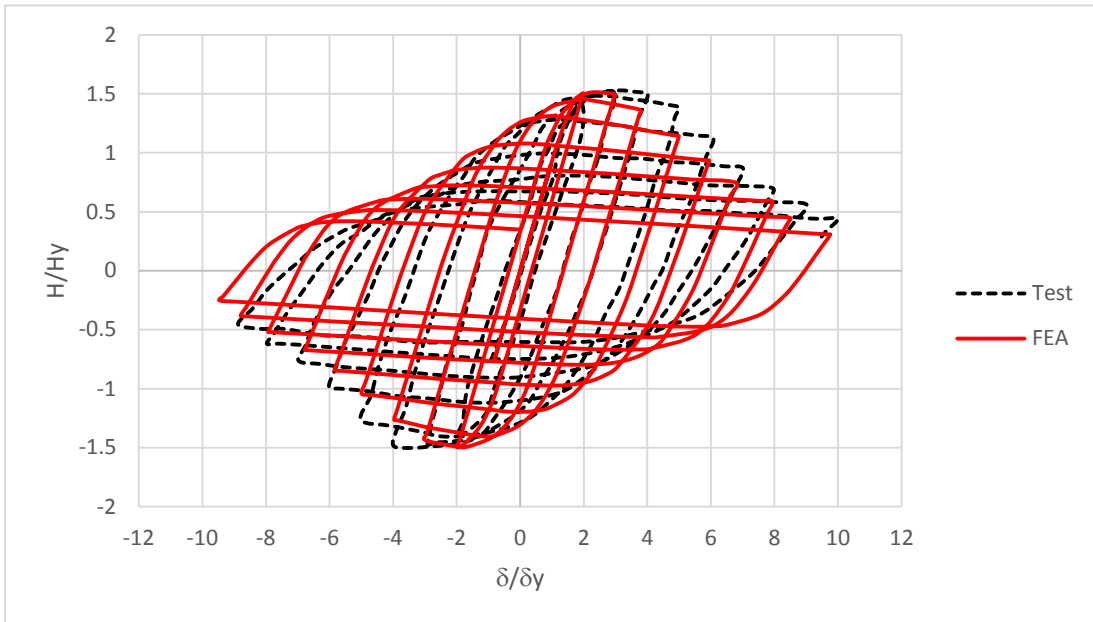

Figure 45. Comparison of Hysteresis Curves of Steel Circular Columns between FEA and Experimental P5-e0
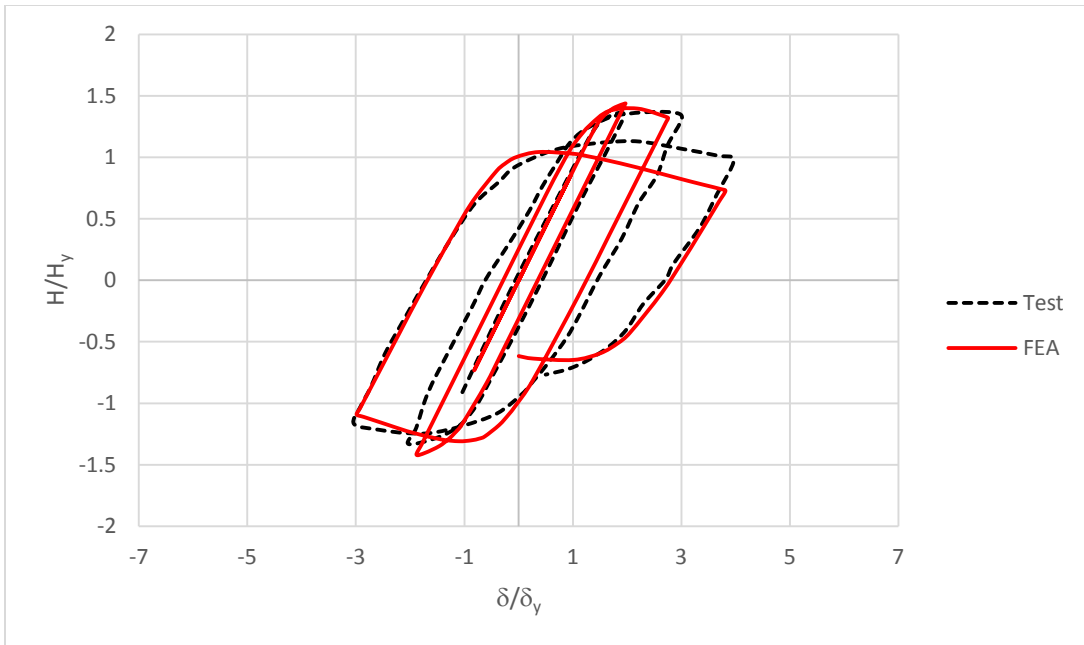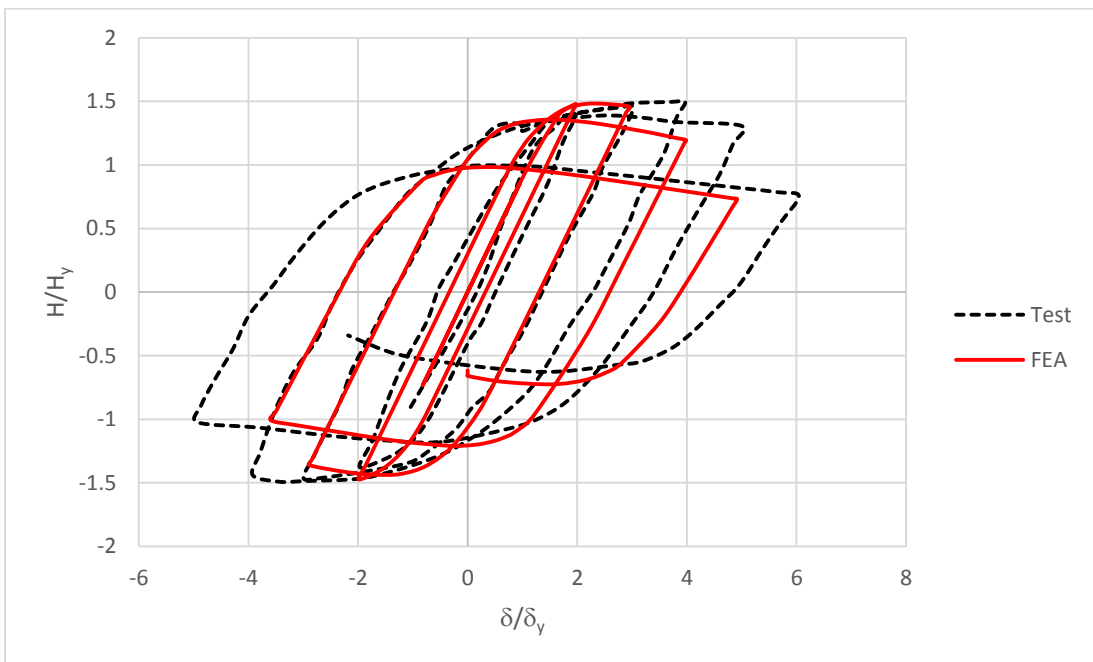
Figure 46. Comparison of Hysteresis Curves of Steel Circular Columns between FEA and Experimental P5-e1
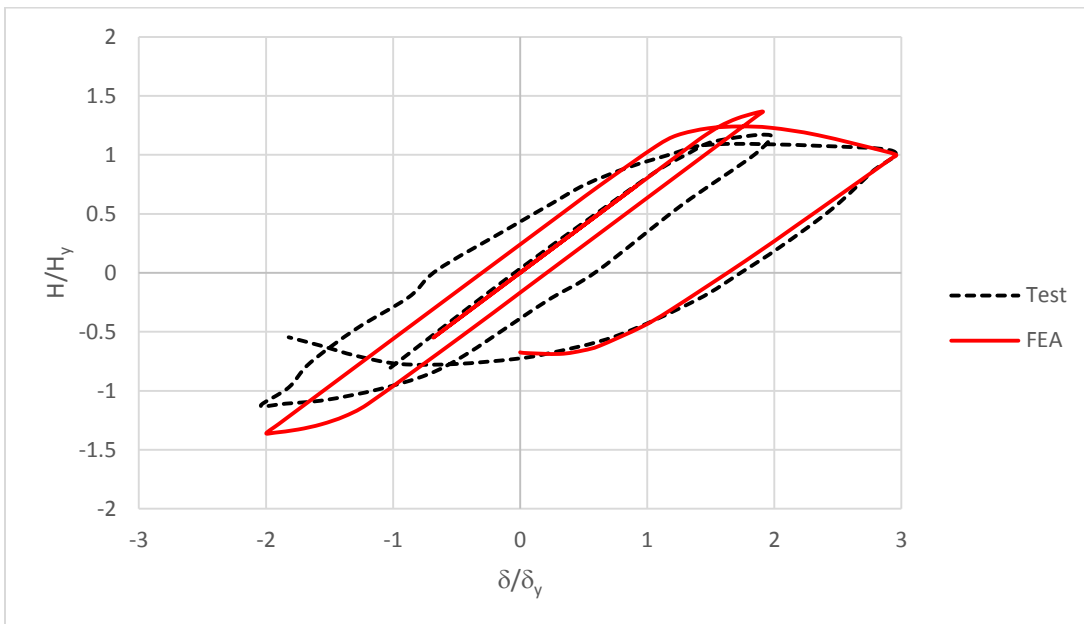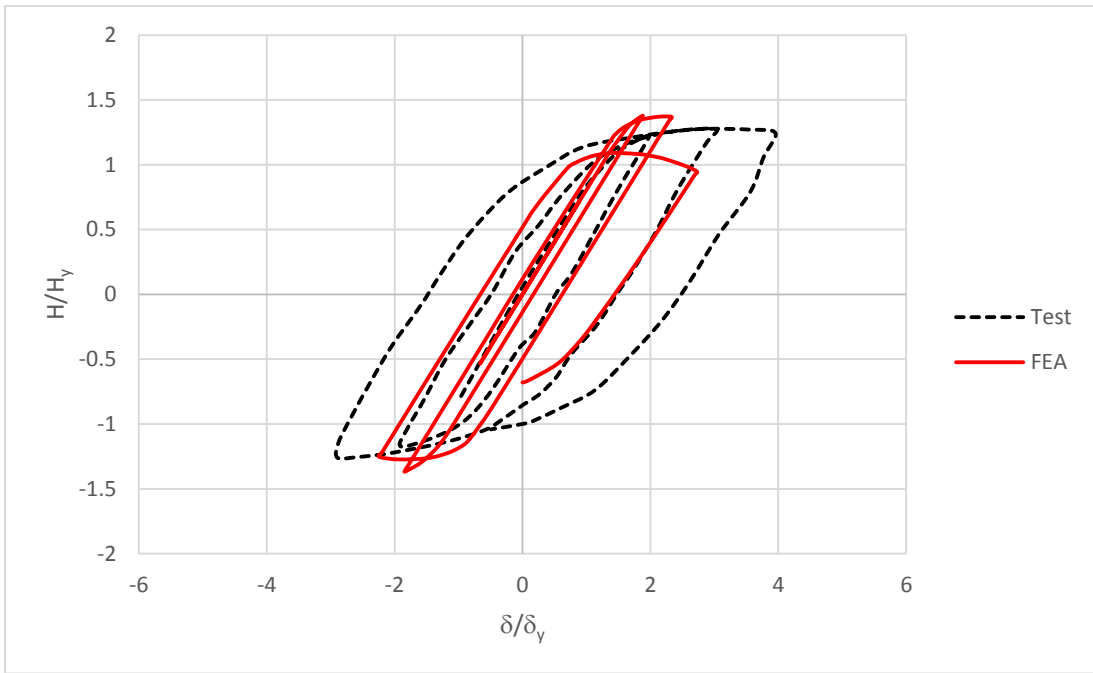

Figure 47. Comparison of Hysteresis Curves of Steel Circular Columns between FEA and Experimental P5-e1
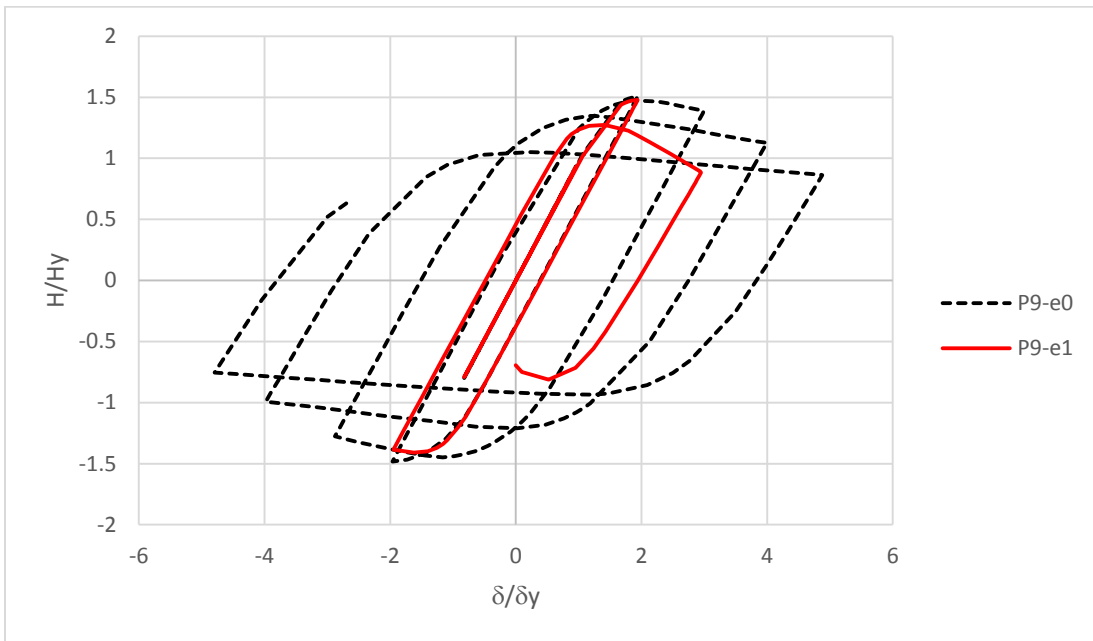
Figure 48. Model P8-e0 and P8-e1 Comparison of Normalized Lateral Load Vs. Lateral Displacement of Centrally Concentric Load and Eccentrically Concentric Load.
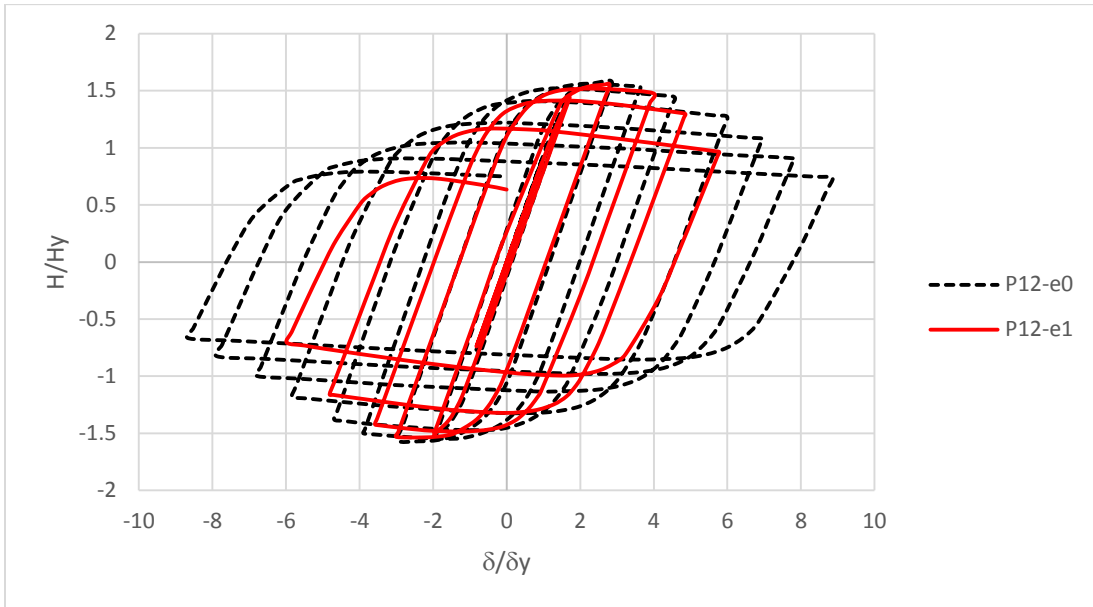

Figure 49. Model P8-e0 and P8-e2 Comparison of Normalized Lateral Load Vs. Lateral Displacement of Centrally Concentric Load and Eccentrically Concentric Load.

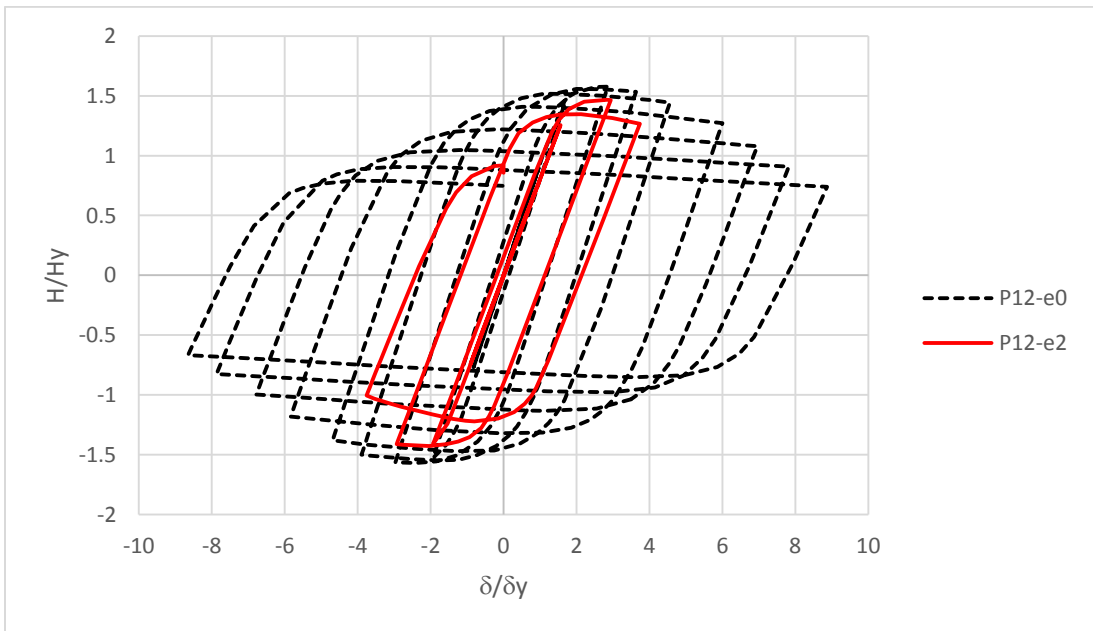Figure 50. Comparison of Hysteresis Curves of Steel Circular Columns between FEA and Experimental P8-e0

Figure 51. Comparison of Hysteresis Curves of Steel Circular Columns between FEA and Experimental P8-e1

Figure 52. Comparison of Hysteresis Curves of Steel Circular Columns between FEA and Experimental P8-e2

Figure 53. Model P9-e0 and P9-e1 Comparison of Normalized Lateral Load Vs. Lateral Displacement of Centrally Concentric Load and Eccentrically Concentric Load.

Figure 54. Model P12-e0 and P12-e1 Comparison of Normalized Lateral Load Vs. Lateral Displacement of Centrally Concentric Load and Eccentrically Concentric Load.

Figure 55. Model P12-e0 and P12-e2 Comparison of Normalized Lateral Load Vs. Lateral Displacement of Centrally Concentric Load and Eccentrically Concentric Load.
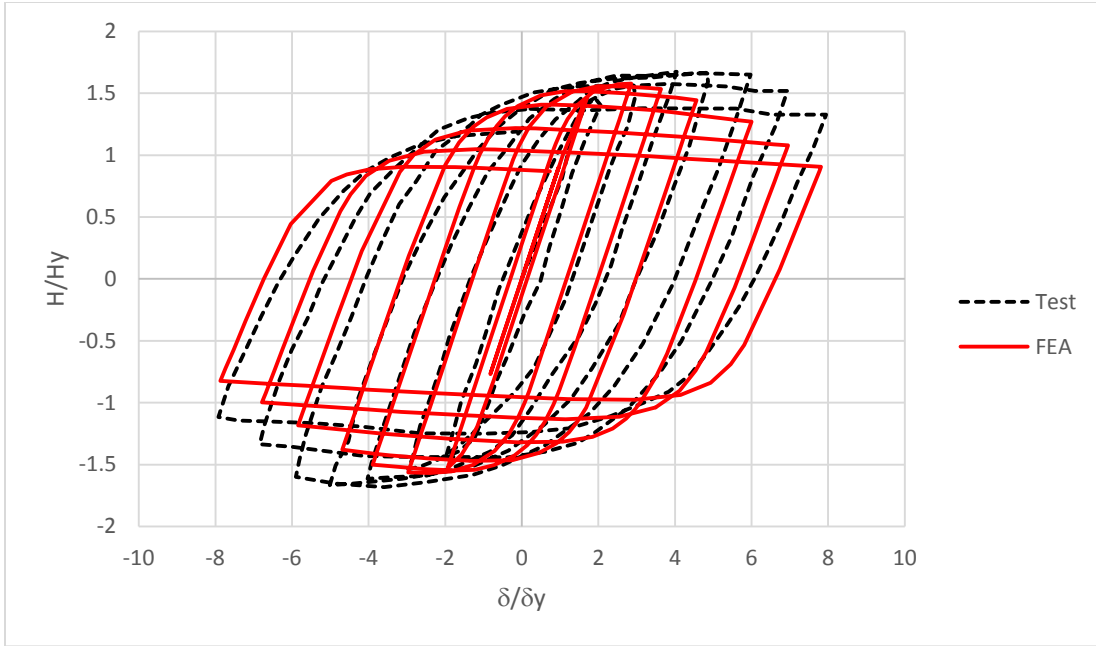
Figure 56. Comparison of Hysteresis Curves of Steel Circular Columns between FEA and Experimental P12-e0
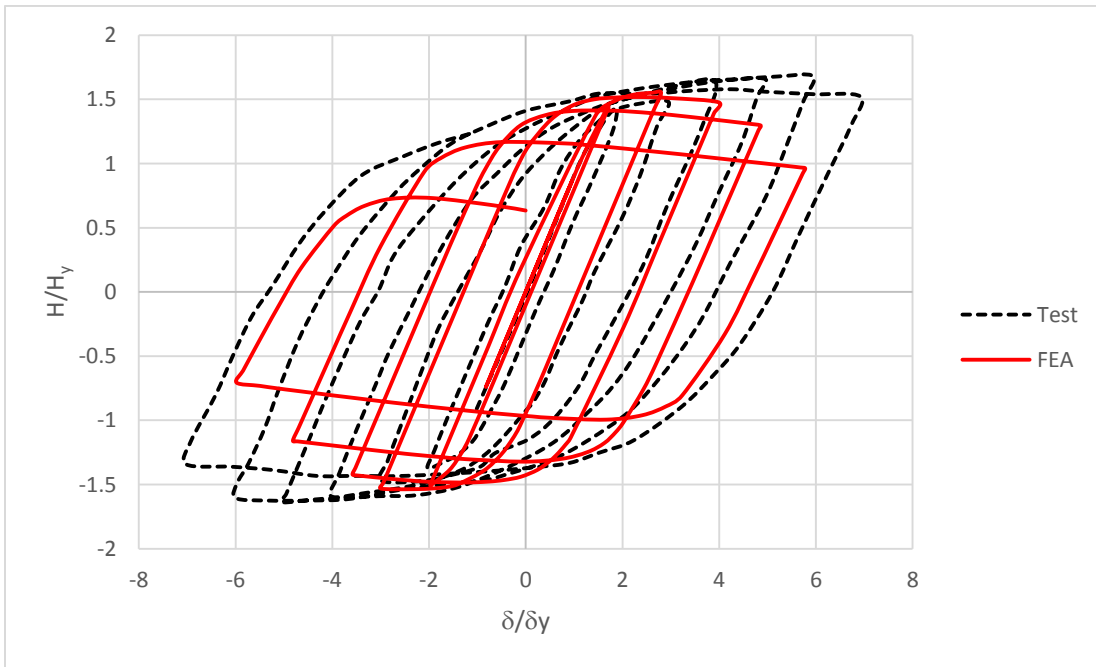

Figure 57. Comparison of Hysteresis Curves of Steel Circular Columns between FEA and Experimental P12-e1
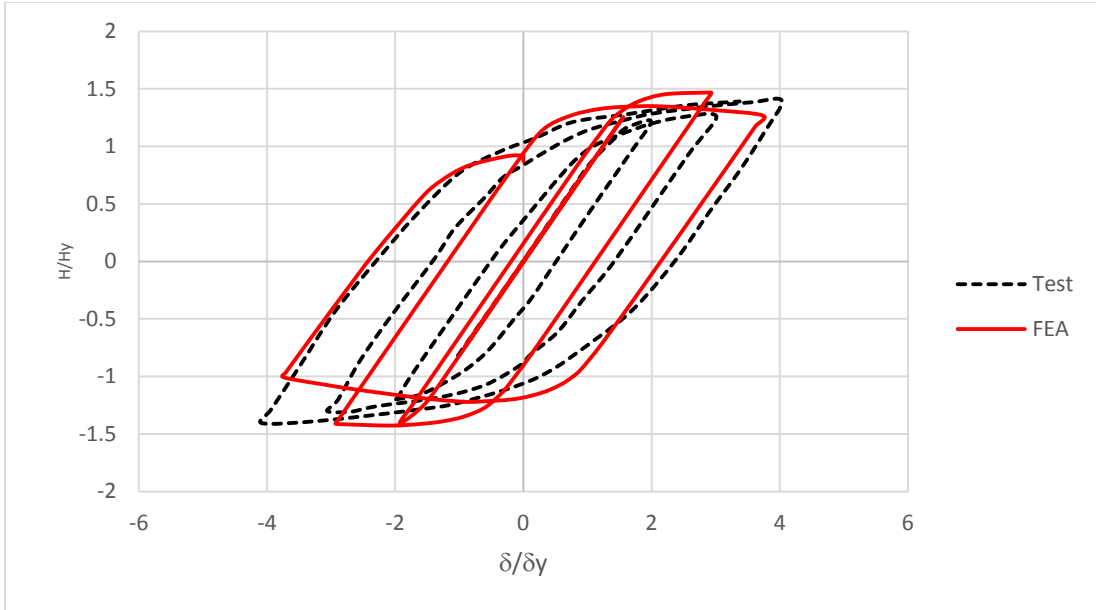
Figure 58. Comparison of Hysteresis Curves of Steel Circular Columns between FEA and Experimental P12-e2
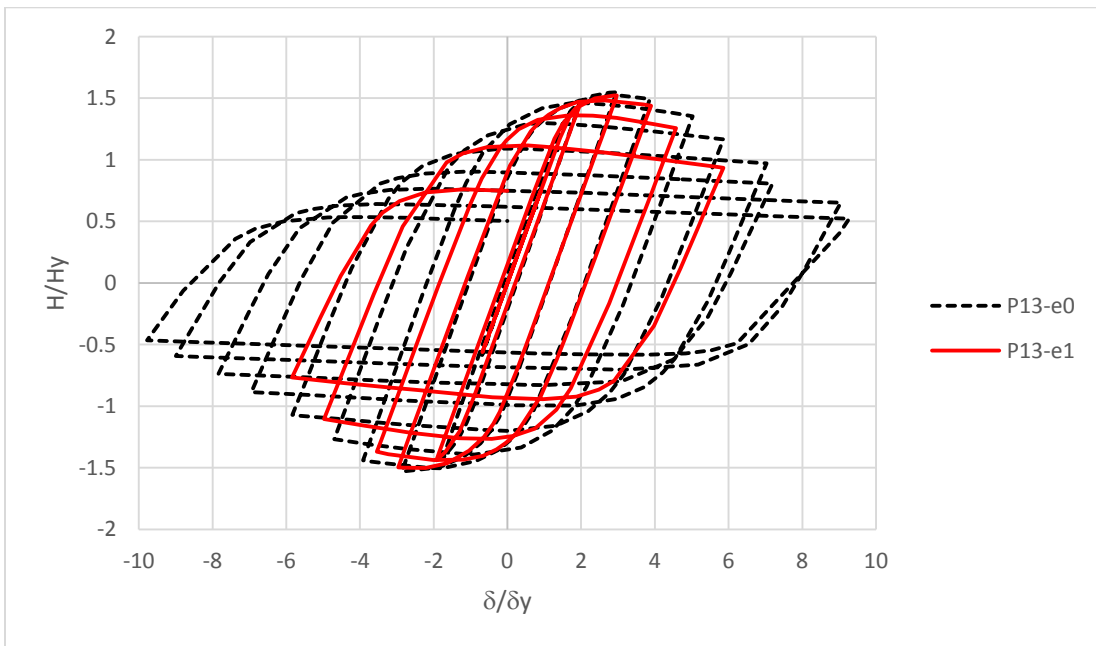

Figure 59. Model P13-e0 and P13-e1 Comparison of Normalized Lateral Load Vs. Lateral Displacement of Centrally Concentric Load and Eccentrically Concentric Load.
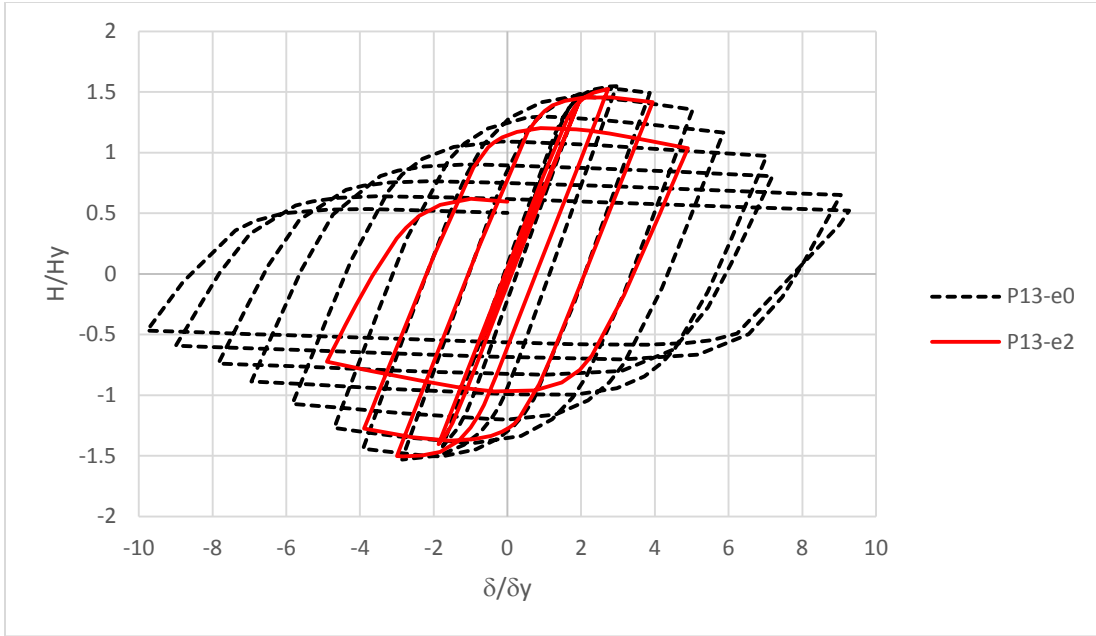
Figure 60. Model P13-e0 and P13-e2 Comparison of Normalized Lateral Load Vs. Lateral Displacement of Centrally Concentric Load and Eccentrically Concentric Load.
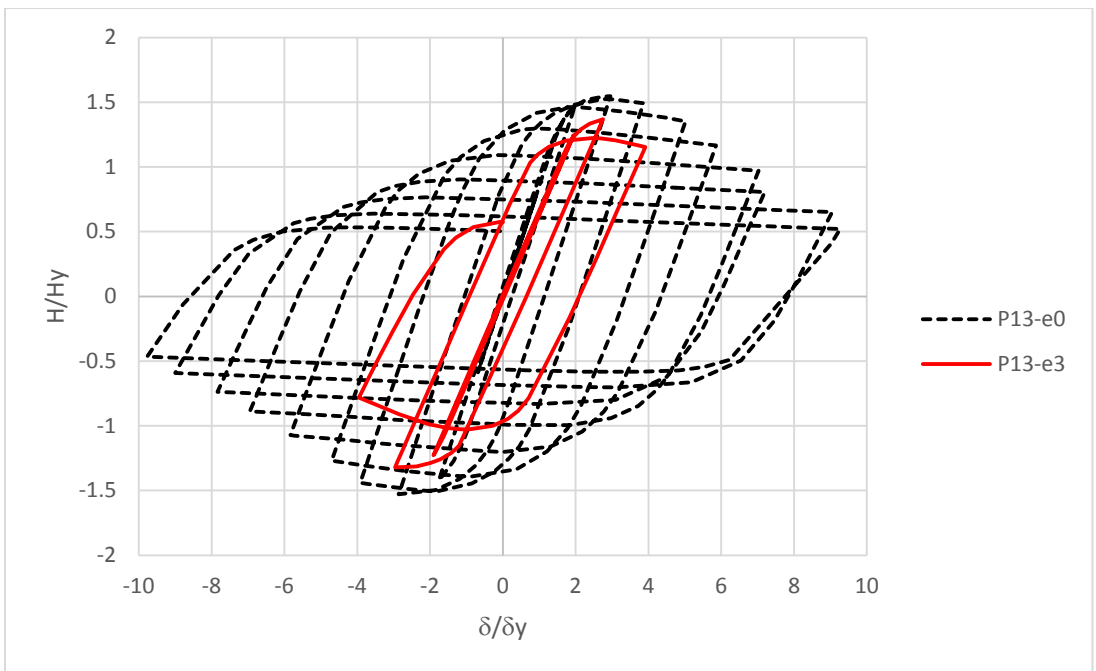

Figure 63. Model P13-e0 and P13-e3 Comparison of Normalized Lateral Load Vs. Lateral Displacement of Centrally Concentric Load and Eccentrically Concentric Load.
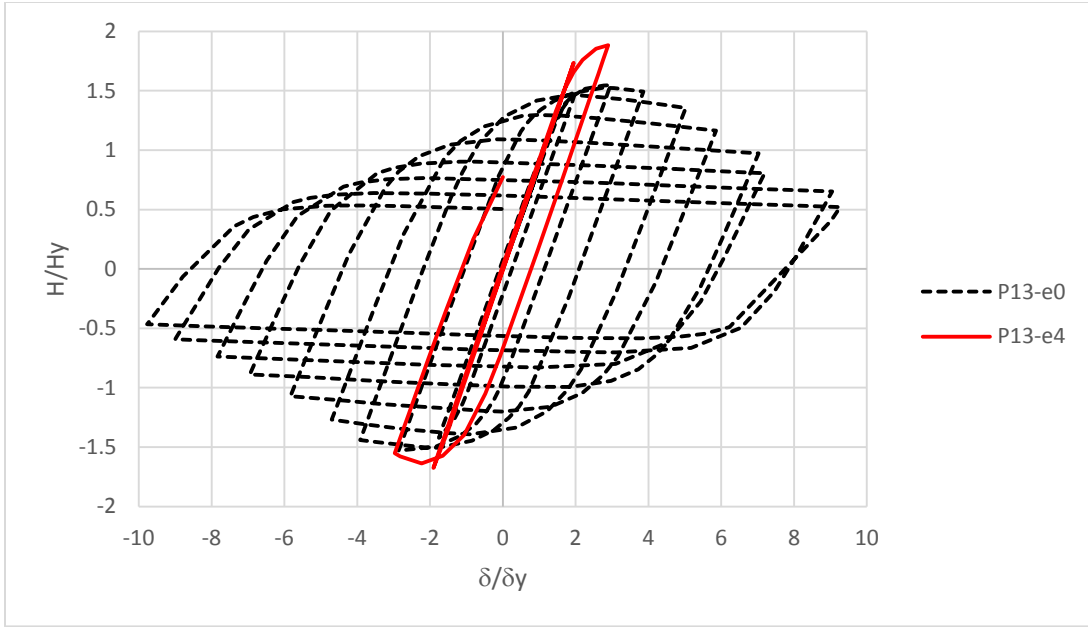
Figure 61. Model P13-e0 and P13-e4 Comparison of Normalized Lateral Load Vs. Lateral Displacement of Centrally Concentric Load and Eccentrically Concentric Load.
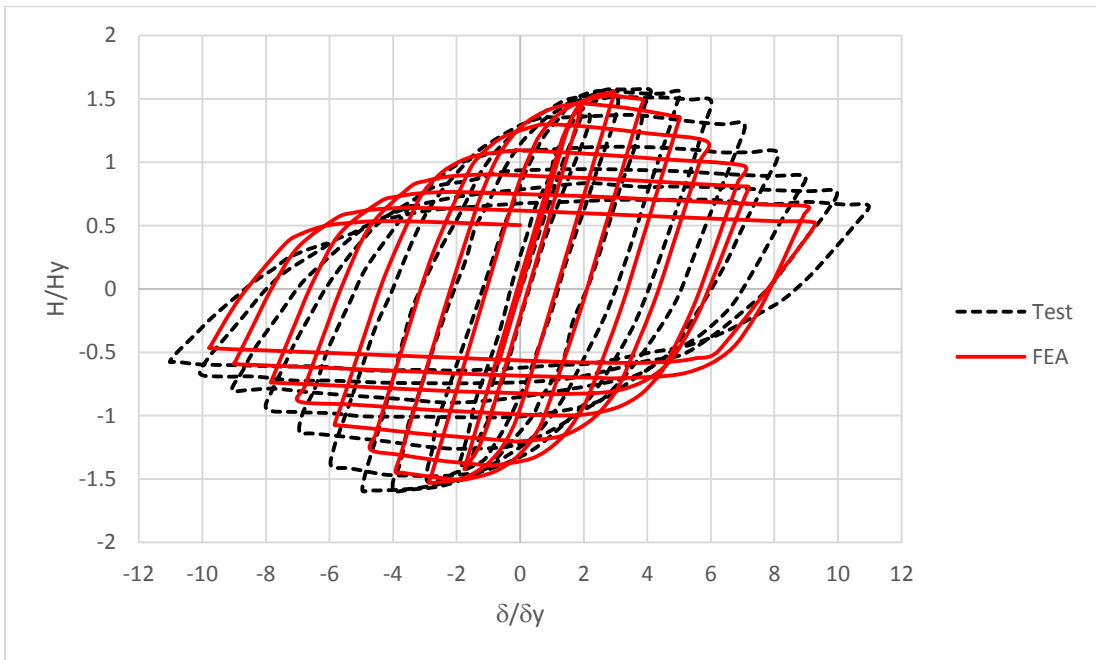

Figure 62: Comparison of Hysteresis Curves of Steel Circular Columns between FEA and Experimental P13-e0

Figure 63. Comparison of Hysteresis Curves of Steel Circular Columns between FEA and Experimental P13-e2

Figure 64. Comparison of Hysteresis Curves of Steel Circular Columns between FEA and Experimental P13-e3

Figure 65. Model P14-e0 and P14-e1 Comparison of Normalized Lateral Load Vs. Lateral Displacement of Centrally Concentric Load and Eccentrically Concentric Load.

Figure 66. Model P14-e0 and P14-e2 Comparison of Normalized Lateral Load Vs. Lateral Displacement of Centrally Concentric Load and Eccentrically Concentric Load.

Figure 67. Comparison of Hysteresis Curves of Steel Circular Columns between FEA and Experimental P14-e0
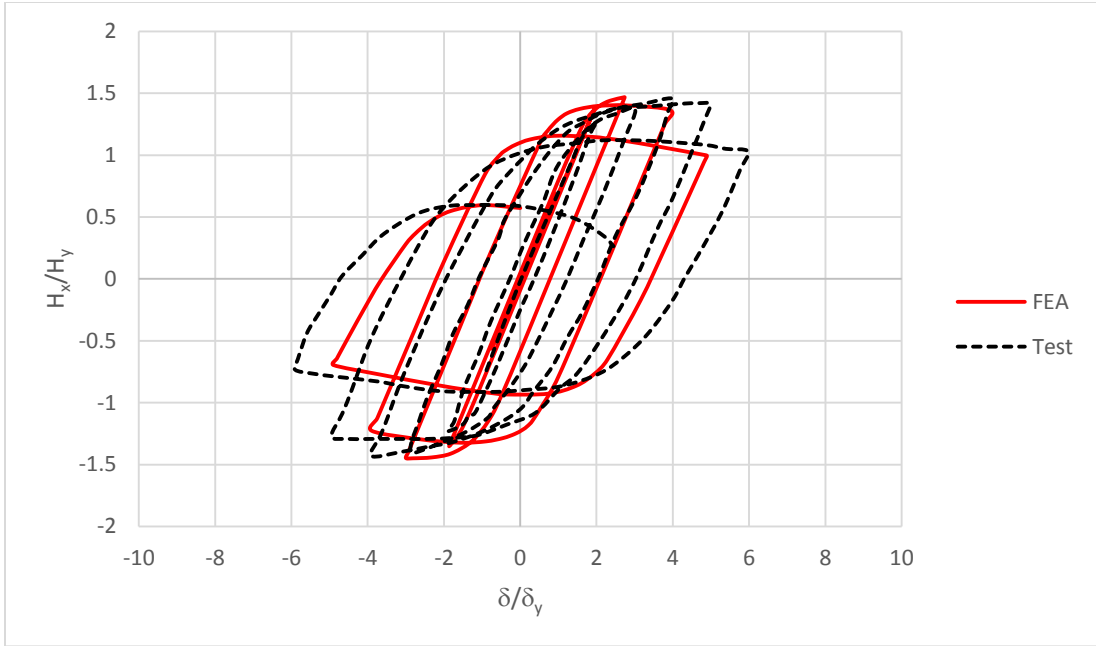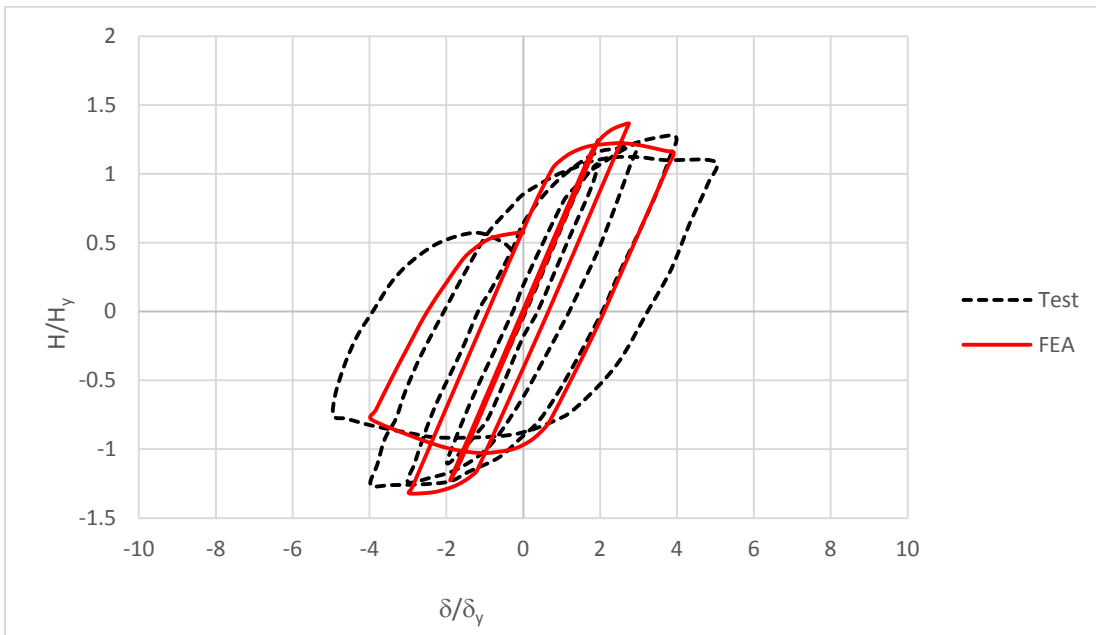

Figure 68. Comparison of Hysteresis Curves of Steel Circular Columns between FEA and Experimental P14-e1

Figure 69. Comparison of Hysteresis Curves of Steel Circular Columns between FEA and Experimental P14-e2
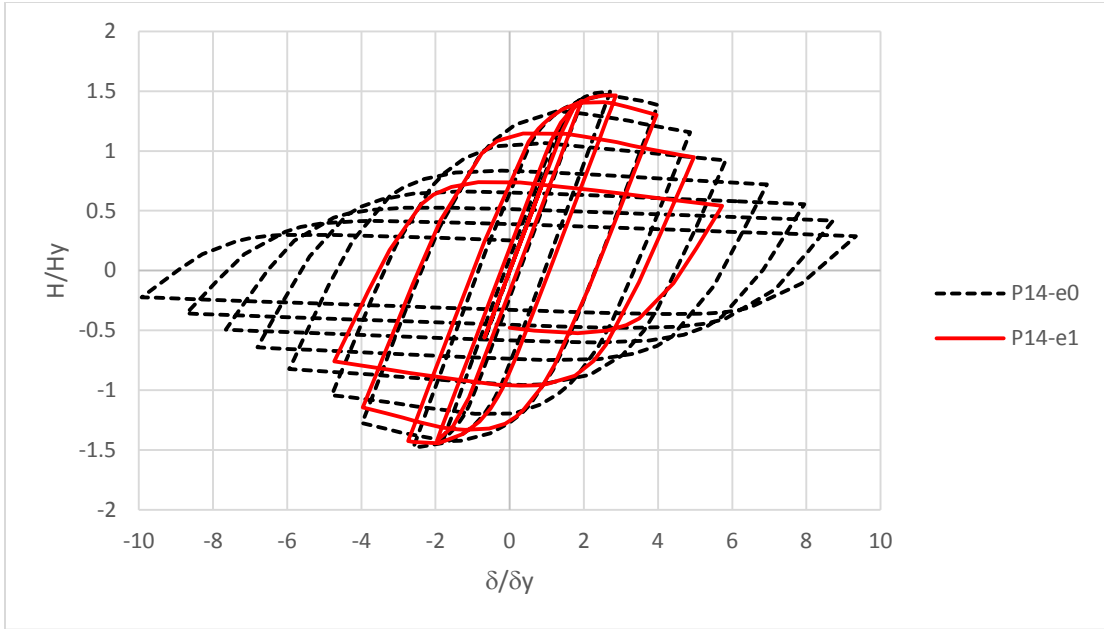

Figure 70. Model P15-e0 and P15-e1 Comparison of Normalized Lateral Load Vs. Lateral Displacement of Centrally Concentric Load and Eccentrically Concentric Load.
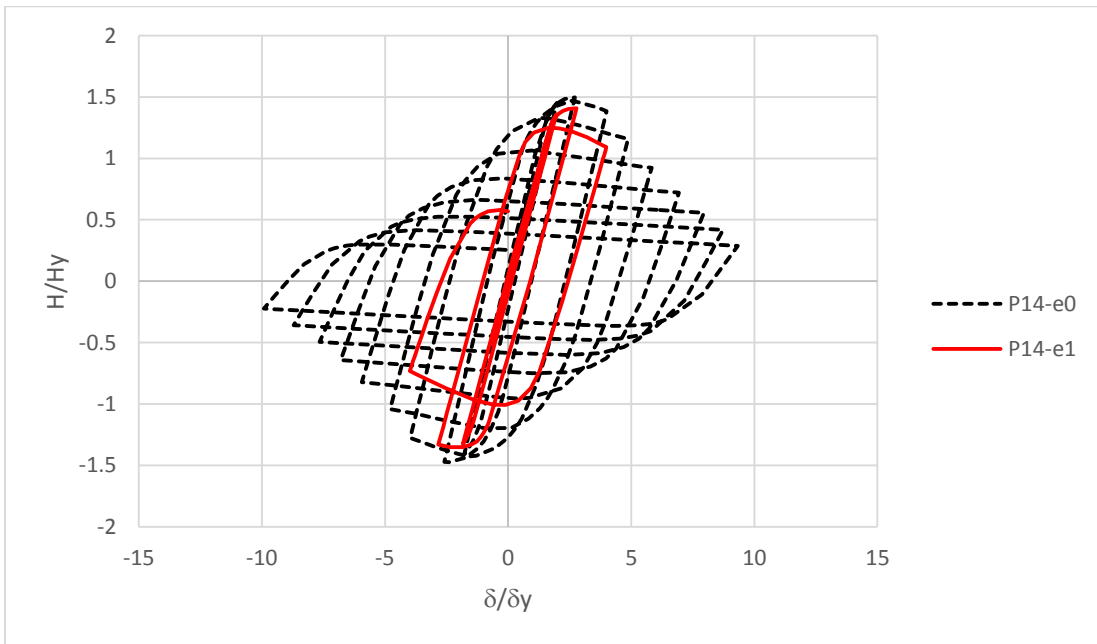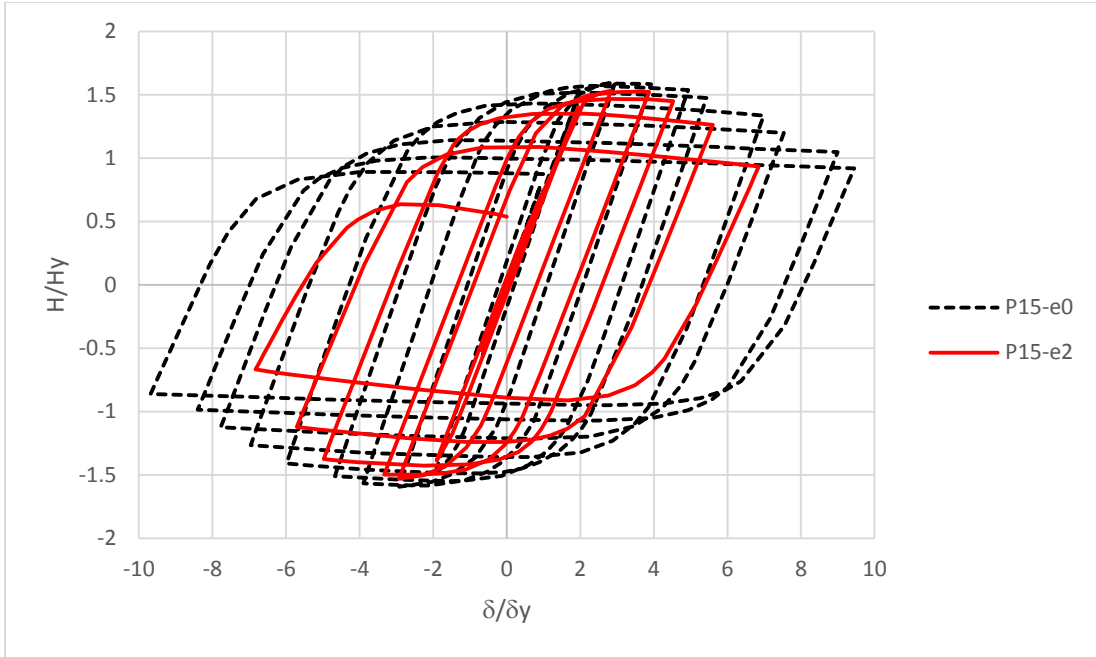
Figure 71. Model P15-e0 and P15-e2 Comparison of Normalized Lateral Load Vs. Lateral Displacement of Centrally Concentric Load and Eccentrically Concentric Load.
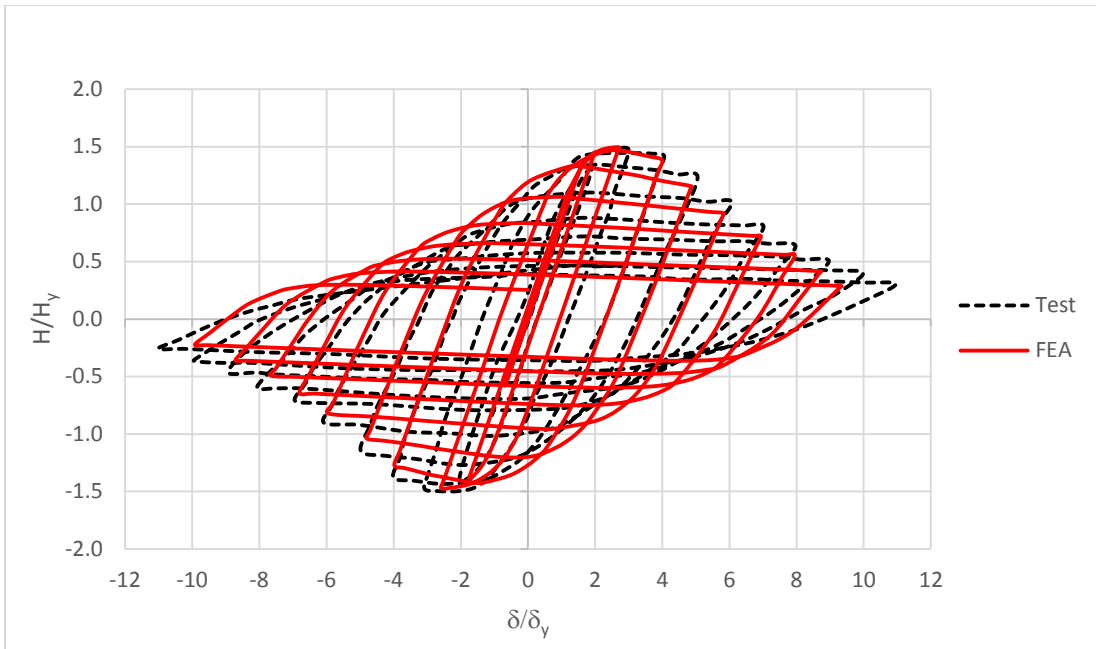

Figure 72. Comparison of Hysteresis Curves of Steel Circular Columns between FEA and Experimental P15-e0
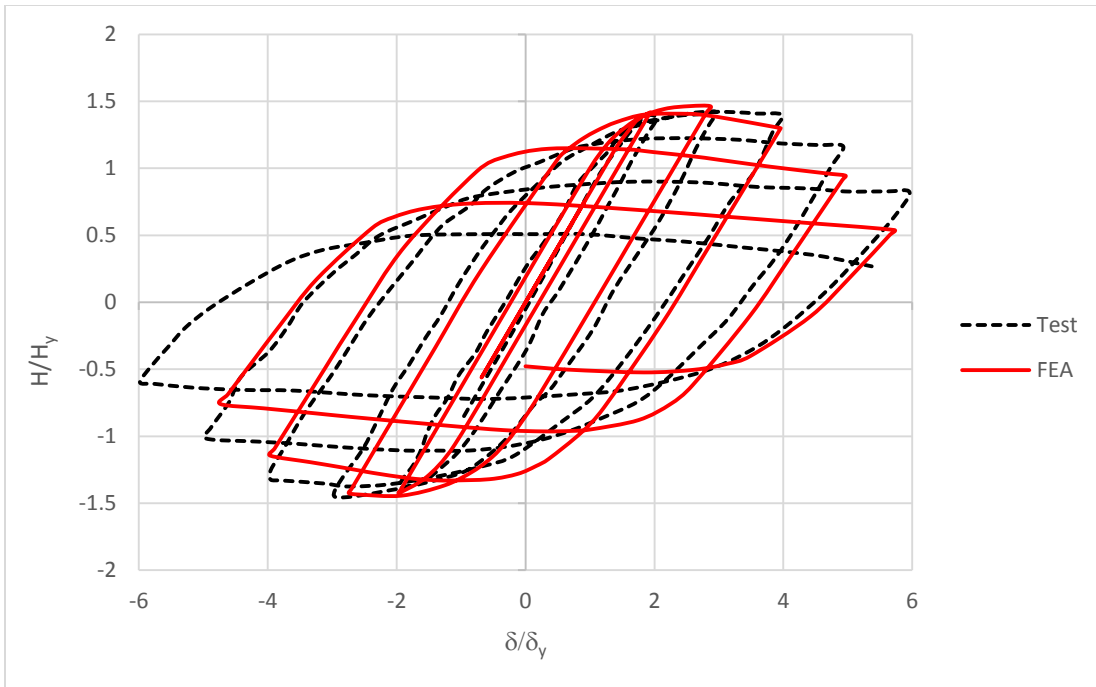
66

Figure 73. Comparison of Hysteresis Curves of Steel Circular Columns between FEA and Experimental P15-e1.

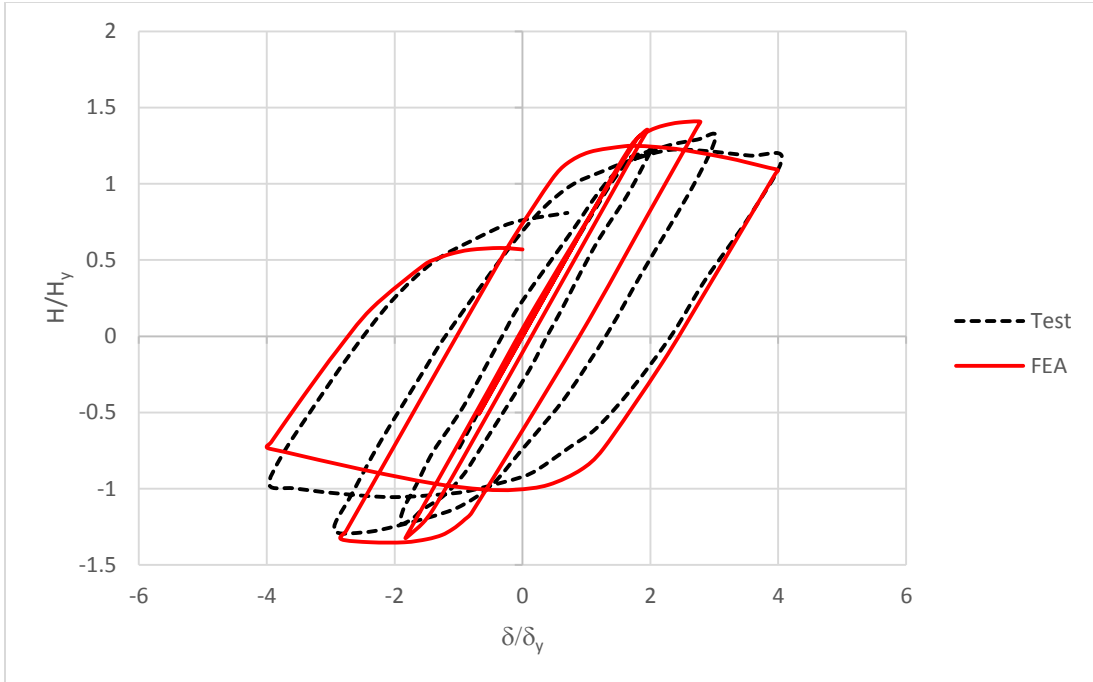Figure 74. Comparison of Hysteresis Curves of Steel Circular Columns between FEA and Experimental P15-e1
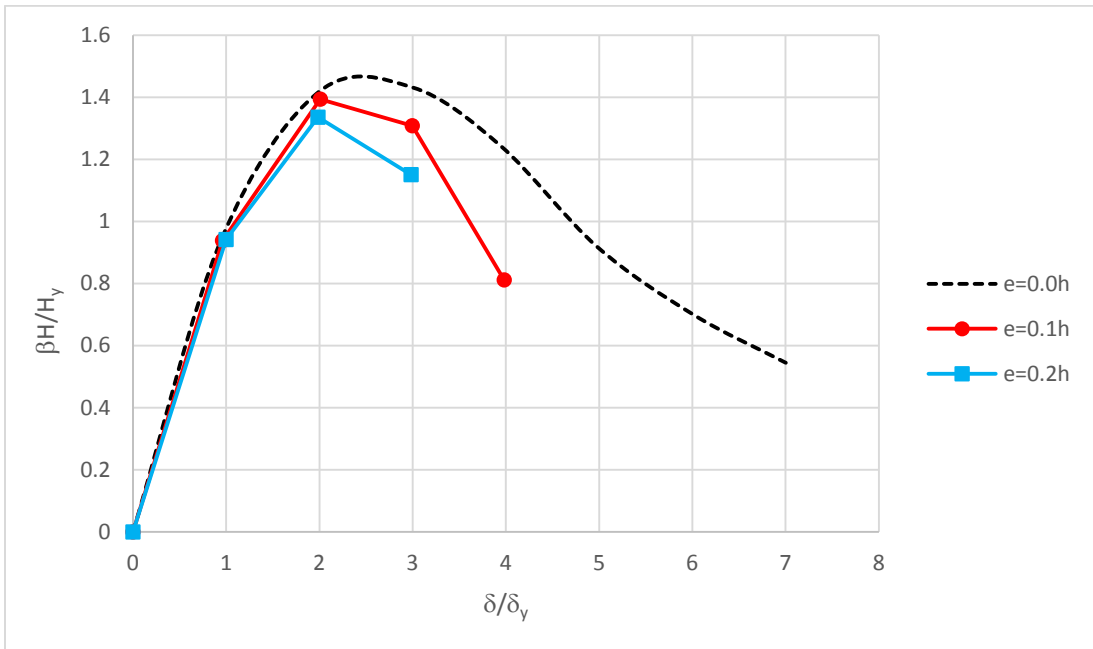
Figure 75. Model P5 Series Envelopment Curves of Horizontal Load Vs. Displacement Relation.
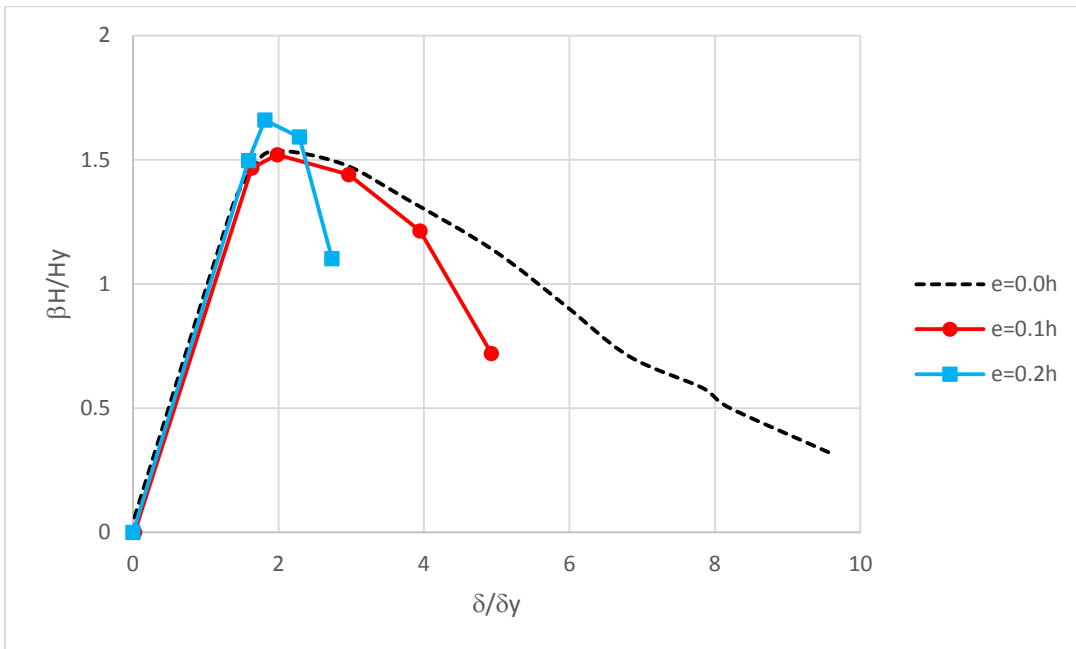
Figure 76. Model P8 Series Envelopment Curves of Horizontal Load Vs. Displacement Relation.
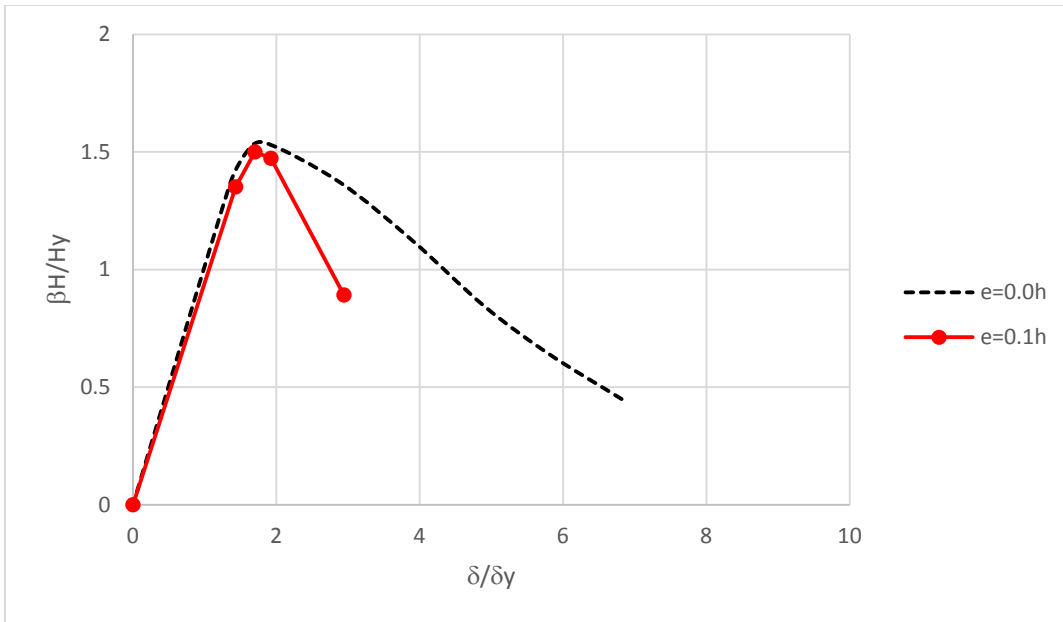
Figure 77. Model P9 Series Envelopment Curves of Horizontal Load Vs. Displacement Relation.
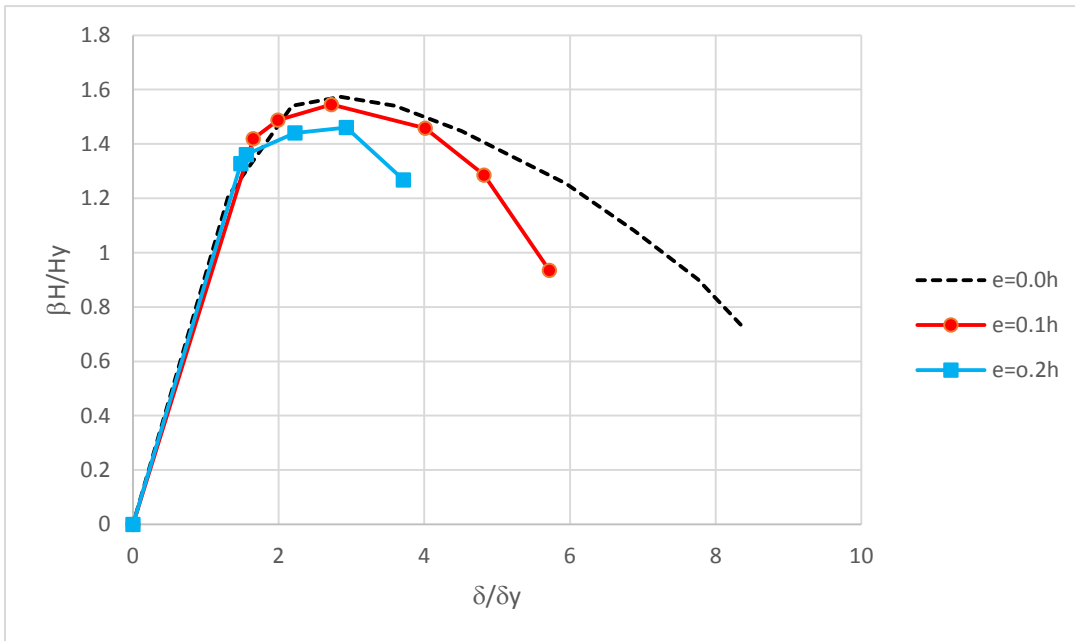
Figure 78. Model P12 Series Envelopment Curves of Horizontal Load Vs. Displacement Relation.
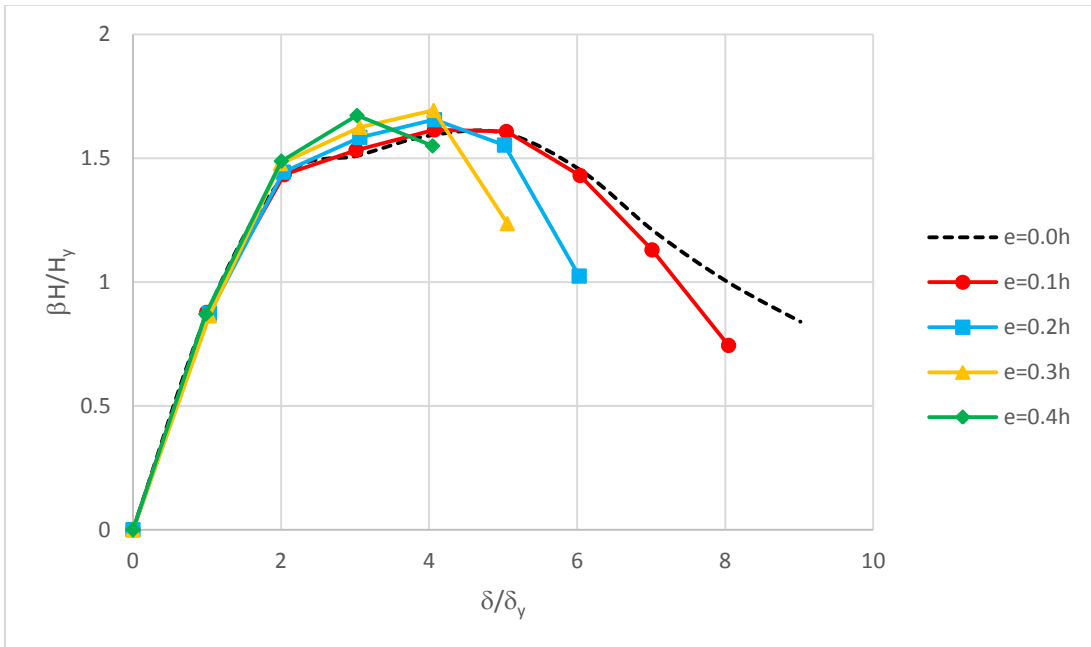
Figure 79. Model P13 Series Envelopment Curves of Horizontal Load Vs. Displacement Relation.
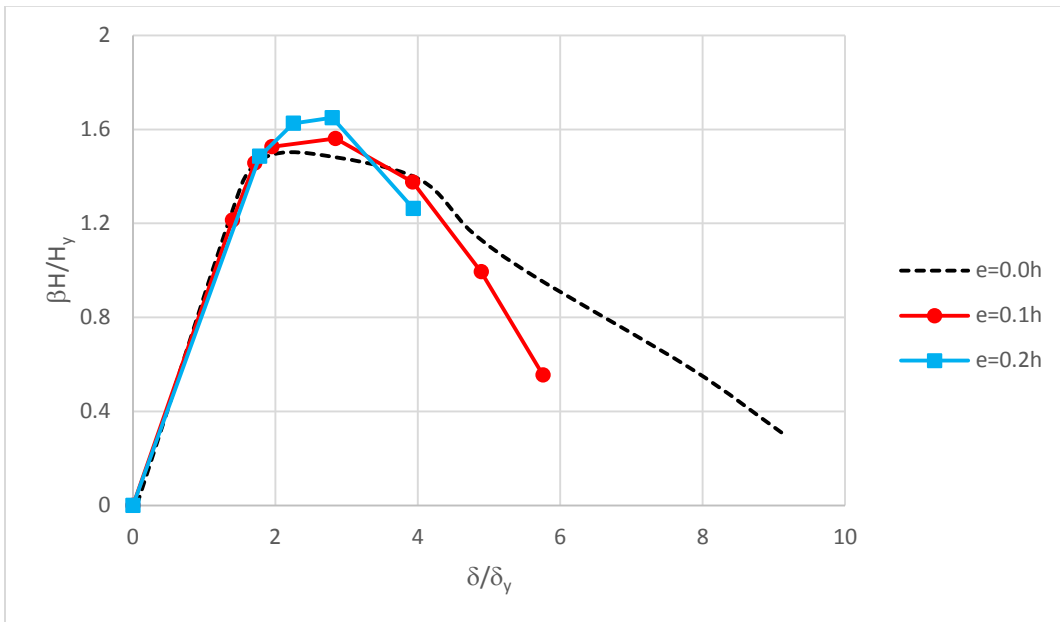
Figure 80. Model P14 Series Envelopment Curves of Horizontal Load Vs. Displacement Relation.
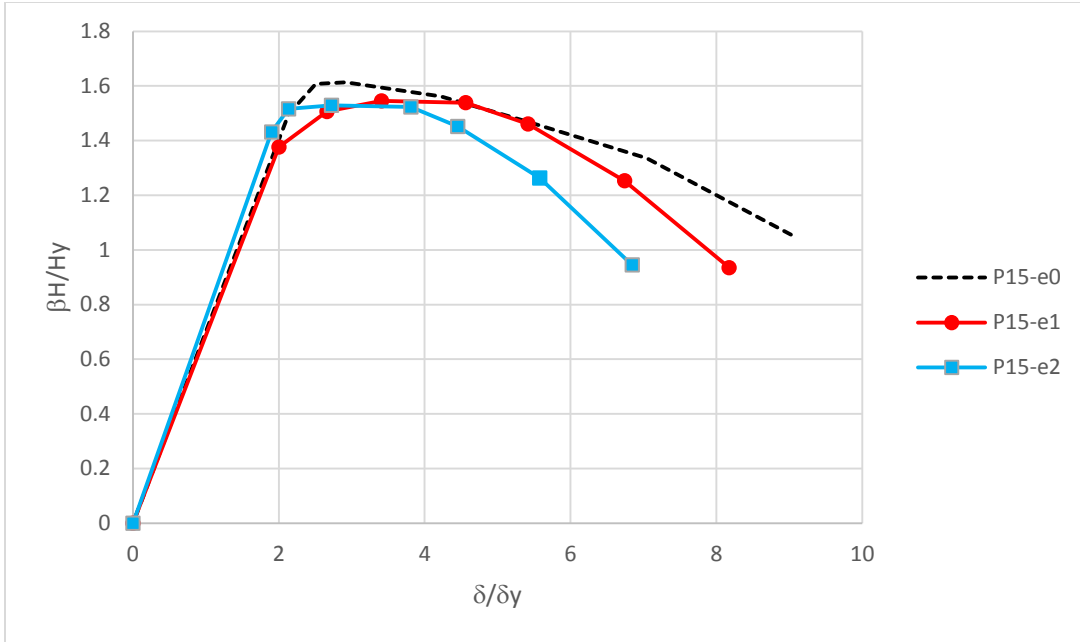
Figure 81. Model P15 Series Envelopment Curves of Horizontal Load Vs. Displacement Relation.
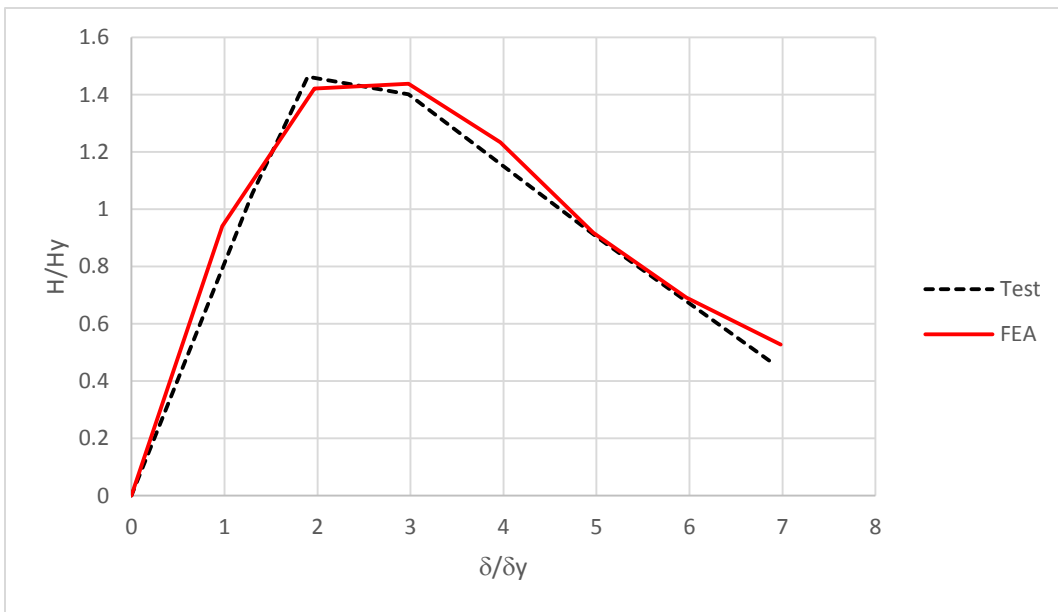
Figure 82. Comparison of Envelope Curves of Steel Circular Columns between FEA and Experimental P5-e0
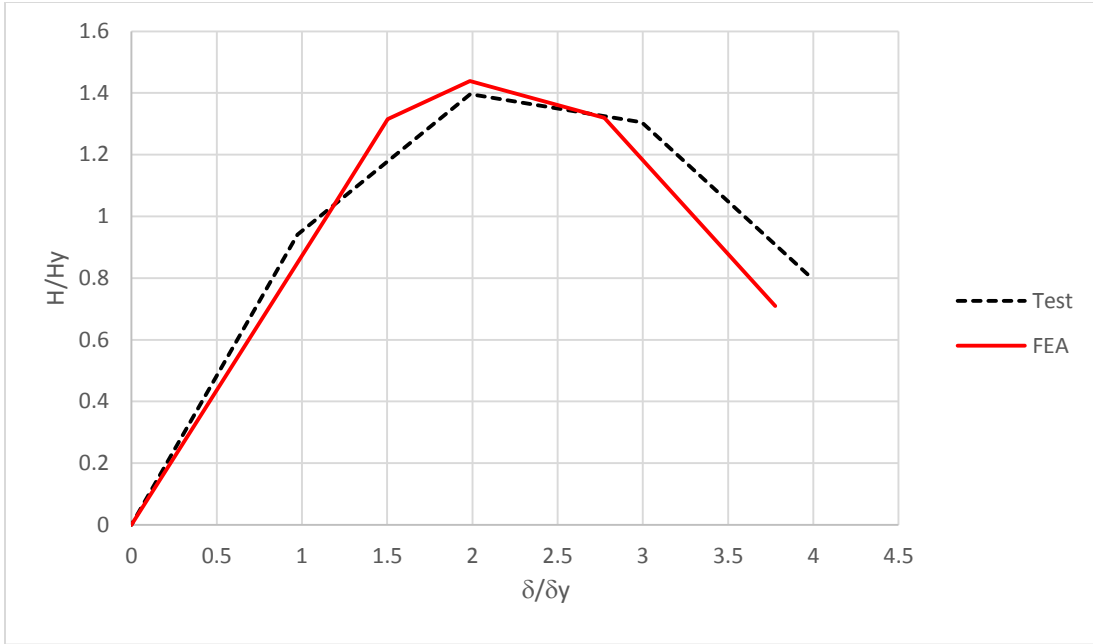
Figure 83. Comparison of Envelope Curves of Steel Circular Columns between FEA and Experimental P5-e1
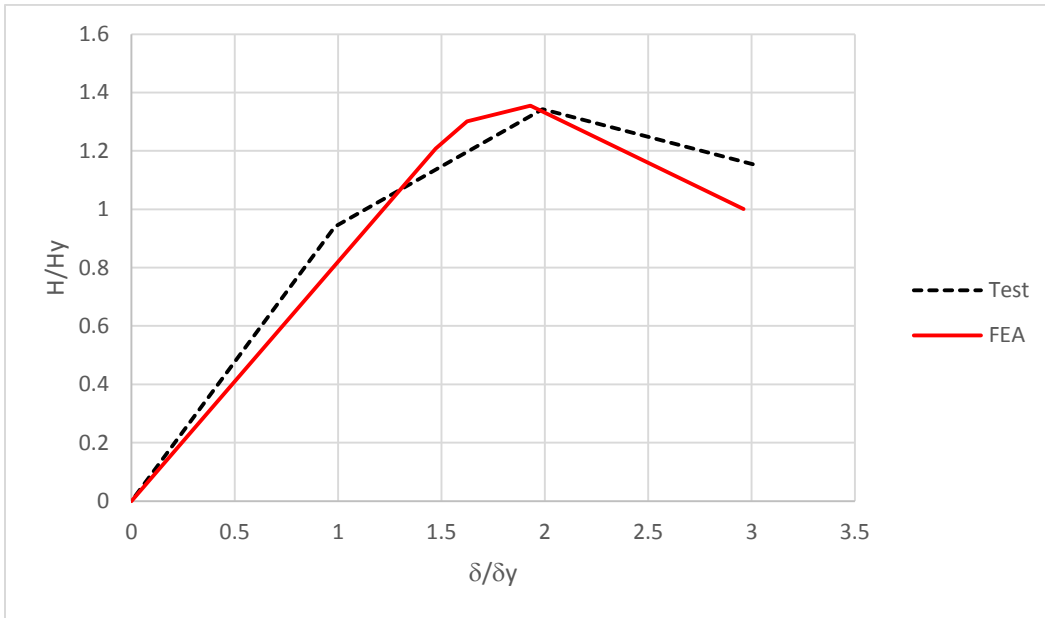
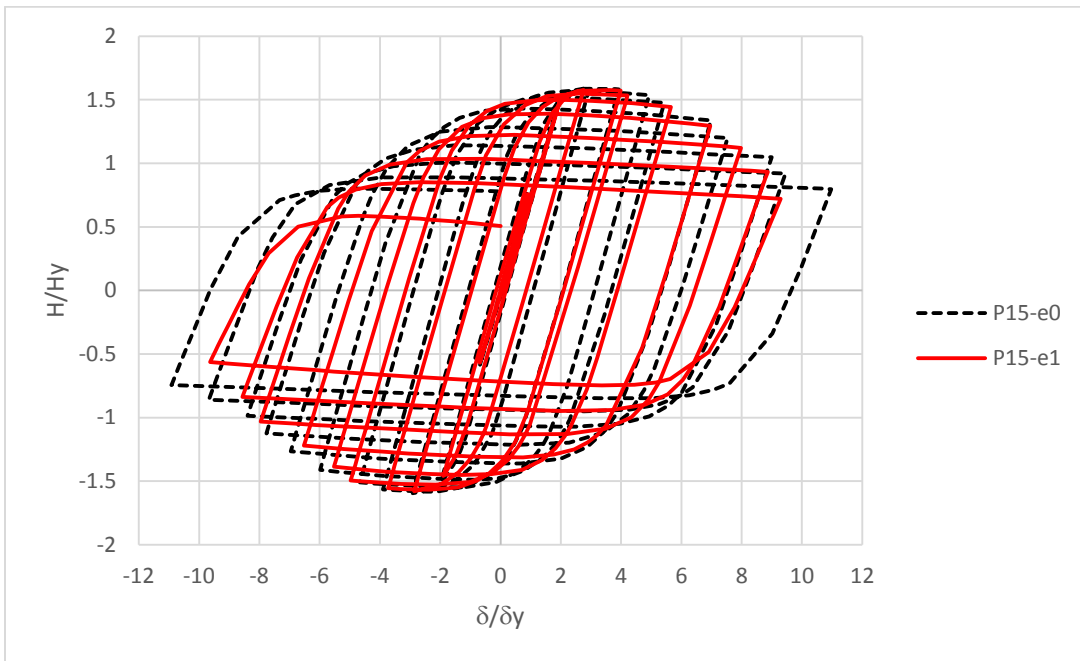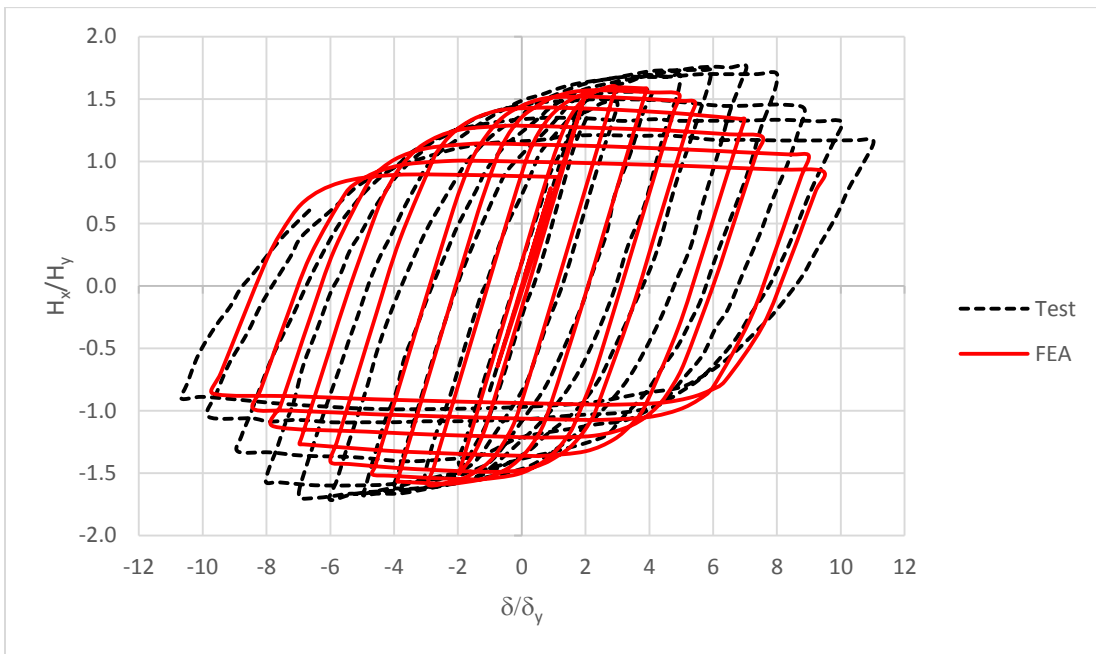Figure 84. Comparison of Envelope Curves of Steel Circular Columns between FEA and Experimental P5-e2
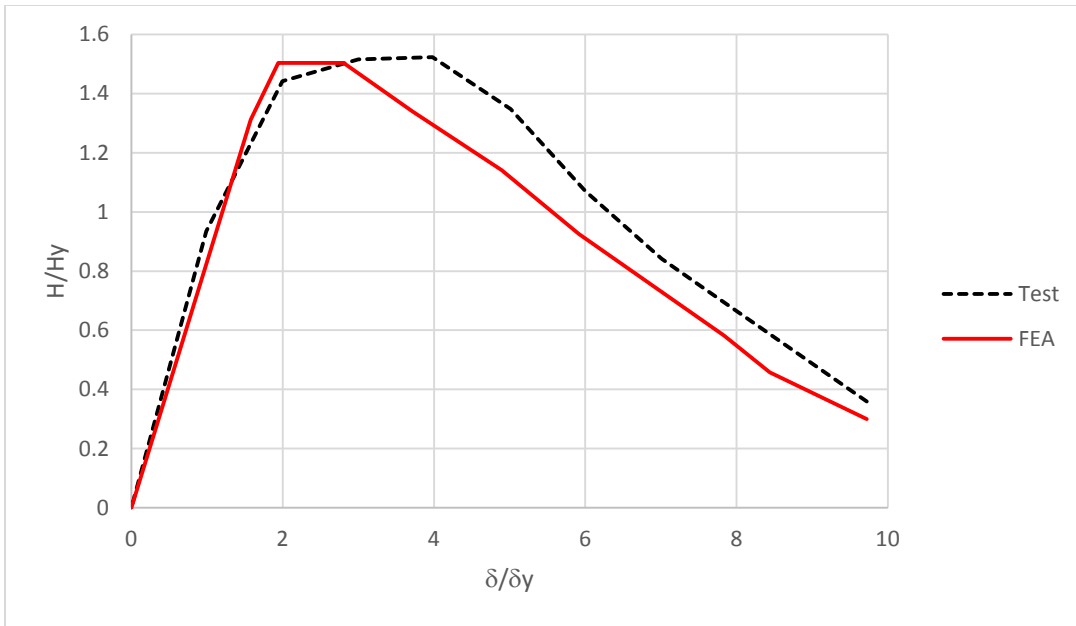
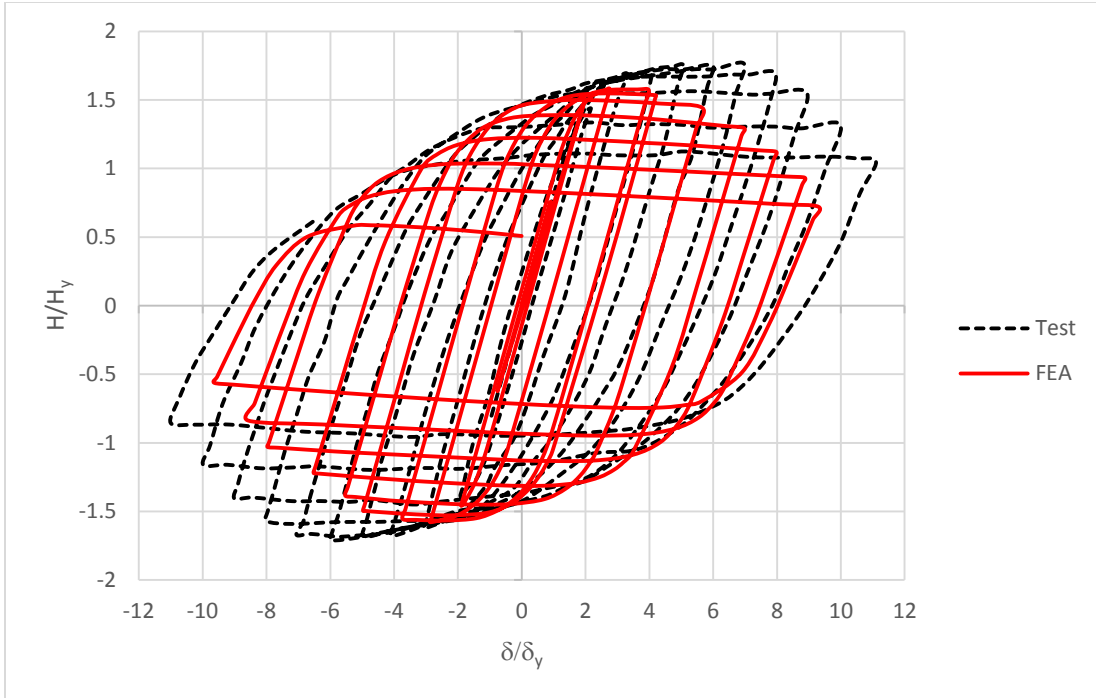Figure 85. Comparison of Envelope Curves of Steel Circular Columns between FEA and Experimental P8-e0
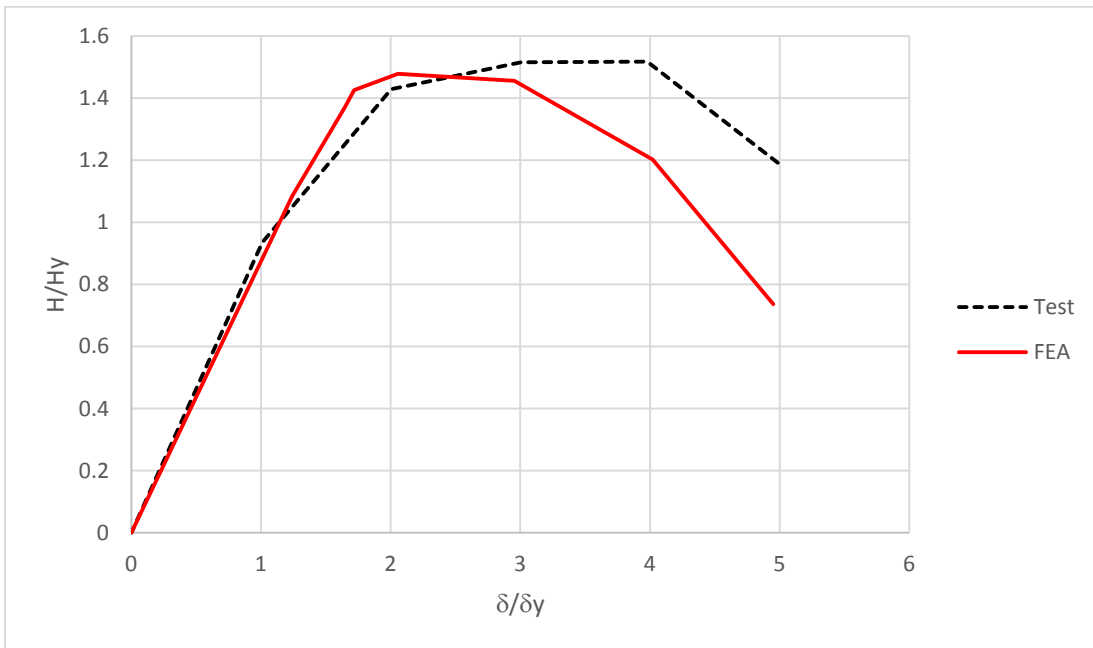
Figure 86. Comparison of Envelope Curves of Steel Circular Columns between FEA and Experimental P8-e1
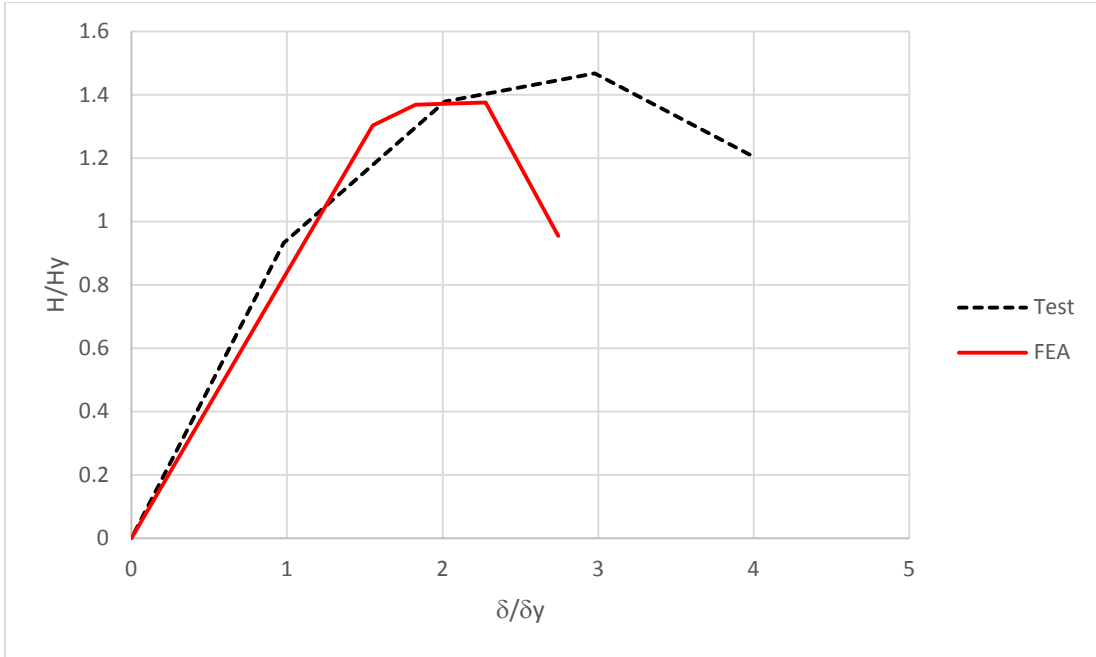
Figure 87. Comparison of Envelope Curves of Steel Circular Columns between FEA and Experimental P8-e2
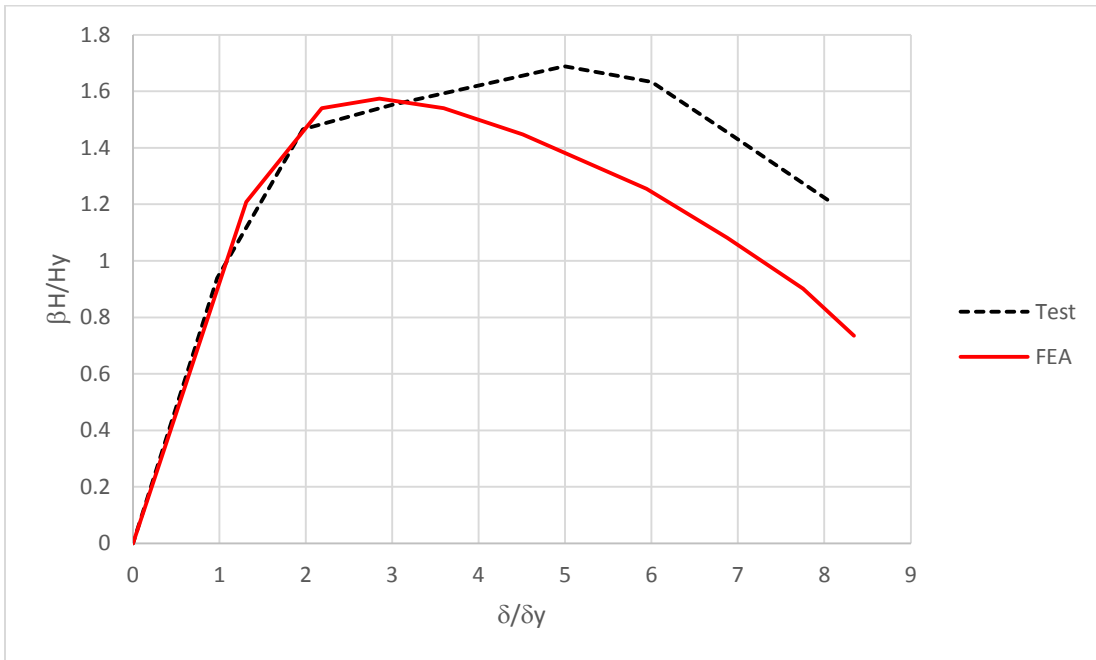
Figure 88. Comparison of Envelope Curves of Steel Circular Columns between FEA and Experimental P12-e0
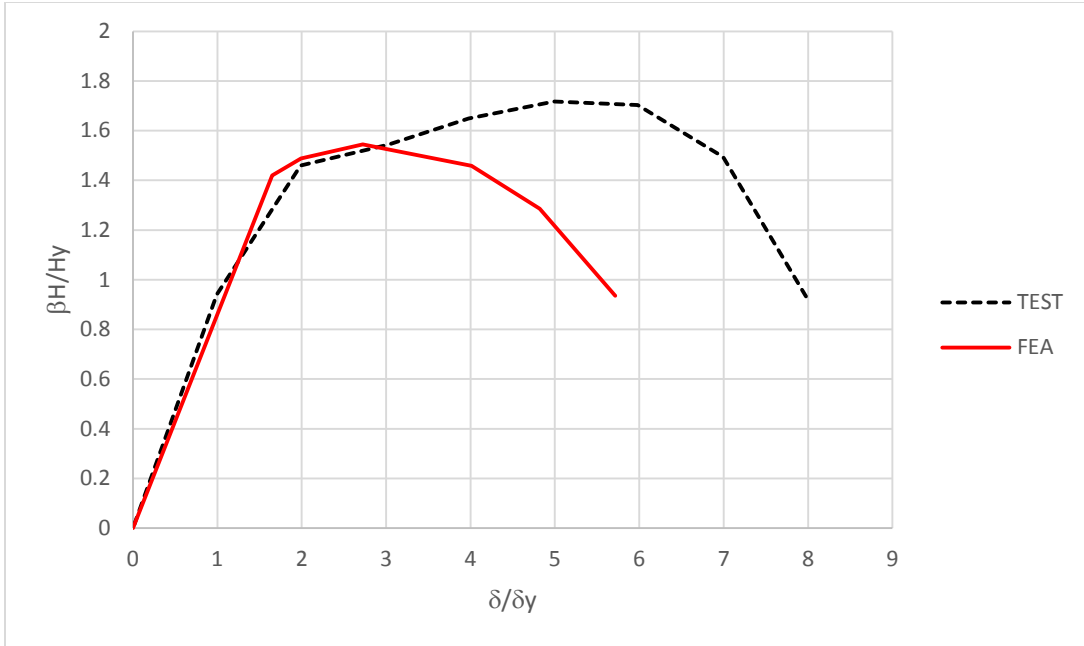
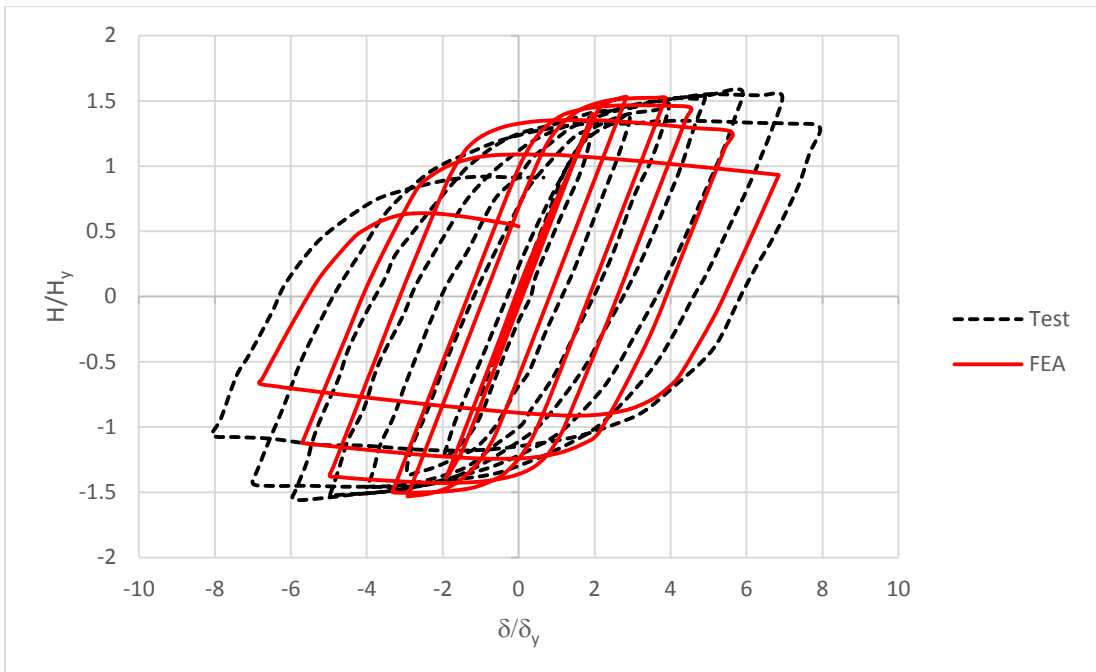Figure 89. Comparison of Envelope Curves of Steel Circular Columns between FEA and Experimental P12-e1
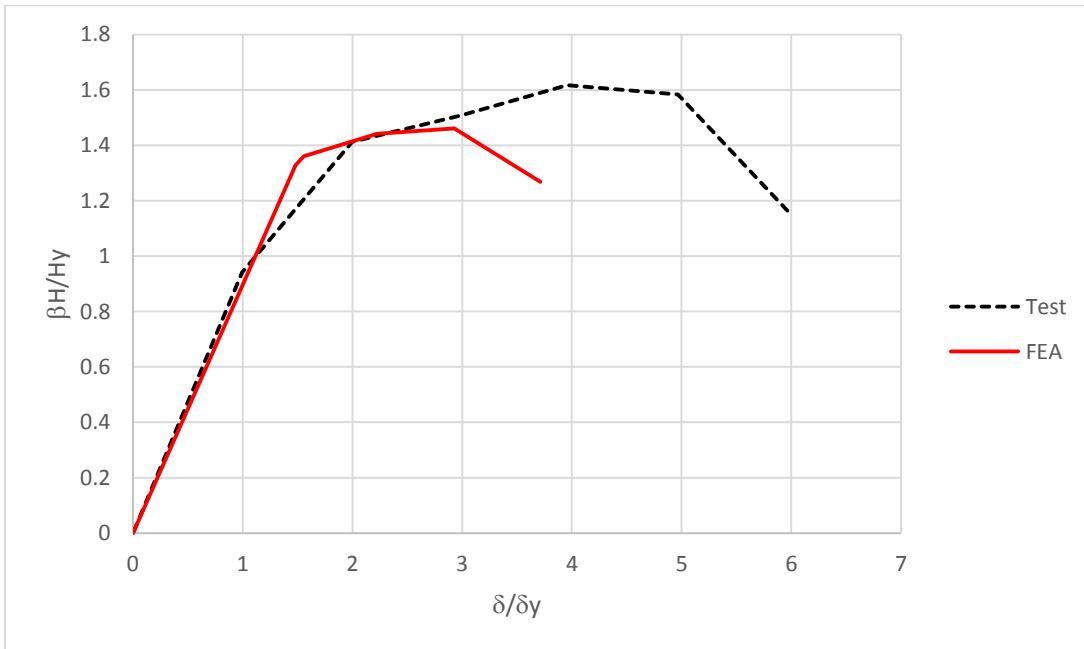
Figure 90. Comparison of Envelope Curves of Steel Circular Columns between FEA and Experimental P12-e2

4.5 Conclusion

In this study, the finite element analysis program ABAQUS (22013) was used to model thin-walled steel bridge piers subjected to out-of-plane cyclic transverse load. The experimental data was used to validate the analysis results. The model was developed for circular cross sections. The results were then plotted on hysteresis loops and compared to the experimental results. As a result, the finite element analysis program ABAQUS (2013) using material models appears to predict the behavior of model with reasonable accuracy.

Based on the analytical results, the following conclusions can be made:

- The load-carrying capacity of the columns is greatly reduced as eccentric, e distance increases.

- In the cases of P13 series $e \leq 0.1h$ and $\lambda \leq 0.20$, or $e \leq 0.1h$ and $R_t \leq 0.075$, the ultimate strength and ductility capacity of the eccentrically loaded columns are almost the same as those of the centrally loaded columns. When eccentricity is higher than e=0.1h, as eccentricity increase by 10% of height, h amplitude $(\delta/\delta y)$ decrease by 1.

- Comparison of the buckling modes indicated in Figure 42 shows that the out-of-plane bending moment dominates the hysteretic behavior of the columns, and the inward deformation on the eccentric side is attributed to the effect of the cyclic twisting moment.

CHAPTER V

CONCLUSION

The usage of thin-walled steel tubular columns as bridge piers have found a wide application in highway bridge systems in Japan as well as other highly populated areas where there are severe constructional limitations since it has small cross-sectional areas and high earthquake resistance. Steel tubular bridge piers, compared with concrete, is light, ductile, and advantageous in environments that cannot support heavy superstructures such as areas with bay areas, soft ground, and reclaimed land. Structural engineers have been continuously looking for new ways to improve design procedures. One area of great concern is the necessity to accurately predict the ultimate behavior of thin-walled steel columns used as bridge piers during severe earthquakes. It is essential to examine the ultimate behavior of thin-walled columns under cyclic in-plane and out-of-plane lateral loading.

In this study, thin-walled steel columns were subjected to in-plane lateral loading and out-of- plane lateral loading having a constant compressive axial force was applied at eccentric distance. The experimental results for cyclic loading thin-walled steel bridge pier model with circular hollow sections conducted by (Gao et al., 2000b) were used to validate finite element analysis of the model using ABAQUS (2013). Results for the models were plotted and compared with the proposed results for the respected models.

Analysis covered in Chapters II and III, the comparison between the hysteresis loops show that there is a reasonably close agreement between the finite element analysis and experimental results. The differences in the models adopted in the analysis can be explained by the fact that they do not accurately consider the reduction of the elastic range due to plastic deformation, known as the Bauschinger effect. The size of the elastic range was taken to be constant, which does not represent the actual behavior of steel. As seen in both Chapters II and III, it can be confirmed that the strength and ductility of the column for the larger R_t becomes lesser. Based on the proposed and numerical results, a seismic design methodology for ultimate strength and ductility evaluation of hollow thin-walled steel tubular columns was presented. The method was based on the empirical ductility equations for column's plate sub-elements and involves an elastoplastic pushover analysis and failure criterion accounting for local buckling. Based on the ultimate strength and ductility capacity, a seismic design verification method for thin-walled tubular beam-columns was presented and discussed. The application of the method was demonstrated by comparing the computed strength and ductility of some cantilever columns with the test results. A good correlation between the computed and test results was achieved. The effects of some important material characteristics and structural parameters, such as, residual stress, width-to-thickness ratio, and column slenderness ratio, on the ultimate strength and ductility of thin-walled steel tubular columns, was investigated. The method is applicable for both the design of new and retrofitting of existing thin-walled steel tubular columns.

References

Banno, S., Mamaghani, I.H.P., Usami, T., & Mizuno, E. (1998). Cyclic elastoplastic large deflection analysis of thin steel plates. Journal of Engineering Mechanics, 124(4), 363-370.

Fukumoto, Y. (2004), "Cyclic Performance Assessment of Stiffened Box Columns with Thickness Tapered Plates", *SSRC 2004 Beedle Award Paper,* Long Beach, California, PP. 1-18.

Zheng, Y., Usami, T., & Ge, H. (2000). Ductility evaluation procedure for thin-walled steel structures. *Journal of Structural Engineering, 126*(11), 1312-1319.

Gao, S., Usami, T., & Ge, H. (1998). Ductility evaluation of steel bridge piers with pipe sections. Journal of Engineering Mechanics, 124(3), 260-267.

Gao, S., Usami, T., & Ge, H. (2000a). Eccentrically loaded steel columns under cyclic in-plane loading. Journal of Structural Engineering, 126(8), 964-973.

Gao, S., Usami, T., & Ge, H. (2000b). Eccentrically loaded steel columns under cyclic out-of-plane loading. Journal of Structural Engineering, 126(8), 974-981.

Goto, Y., Jiang, K., & Obata, M. (2006). Stability and ductility of thin-walled circular steel columns under cyclic bidirectional loading. Journal of Structural Engineering, 132(10), 1621-1631.

Goto, Y., Wang, Q., & Obata, M. (1998). FEM analysis for hysteretic behavior of thin-walled columns. Journal of Structural Engineering, 124(11), 1290-1301.

Japanese Road Association. (1996). Specification for Highway Bridges, part V, *Seismic Design*, Tokyo, Japan,

Guo, L., Zhang, S., Kim, W., & Ranzi, G. (2007). Behavior of square hollow steel tubes and steel tubes filled with concrete. *Thin-Walled Structures, 45*(12), 961-973.

JSCE Earthquake Engineering Committee. (2000). Earthquake Resistant Design Codes in Japan. *Japan Society of Civil Engineers (JSCE)*.

Hajjar, J.F. (2000). Concrete-filled Steel Tube Columns under Earthquake Loads, Progress in Structural Engineering and Materials, Vol. 2(1), pp. 72–82.

Han, L., Yao, G., & Tao, Z. (2007). Performance of concrete-filled thin-walled steel tubes under pure torsion. *Thin-Walled Structures, 45*(1), 24-36.

Japanese Road Association (JRA). (1996). Specification for Highway Bridges, Part V, Tokyo (in Japanese).

Kitada, T., Nakai, H., Matsumura, M. and Kagayama, T. (2000). Experimental Study on Seismic Retrofitting Method of Stiffened Plates in Existing Steel Bridge Piers Under Cyclic Loading, *Journal of Structural Engineering, JSCE*, Vol. 46, pp. 127–134 (in Japanese).

Mamaghani, I. H. P. (1996). Cyclic Elastoplastic Behavior of Steel Structures: Theory and
 Experiment, *Ph.D. Thesis*, Nagoya University, Nagoya, Japan.

Mamaghani, I.H.P. (2005). Seismic performance evaluation of thin-walled steel tubular columns, *Structural Stability Research Council*, Montreal, Quebec, Canada. pp.489-506.

Mamaghani, I.H.P. (2006a). Cyclic elastoplastic analysis and seismic performance evaluation of thin-walled steel tubular bridge piers. Paper presented at the *ASCE Structures Congress 2006,* 17th Analysis and Computation Specialty Conference, 1-13.

Mamaghani, I.H.P. (2006b). Cyclic elastoplastic analysis and seismic performance evaluation of thin-walled steel tubular bridge piers. Paper presented at the *ASCE Structures Congress* 2006, 17th Analysis and Computation Specialty Conference, 1-13.

Mamaghani, I.H.P. (2006c). Inelastic Cyclic Analysis and Stability Evaluation of Steel Braces, *Structural Stability Research Council,* February 8-11, San Antonion, Texas, pp. 281-300.

Mamaghani, I.H.P. (2008). Seismic Design and Ductility Evaluation of Thin-Walled Steel Bridge Piers of Box Sections, *Journal of the Transportation Research Board*, No. 2050, Washington D.C., pp. 137-142.

Mamaghani, I.H.P. (2011) Elastoplastic Large Displacement Analysis of Steel Tubular Columns under Cyclic Loading, *Modern Methods and Advances in Structural Engineering and Construction*, Cheung, S. O., Yazdani, S., Ghafoori, N., and Singh, A. (eds.), ISEC-6, June 21–26, Zürich, Switzerland.

Mamaghani, I.H.P. (2014a). Cyclic Elastoplastic Analysis and Hysteretic Behavior of Thin Steel Plates, *7th European Conference on Steel and Composite Structures, EuroSteel2014*, Napoli, Italy, September 10-12, Paper ID: 460.

Mamaghani, I. H.P. (2014b) Seismic Design and Ductility Evaluation of Steel Bridge Piers, *SMSB 2014 – the 9th International Conference on Short and Medium Span Bridges*, paper ID # 172.

Mamaghani, I. H.P. (2015). Eccentrically Loaded Thin-walled Steel Tubular Bridge Piers under Cyclic In-Plane and Out-of-Plane Loading." *8th International Symposium on Steel Bridges: Innovation & New Challenges 2015 (SBIC 2015),* 14-16 September, Istanbul, Turkey.

Mamaghani, I.H.P., and Packer J.A. (2002), "Inelastic Behavior of Partially Concrete-Filled Steel Hollow Sections", *4th Structural Specialty Conference*, The Canadian Society for Civil Engineering, Montréal, Québec, Canada, pp. s71:1-10.

Mamaghani, I.H.P., Shen, C., Mizuno, E., and Usami, T. (1995). Cyclic behavior of structural steels. I: experiments, *Journal of Engineering Mechanics, ASCE*, 121(11), 1158-1164.

Mamaghani, I. H. P., T. Usami, and E. Mizuno, (1996a). Inelastic large deflection analysis of steel structural members under cyclic loading, *Engineering Structures*, UK, Elsevier Science, 18(9), 659-668.

Mamaghani, I.H.P., Usami, T., and Mizuno, E. (1996b). Cyclic elastoplastic large displacement behaviour of steel compression members, *Journal Structural Engineering, JSCE*, Vol. 42A, 135-145.

Mamaghani, I.H.P., Usami, T., and Mizuno, E. (1997). Hysteretic behavior of compact steel box beam-columns. *Journal of Structural Engineering, JSCE*, Japan, Vol. 43A, 187-194.

Mamaghani, I.H.P., Khavanin, M., Erdogan, E., & Falken, L. (2008). Elastoplastic analysis and ductility evaluation of steel tubular columns subjected to cyclic loading. Paper presented at the *Structures Congress*, pp. 1-12.

Mamaghani, I.H.P., Montazeri, S. (2010). Cyclic Elastoplastic Large Displacement Analysis of Cold-Formed Steel Box Columns under Combined Axial and Bidirectional Lateral Loading, *Cold-formed Steel Structures-2010, 20th International Specialty Conference,* November 3-4, St. Louis, Missouri, pp. 61-75.

Mamaghani, I.H.P., Nemati, N., and Erdogan, E. (2011), Cyclic Behavior and Ductility Evaluation of Thin-walled Stiffened Steel Box Columns, *Structural Stability Research Council,* May 11-14, Pittsburgh, PA.

Mamaghani, I.H.P., Ahmad, F., Dorose, B. (2014a). Cyclic Large Displacement Analysis of Steel Tubular Bridge Piers under Combined Axial and Bidirectional Lateral Loading, *International Journal of Applied Science and Technology (IJAST)*, Vol. 4, No. 6, November, PP. 38-47.

http://www.ijastnet.com/journals/Vol_4_No_6_November_2014/6.pdf

Mamaghani, I.H.P., Dorose, B., Ahmad, F. (2014b). Cyclic Elastoplastic Analysis of thin-walled Steel tubular columns and Frames, *Istanbul Bridge Conference*, Istanbul, Turkey, August 11-13, Paper ID 61.

Mamaghani, I.H.P., Wesley, K, Ahmad, F., Dorose, B. (2014c). Seismic Design and Ductility Evaluation of Thin-walled Steel Box Columns with Enhanced Energy Dissipating Mechanisms, *Istanbul Bridge Conference*, Istanbul, Turkey, August 11-13, paper ID 62.

Mamaghani, I.H.P., Wesley, K., Ahmad, F. (2014d). Cyclic Elastoplastic Analysis and Ductility Evaluation of Thin-walled Steel Box Columns, *4th International Structural Specialty Conference,* Halifax-Canada, May 28-31, Paper ID: CST-165.

Mamaghani, I.H.P., Ahmad, F., Dorose, B. (2015a). Stability Evaluation of Thin-Walled steel Tubular Bridge Piers under Cyclic Multidirectional Loading, *Transportation Research Board, TRB 94th Annual Meeting,* January 11-15, 2015, Washington, D.C., Paper ID: 15-4359. http://amonline.trb.org/trb57535-2015-1.1793793/t004-1.1821073/589-1.1821299/15-4359-1.1821300/15-4359-1.1821301?qr=1

Mamaghani, I.H.P., Dorose, B., Ahmad, F. (2015b). Seismic Design of Concrete-filled Steel Tubular Columns with Enhanced Energy Dissipating Mechanisms, *ISTS15 - 15th International Symposium on Tubular Structures,* 27-29 May 2015, Paper ID: 77, Rio, Brasil.

Mamaghani, I.H.P., Dorose, B., Ahmad, F. (2015c). Cyclic Inelastic Finite Element Analysis and Ductility Evaluation of Steel Braced Frames, *ASCE, 2015 Structures Congress,* Portland, OR., April 23-25, 2015, Paper ID: 250.

Mamaghani, I.H.P., Ahmad, F., Dorose, B. (2015d). Strength and Ductility Evaluation of Steel Tubular Columns under Cyclic Multiaxial Loading, *ISTS15 - 15th International Symposium on Tubular Structures*, 27-29 May 2015, Paper ID: 78, Rio, Brasil.

Mamaghani, I.H.P., Dorose, B. (2015e). Stability and Ductility Evaluation of Thin-walled Circular Steel Bridge Piers under Cyclic Multidirectional loading, *UND Scholarly Forum, University of North Dakota,* Grand Forks, ND, March 10-11, 2015.

Nakanishi, K., Kitada, T. and Nakai, H. (1999), "Experimental Study on Ultimate Strength and Ductility of Concrete Filled Steel Columns Under Strong Earthquake", *Journal of Constructional Steel Research,* No. 51, pp. 297–319.

Nishikawa, K., Yamamoto, S., Natori, T., Terao, K., Yasunami, H. and Terada, M. (1998), "Retrofitting for Seismic Upgrading of Steel Bridge Columns", *Engineering Structures*, Vol. 20, Nos. 4~6, pp. 540-551.

Nishikawa K, Yamamoto S, Natori T, Terao K, Yasunami H, Terada M. (1996). "An experimental study on improvement of seismic performance of existing steel bridge piers." *J. of Struct. Engrg., JSCE* 1996; 42A, 975-986 (in Japanese).

Obata, M., and Goto, Y. (2004). Development of 3D pseudo-dynamic experiment system for bridge piers and columns. *J. Struct. Mech. Earthquake Eng., JSCE*, No. 753/I-66, 253–266 (in Japanese).

Schneider, S. P. (1998). Axially loaded concrete-filled steel tubes. *Journal of Structural Engineering, 124*(10), 1125-1138.

Shen, C., Mamaghani, I.H.P., Mizuno, E. and Usami, T. (1995). Cyclic behavior of structural steels. II: theory. *Journal of Engineering Mechanics, ASCE*, USA, Vol.121, No.11, 1165-1172.

Tao, Z., Wang, Z., & Yu, Q. (2013). Finite element modelling of concrete-filled steel stub columns under axial compression. *Journal of Constructional Steel Research, 89*, 121-131.

Uenoya, M., Nakamura, M., Fukumoto, Y., Yamamoto, S. (2003), "Cyclic Performance of Square Box Columns with Thickness Tapered Plates", *J. of Structural Engineering, JSCE,* Vol. 49A, pp. 115-125 (in Japanese).

Usami, T. (1996), "Interim Guidelines and New Technologies for Seismic Design of Steel Structures", Committee on New Technology for Steel Structures, JSCE, Tokyo (in Japanese).

Usami, T., Ge, H., & Amano, M. (1999). *Strength and ductility of plates in shear* Elsevier.

Usami, T., Suzuki, M., Mamaghani, I.H.P., and Ge, H.B. (1995), "A Proposal for Check of Ultimate Earthquake Resistance of Partially Concrete Filled Steel Bridge Piers", *Journal of Structural Mechanics and Earthquake Engineering, JSCE*, Tokyo, 525/I-33, 69-82, (in Japanese).